NASA CONTRACTOR REPORT

NASA CR-288

DEVELOPMENT OF LAUNCH VEHICLE MALFUNCTION EFFECTS MODEL

Prepared under Contract No. NAS 8-11229 *by*
SPERRY GYROSCOPE COMPANY
Carle Place, N.Y.
for

NATIONAL AERONAUTICS AND SPACE ADMINISTRATION • WASHINGTON, D. C. • AUGUST 1965

NASA CR-288

DEVELOPMENT OF LAUNCH VEHICLE MALFUNCTION EFFECTS MODEL

Prepared under Contract No. NAS 8-11229 by
SPERRY GYROSCOPE COMPANY
Carle Place, N. Y.

for

NATIONAL AERONAUTICS AND SPACE ADMINISTRATION

For sale by the Clearinghouse for Federal Scientific and Technical Information
Springfield, Virginia 22151 – Price $4.00

TABLE OF CONTENTS

TABLE OF CONTENTS (Cont'd)

SECTION I

INTRODUCTION AND CONCLUSIONS

1.1 READI CONCEPT

The READI concept comprises an on-board instrumentation and control system that senses abnormal operation of rocket engine propulsion systems and institutes emergency remedial actions to reduce the consequences of malfunctions upon mission success and crew safety. The remedial actions function to limit the secondary effects of the malfunction and, when possible, capitalize on inherent vehicle redundancy to replace lost functions. The concept emphasizes accurate and early identification of malfunctions to avoid unnecessary aborts and allow adequate lead time for crew escape when abort is necessary.

1.2 PREVIOUS INVESTIGATIONS

The preceding two phases have provided answers to some of the major questions concerning the READI concept. Phase I established that the effectiveness of a READI system for a typical engine and launch vehicle stage could justify the additional on-board equipment required and still produce a substantial gain in terms of cost effectiveness. Design procedures were developed to achieve the optimum READI system design and level of complexity. During the Phase II investigation the development of design procedures was continued and an experimental system was built to demonstrate that a very high reliability could be achieved. The experimental system made extensive use of microcircuitry, information redundancy, and special signal validity tests to achieve very low false alarm rates.

1.3 OBJECTIVES OF THE PRESENT INVESTIGATION

The READI design procedure developed in the previous two phases of the program is shown in figure 1-1. The shaded boxes represent key steps in this procedure that involve the development of mathematical models for the mission, vehicle stages, and subsystems to describe their operation under malfunction conditions. The objective of the present investigation was to develop a set of these malfunction effect models which would be applicable to a real mission-vehicle-engine combination.

Specifically the Apollo Manned Lunar Landing Mission and the Saturn V launch vehicle have been selected for analysis in this study because of the availability of real data and current interest in these programs. The J-2 engine was selected as an example of the vehicle subsystems since it is used in two stages of the Saturn V launch vehicle.

The malfunction effects models have been utilized in a concurrent program, Contract No. NAS 8-11290, to actually synthesize and evaluate a READI system for the Saturn V. The final report on that program describes in detail the functional design and effectiveness estimates for the systems.[1]

- - - - - - -

[1] Refer to reference 1, Appendix C.

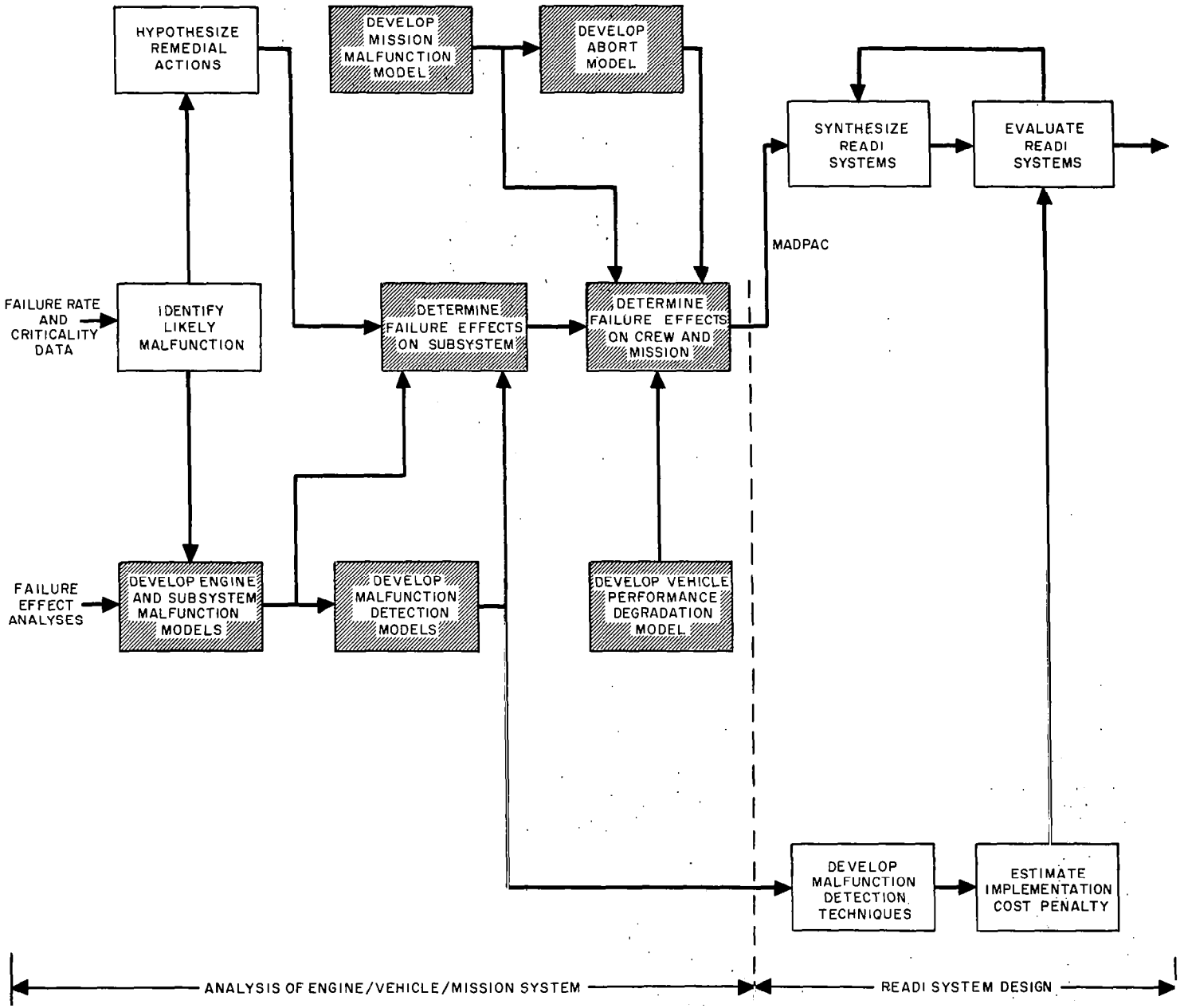

FIGURE I-1. READI DESIGN PROCEDURE

It should be noted that the malfunction effects models by themselves do not constitute a complete solution to the problem of designing a READI system. Their purpose is to provide the designer with a set of tools which enables him to determine, in a logical and systematic manner, the ultimate effect of a malfunction and decision pair upon the mission success and crew safety. The summation of this data over the set of probable malfunctions which can occur during a flight comprises the input data to the Malfunction and Decision Pair Analysis Compilation (MADPAC). The result of MADPAC is a computer printout which, as shown in figure 1-1, contains the necessary data to synthesize and evaluate READI systems. Details of the format of this document are contained in this report, since an organized data handling procedure such as this is believed to be essential in applying the design techniques to large scale problems.

1.4 CONCLUSIONS

Mathematical relationships relating malfunction and remedial actions to their effects on crew safety and mission success have been derived and are presented as a series of mathematical models and computational procedures. The application of these techniques to the Saturn V launch vehicle has demonstrated that the large volume of reliability and failure effects data, typical of a complex multistage launch vehicle, can be assimilated, processed, and used effectively to assure that the READI system design considers these data in a proper perspective.

The models and computational procedures have also proved to be of great value in organizing and assigning tasks to the team of design engineers and in providing a standardized format for record keeping and communication among the various specialists who are required during the analysis of the vehicle.

1.5 ORGANIZATION OF REPORT

Figure 1-2 illustrates the application of the various malfunction effects models to assess the effect on mission success and crew safety of a particular malfunction coupled with a specific remedial action. The probability of crew and mission loss is computed from a chain of conditional probabilities based on the models. Since the mission and abort models have the most direct relationship with the final outputs of crew and mission risk, these models are discussed first in Sections II and III. The vehicle performance degradation models are discussed in Section IV followed by the engine or subsystem malfunctions effects models in Section V. The MADPAC format is detailed in Section VI, and the malfunction sensing model is presented in Section VII to complete the chain from the initial malfunction through all the intermediate effects to the final losses.

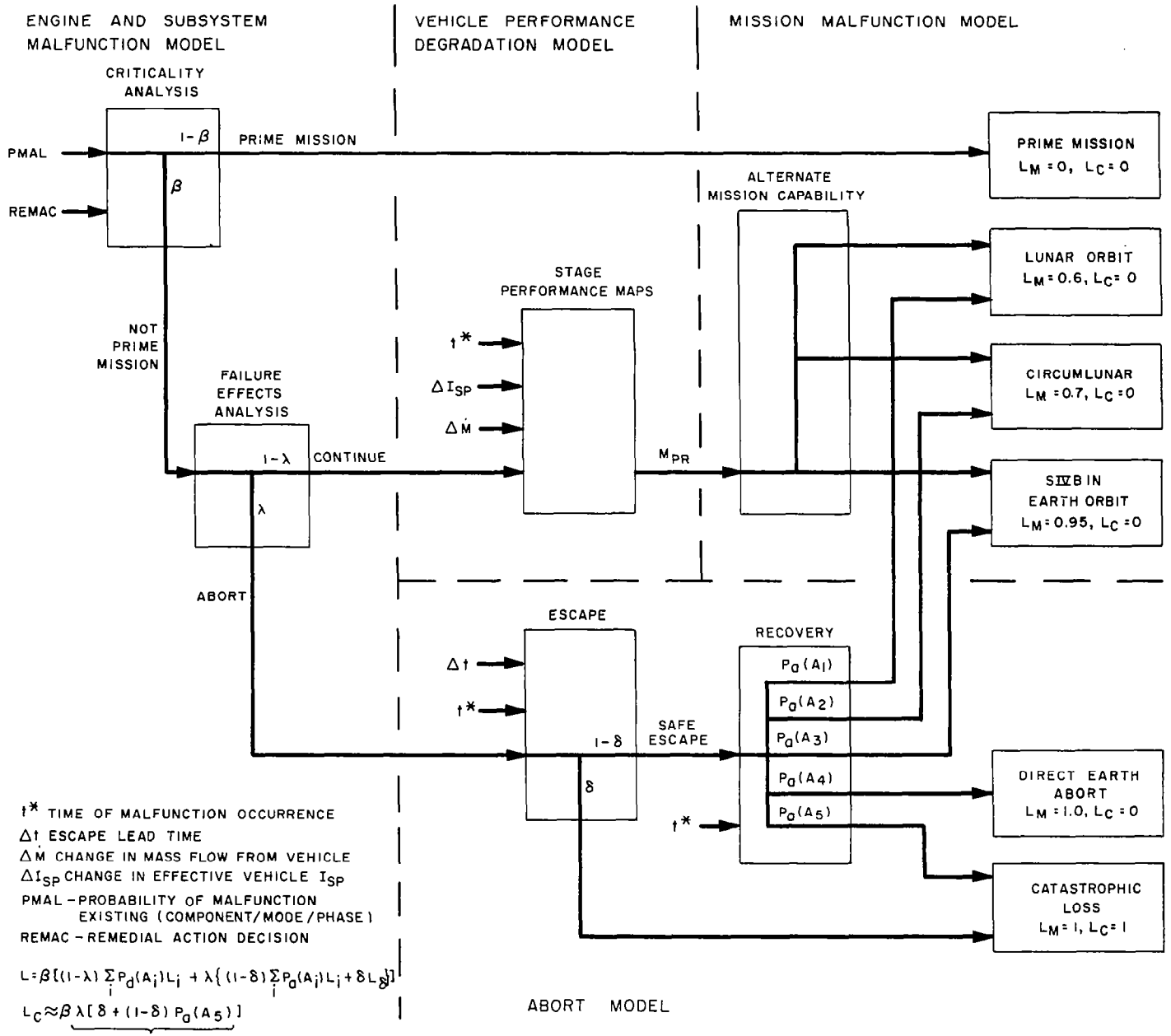

FIGURE I-2. APPLICATION OF MALFUNCTION EFFECTS MODELS

SECTION II

MISSION MODEL

2.1 INTRODUCTION AND SUMMARY

The mission model discussed in this section is a mathematical representation of the mission which permits an assessment of the degree of mission success and crew safety, given certain conditions of vehicle performance degradation.

The mission chosen for analysis is the Apollo Manned Lunar Landing Mission. The prime mission is, of course, well defined; however, in the event performance degradations preclude attainment of the prime mission, there are various less well defined alternate missions that may still be possible as indicated in figure 2-1. The mission model must recognize the value of these alternates in order to be realistic. A single number representative of mission success can be obtained if the various alternate missions are assigned weighting values that represent the worth of each alternate mission relative to the prime mission.

The capability of attaining the prime and alternate missions, having achieved earth orbit and assuming perfect spacecraft operation, can be expressed in terms of the residual propellants contained by the SIVB in a standard 100 nm orbit. These relationships, which are the result of the mission analysis, are summarized in figure 2-2. Effects on mission capability prior to achievement of earth orbit, due to staging and other constraints, are shown separately for the three stages in figures 2-3, 2-4, and 2-5.

2.2 ALTERNATE MISSIONS

The missions considered as favorable alternates to the lunar exploration mission have not to date been designated by NASA. For the purposes of this study, therefore, a set of alternate missions has been assumed that is believed to represent the preliminary results of NASA's thinking at this time.

Likewise, relative worth values were assigned to the alternate missions on a rather arbitrary basis with the realization that these weighting values will change with each particular mission depending upon the accomplishments of previous missions. The weighted numbers affect only the optimization of READI design; the latter does not appear to be a strong function of the exact values used.

The set of alternate missions used and the assigned relative worth values are given below:

	Mission	Relative Value
Prime Mission	Lunar Landing	1.0
Alternate Missions	Lunar Orbit	0.4
	Circumlunar	0.3
	Earth Orbit	0.05
	Earth Direct Abort	0.0

2.3 ALTERNATE MISSION CAPABILITY

The capability of the Saturn V vehicle to achieve the prime or an alternate mission can be expressed in terms of the residual propellant aboard the SIVB stage

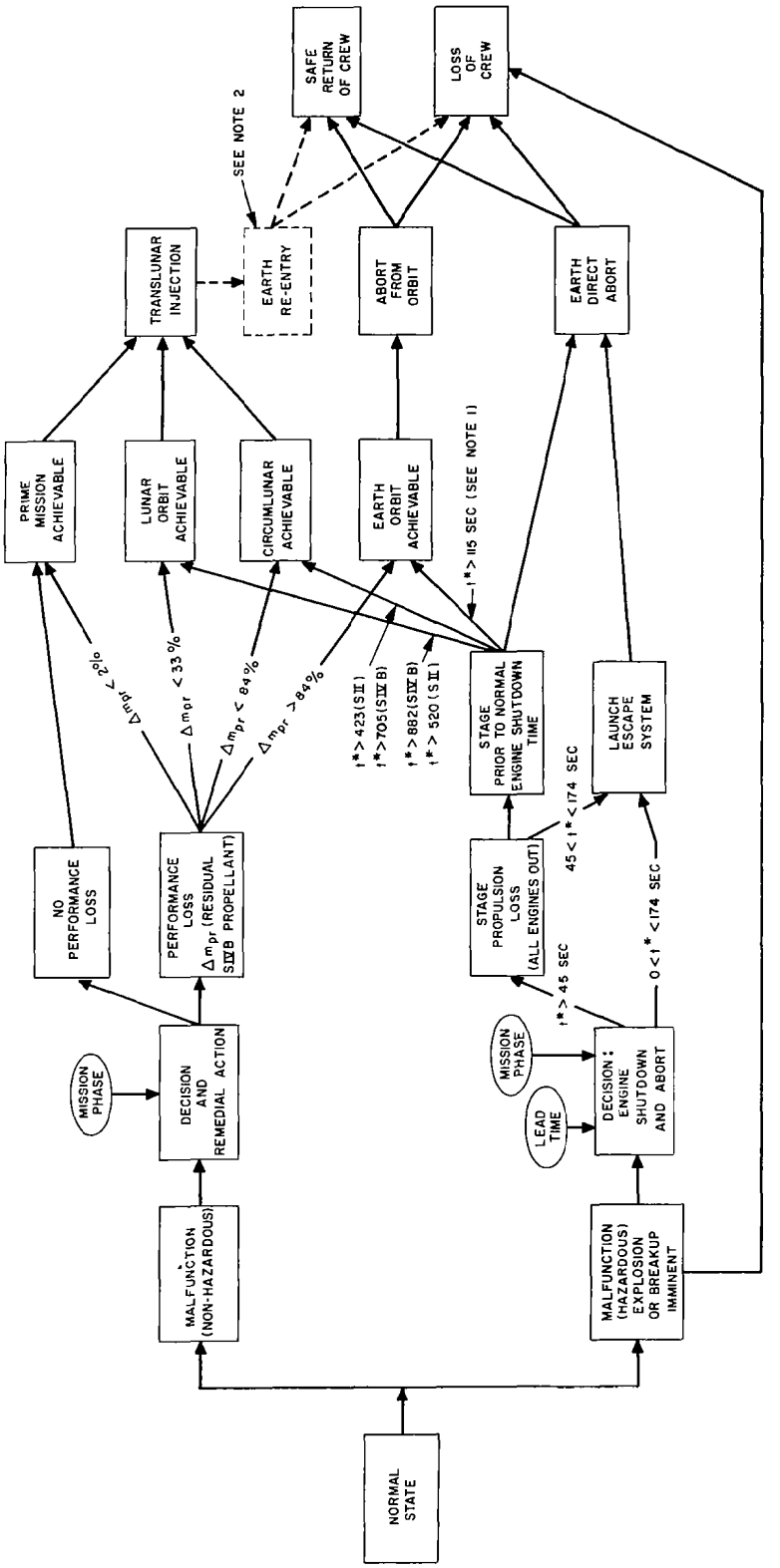

NOTES:
(1) t* IS TIME AFTER LAUNCH AT WHICH MALFUNCTION OCCURS
(2) SATURN V MISSION COMPLETE WITH SEPARATION OF S IVB STAGE FROM SM AND CM. EVALUATION OF READI STOPS AT THIS EVENT

FIGURE 2-1. POSSIBLE TRANSITIONS DURING SATURN V MISSION

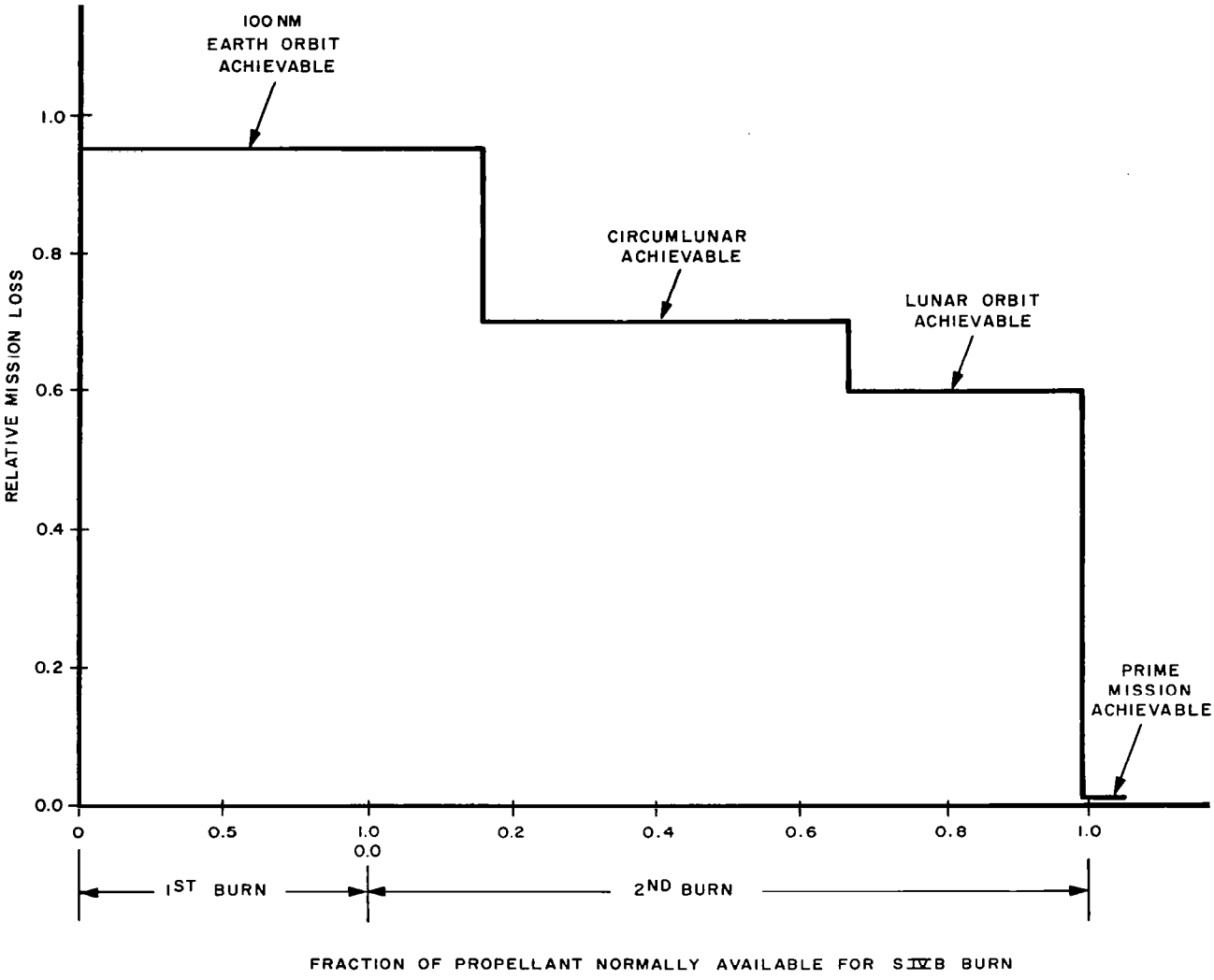

FIGURE 2-2. ALTERNATE MISSION CAPABILITY

after it has reached 100 nm orbit. If a normal ascent to orbit has occurred, the SIVB stage will have a certain propellent mass, M_{PRN}, available for injecting the payload into a translunar trajectory. With the vehicle parameters assumed for the mission model, over 98.1 percent of this propellent mass is required during SIVB second burn to attain the necessary velocity increment (ΔV) for translunar injection. If more than two percent of the normally available propellant had been used during SIVB first burn to reach orbit, then the ΔV required for translunar injection cannot be supplied by the SIVB stage alone; the deficit must be made up by the Service Module (SM). Depending upon the amount of propellant expended by the SM for this purpose, its capability for achieving the prime mission will either be eliminated or, at the very least, reduced in safety margin.

The reduction in the propellant available for SIVB second burn is caused by performance losses during the boost phase which are compensated for by a longer-than-normal SIVB first burn. It is assumed that the adaptive guidance system of the Saturn V launch vehicle automatically controls the SIVB burn time until orbital conditions have been attained. For example, assume that READI initiates SII engine cutoff 20 seconds before normal depletion cutoff in anticipation of an explosion hazard. In order to achieve 100 nm orbit, the SIVB stage would have to burn longer than normally planned, and a reduction in the propellant available for second burn results. Performance maps have been prepared to relate the effects of various malfunction and decision pairs to a reduction in M_{PR}. These performance maps are discussed in Section IV of this report. This section describes the alternate mission capability as a function of M_{PR}, the propellant available for SIVB second burn.

2.4 CALCULATIONS OF ΔV

The approach taken in determining the alternate mission capability is summarized by the following steps:

(a) Determine the velocity increments (ΔV's) required during various phases of the prime (lunar landing) mission.

(b) Use these ΔV's to determine the amount of SM propellant needed for alternate missions, and calculate the unused propellant on-board the SM.

(c) Calculate the contribution this "excess" SM propellant could make to the velocity increment required for lunar injection from 100 nm earth orbit.

(d) Compute the amount of SIVB propellant needed to complete the ΔV required for lunar injection.

The following are the input data which have been used in determining the alternate mission capability for the Saturn V mission model:

- Mass in 100 nm orbit		277,800 lbs
- Mass of propellant vented in orbit	(-)	6,000
		271,800
- Mass of propellant available for SIVB second burn	(-)	144,500
		127,300

- Mass of empty SIVB, IU	(-)	37,300
		90,000
- Mass of SIVB adapter and shroud	(-)	3,400
- Mass of payload after lunar injection		86,600
- Mass of Service Module (SM) propellant	(-)	37,500
		49,100
- Mass of Lunar Excursion Module (LEM)	(-)	28,000
- Mass of empty Command Service Module (CSM)		21,100

- Service Module engine specific impulse I_{sp} = 310 sec (these values were estimated for the purpose of generating the model, and do not represent actual values.)(2)
- Service Module propellant flow rate = 70 lbs/sec
- SIVB engine specific impulse I_{sp} = 425 sec (estimated).

The velocity increments (ΔV's) required of the SM during the lunar landing mission were calculated using the assumed values of I_{sp} in the following equation

$$\Delta V = I_{sp}\, g_o \ln \frac{m_o}{m_f} \qquad (1)$$

where

I_{sp} = specific impulse of engine

g_o = gravitational constant = 32.2 ft/sec^2

m_o = initial mass of vehicle before thrusting

m_f = final mass of vehicle after thrusting.

- - - - - - -

(2)Refer to Reference 2, Appendix C.

The calculations are summarized in table 2-1.

2.5 LUNAR ORBIT MISSION

A lunar orbit mission might be undertaken if the following conditions existed:

- The SIVB and payload were in 100 nm earth orbit with insufficient SIVB propellant to complete the prime mission.
- The CSM systems were in a "go" condition.

For the purpose of generating the model, the lunar orbit mission was assumed to consist of the following steps:

- The available SIVB propellant is used to escape from earth orbit and start the payload towards a translunar trajectory.
- At SIVB burnout, the CSM separates and thrusts to provide the additional ΔV required to attain the nominal velocity needed for a 72-hour transit time. The LEM is left behind.
- The CSM retrofires and goes into lunar orbit. The only difference between the prime and alternate missions after this point is that no lunar descent takes place.

In order to determine the mass of SIVB propellant required for lunar orbit, it is necessary to first calculate the "excess" propellant aboard the SM. If a safety factor of 500 pounds of SM propellant is assumed, the weight of the CSM at earth re-entry will be 21,100 + 500 = 21,600 pounds. By using this number and the ΔV's computed for the prime mission in subsection 2.4 the "excess" SM propellant is found to be 11,900 pounds. The calculations are summarized in table 2-2.

Table 2-1. SERVICE MODULE ΔV's REQUIRED DURING LUNAR LANDING MISSION

Operation	Burn Time (sec)	m_o (lbs)	m_f (lbs)	ΔV(ft/sec)
(a) Midcourse corrections	(45)	86,600	83,475	375
(b) Retrofire to lunar orbit	(350)	83,475	59,175	3450
(c) Transearth injection	115	31,175(2)	23,200	(2940)(1)
(d) Midcourse corrections	(30)	23,200	21,100(3)	940

The numbers in parentheses were used as the input data for the calculation across the row, as they were considered to be the most reliable information.

(1) ΔV = 2940 = (8230-5290) = (lunar escape velocity for 72-hour transit time - lunar 80 nm orbital velocity)

(2) m_o = 31,175 = (59,175-28,000) = (mass in lunar orbit - mass of LEM)

(3) m_f = 21,100 = mass of CSM at re-entry.

Table 2-2. CALCULATIONS TO DETERMINE EXCESS SM PROPELLANT

Operation	ΔV Req'd (ft/sec)	m_f (lbs)	m_o (lbs)
(d) Midcourse correction (earth return)	940	21,600	23,800
(c) Transearth injection	2940	23,800	31,900
(b) Retrofire to lunar orbit	3450	31,900	44,950
(a) Midcourse correction (to moon)	375	44,950	46,700

It can be seen from the data listed in table 2-2 that the mass of the CSM after injection to lunar orbit is 46,700 pounds. Since the initial weight of the CSM was 58,600 pounds (payload - LEM), the "excess" SM propellant is 11,900 pounds. The ΔV available for translunar injection from this propellant is found by solving equation (1) and is equal to 2280 ft/sec. Since the total velocity increment needed for lunar injection from 100 nm earth orbit is 10,050 ft/sec., the remainder must be supplied by the SIVB second burn. That is,

ΔV_{SIVB} = ΔV required for injection - ΔV supplied by SM

= 10,050 - 2280 = 7770 ft/sec.

Using the assumed I_{sp} of 425 seconds and a m_f of 127,300 pounds for the SIVB (see page 2-3), equation (1) can be solved for m_o, the initial weight of the SIVB prior to lunar injection:

$$m_o = m_f \exp\left(\frac{\Delta V}{I_{sp}\, g_o}\right) = 225{,}000 \text{ lbs.} \qquad (2)$$

The mass of the SIVB propellant which contributes to the translunar injection

velocity is the difference between m_o and m_f, or 97,700 pounds. Since the propellent mass available for SIVB second burn under normal conditions is 144,500 pounds, the percentage required to achieve a lunar orbit mission is seen to be approximately 67 percent.

2.6 CIRCUMLUNAR MISSION

A circumlunar mission might be substituted for the prime mission in either of the following situations:

- The SIVB and payload are in 100 nm earth orbit with insufficient SIVB propellant to complete either a lunar landing or lunar orbit mission.
- A malfunction during SIVB second burn necessitates engine cutoff before attaining a velocity sufficient to complete a lunar orbit mission.

In the latter situation the premature engine cutoff can be equated to the mass of propellant which would result in the same velocity increment so that, for the purpose of the model, the two situations are identical.

The amount of SIVB propellant necessary to achieve a circumlunar mission is calculated in the same manner as was described in subsection 2.5 for the lunar orbit mission. The major difference is that the ΔV required to prescribe an elliptical orbit around the moon is less than that required to go into and escape from a lunar orbit. It is assumed that, in addition to the midcourse corrections, the total ΔV required for velocity and path corrections for a circumlunar mission is 1000 ft/sec. Using the same safety factor of 500 pounds of SM propellant, the SIVB propellant required for a circumlunar mission was calculated. The results are summarized below:

- SM propellant required for circumlunar operations — 6,150 lbs
- SM propellant available for translunar injection — 31,350 lbs
- ΔV for translunar injection supplied by SM — 7,710 ft/sec
- ΔV for translunar injection supplied by SIVB — 2,340 ft/sec
- SIVB propellant required for translunar injection — 23,700 lbs
- Percent of normal SIVB residual propellant, M_{PRN} — $\approx$ 16%.

2.7 STAGE TRANSITION MODELS

In order to determine the increase in mission value resulting from a READI decision, the capability of the launch vehicle to achieve alternate missions must be known. The transition block diagram of figure 2-1 illustrates the wide range of possible deviations from a normal mission, and emphasizes the capacity of the Saturn V vehicle to achieve an alternate mission in the event of a malfunction. It can be seen from figure 2-1 that the alternate mission selected depends upon the nature of the malfunction and decision, and the time at which it occurs.

Those malfunctions which are non-hazardous generally cause a performance loss and can be analyzed in terms of their effect upon M_{PR}, the residual SIVB propellant in 100 nm orbit. Malfunctions

which may be termed hazardous require either an immediate abort or the shutting down of one or more engines, depending upon the mission phase. In order to show these transition possibilities more clearly, the mission has been divided into phases corresponding to the SIC, SII, and SIVB stages, and transition models have been prepared for each, figures 2-3, 2-4, and 2-5. The stage models are subdivided into phases which are defined by discrete operational events. These events, represented as nodes on the diagrams, serve to group the types of malfunctions which can occur during a phase.

For example, consider the SII stage transition model, figure 2-4. The model is characterized by an initial condition state (corresponding to normal SIC burn out) and six possible end condition states. The model shows that the decision to shut down a single SII engine can result in one of two different end states, depending upon when the malfunction and decision occurs. For the interval between SII ignition and a time approximately 410 seconds after liftoff (t = 410), a single engine cutoff will result in loss of prime mission capability, but a lunar orbital mission is still possible. (Normal operation of the following stages is assumed.) For the interval between t = 410 seconds and normal engine cutoff, the model shows that prime mission is achievable even with one engine out. Thus, the increase in mission value resulting from the remedial action decision to shut down an SII engine, as compared with the no-decision case, must be summed over the two time intervals involved. Similar procedures are used to analyze other paths of the stage transition models.

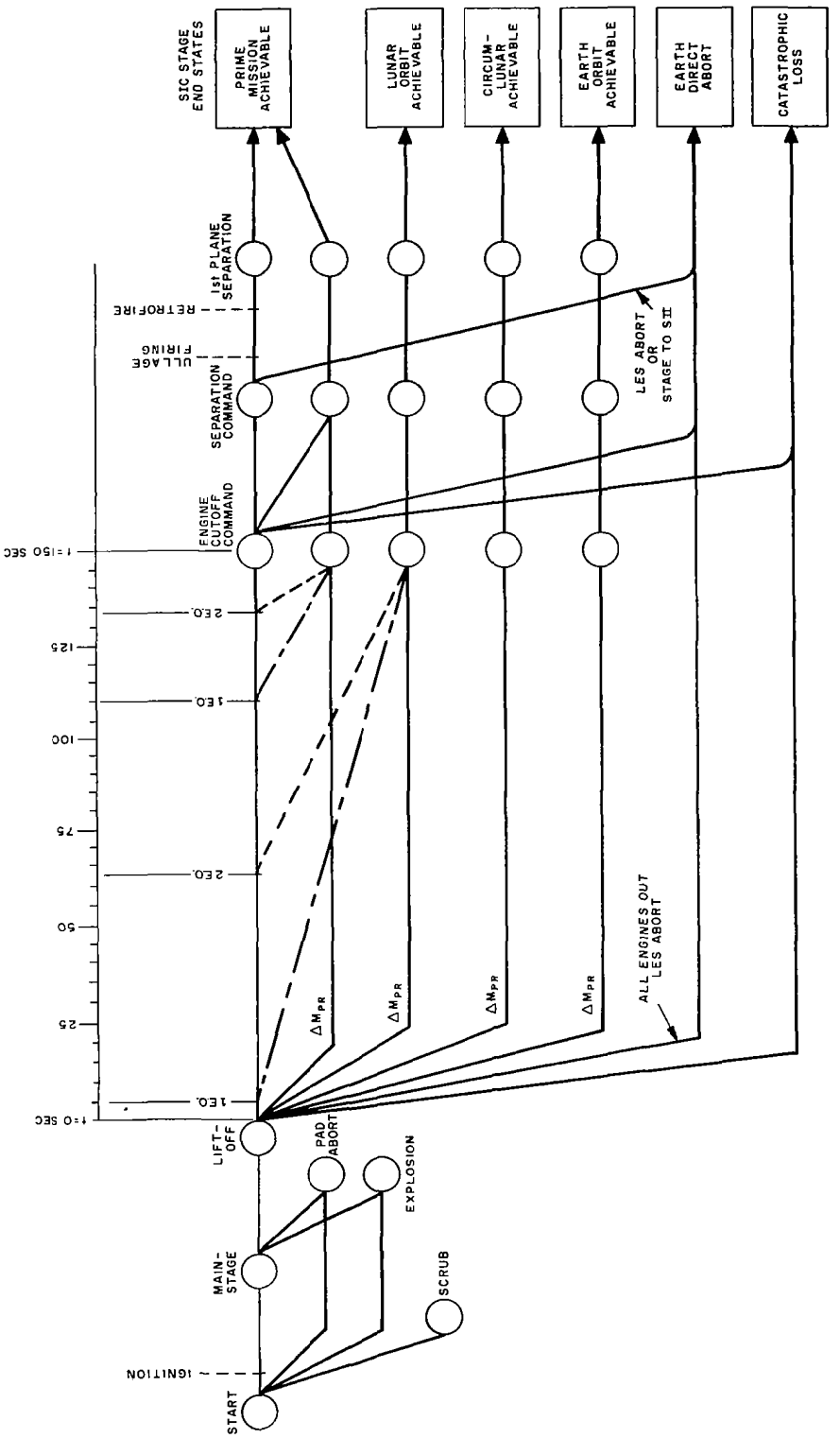

FIGURE 2-3. SIC STAGE TRANSITION MODEL

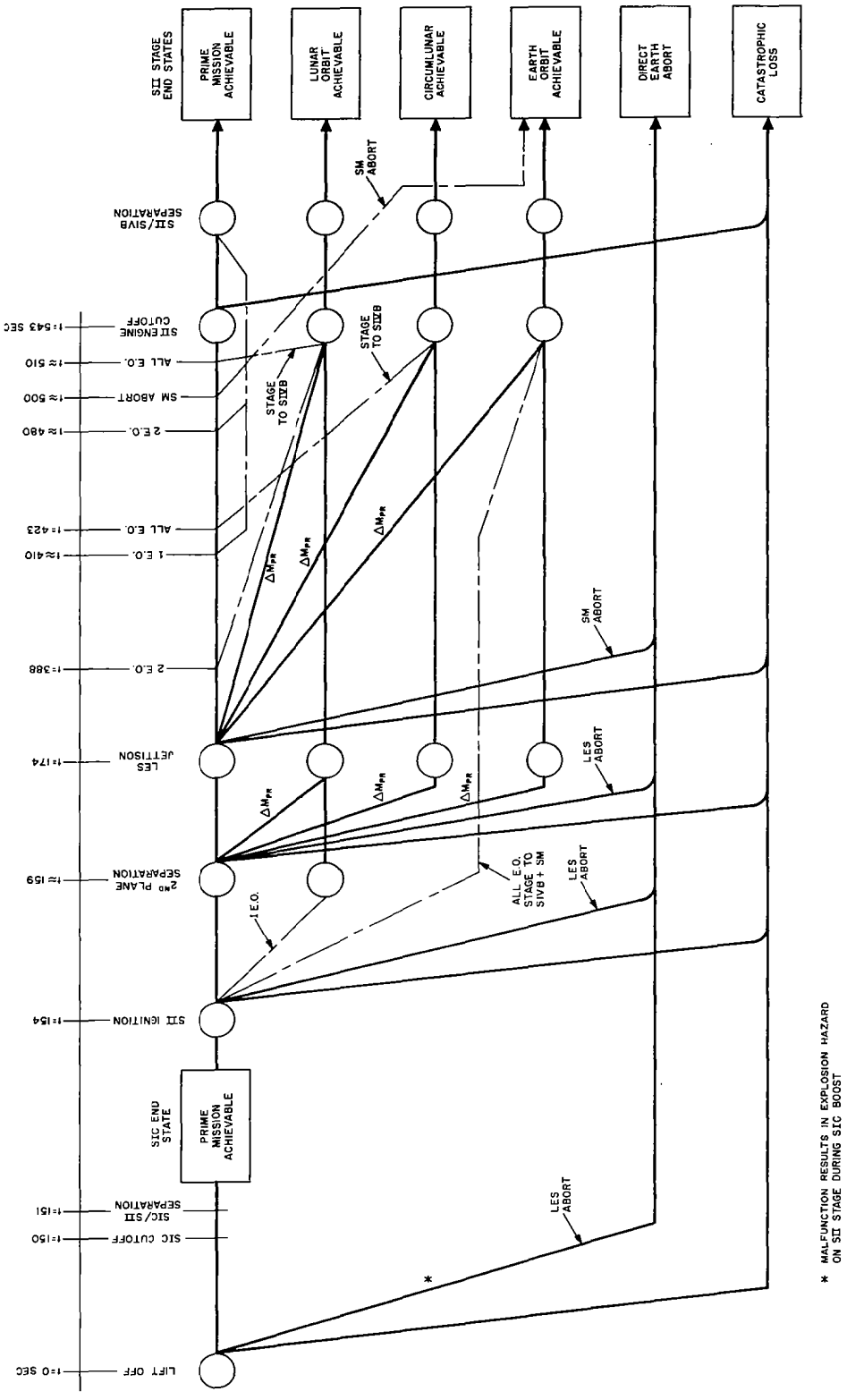

FIGURE 2-4. S II STAGE TRANSITION MODEL

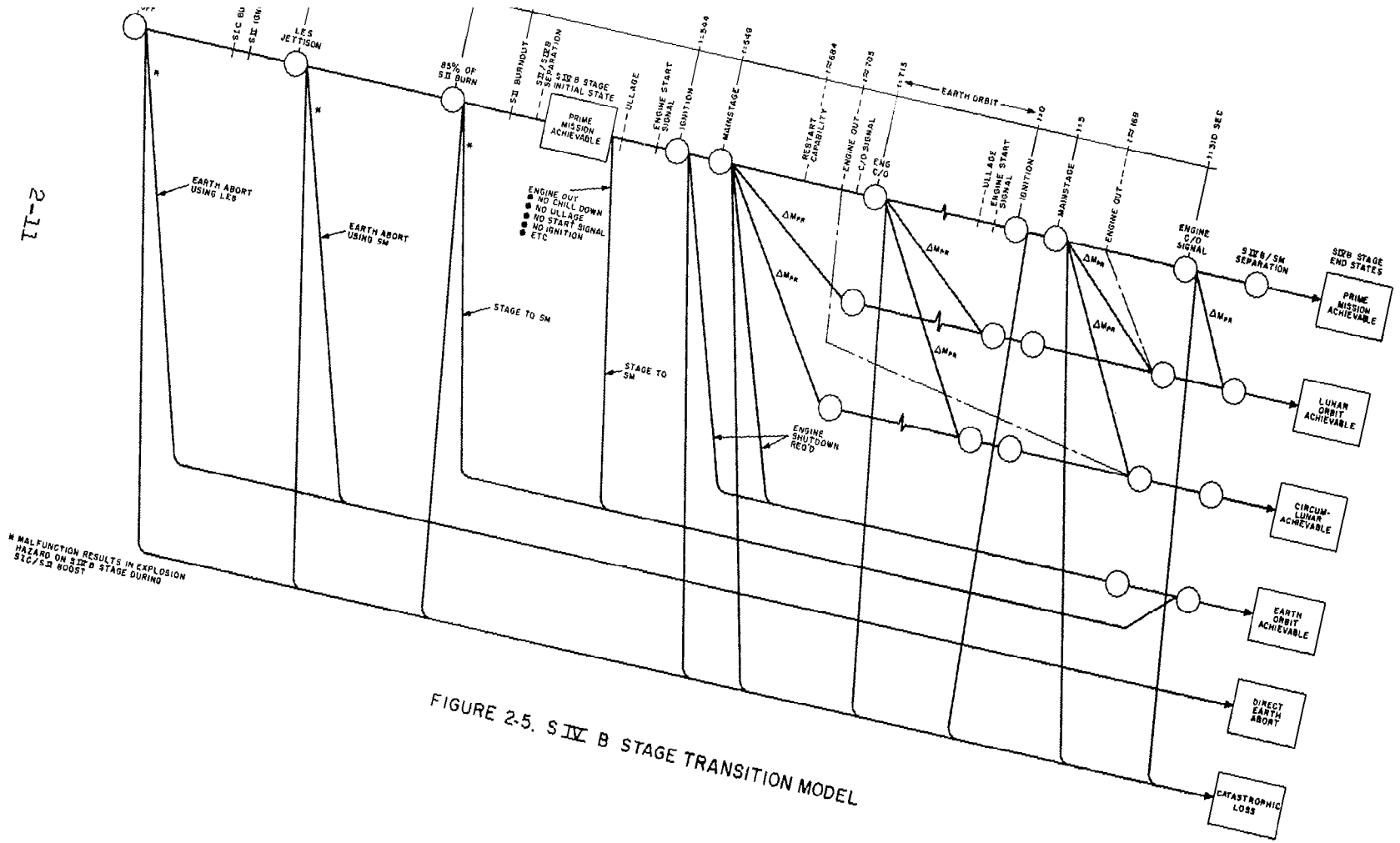

FIGURE 2-5. S IV B STAGE TRANSITION MODEL

SECTION III

ABORT MODEL

3.1 INTRODUCTION AND SUMMARY

The abort model is used to determine the effects on mission success and crew safety in the event that an abort is required at some time during the launch operation. Abort as used here refers to the process of separating the crew from a failed stage to avoid the possibility of crew loss caused by structural breakup or explosion. This action is necessary for certain uncorrectable malfunctions that result in severe loss of performance, excessive vehicle rates, or explosions.

The abort model is comprised of two parts, the escape model and the recovery model. The escape model describes the probability of safely separating from and clearing the failed stage as a function of mission time and lead (or warning) time. The recovery model describes the ensuing capability for alternate mission accomplishment and safe crew recovery.

Figure 3-1 summarizes the preferred method of abort, alternate mission that is achievable, and assumed value of recovery crew risk for the first and second stages of Saturn V; figure 3-2 summarizes the above data for the third stage. Figures 3-4, 3-7, and 3-9 summarize the lead-time required for safe crew escape under various hazardous conditions.

3.2 ABORT MODES

3.2.1 PRELIMINARY CONSIDERATIONS

The preferred method of abort is dependent upon factors such as the nature of the contingency and the mission phase during which it occurs. The objective of the abort decision is to attain the highest valued alternate mission possible without endangering the crew. Because the upper stages of the Saturn V have a high performance capability, a malfunction in the launch vehicle can often be left behind while the spacecraft fulfills an alternate mission. For example, assume an explosion hazard is detected during the first 20 seconds of SII burn, before the Launch Escape System (LES) has been jettisoned. If the malfunction is detected sufficiently in advance of the explosion, it may be possible to shut down the SII engines, stage to the SIVB, and achieve earth orbit with the aid of the (SM) propulsion system. If, on the other hand, the need for an immediate abort is indicated, the LES would be used to separate the spacecraft from the launch vehicle and return it directly to earth. This example emphasizes the importance of detecting the malfunction as far in advance of the resultant explosion or breakup as possible. Not only is the crew safety enhanced by early detection, but the probability of completing an alternate mission with greater scientific value is also increased.

3.2.2 METHODS OF ABORT

The example described in paragraph 3.2.1 also serves to illustrate the two general methods of abort which were used in construction of the abort model, namely

- Abort using the LES
- Abort from the Saturn V vehicle by premature engine shut down and staging.

The former method would be used during SIC boost and the first 20 seconds of SII boost before the LES is jettisoned. The only alternate mission which can be achieved using the LES is a direct earth return. If abort is required during the SII burn after the LES is jettisoned, the normal procedure would be to shut down engines and stage to the SIVB. However, the nature of the malfunction may require staging directly to the SM. During SIVB burn, abort would be accomplished by engine shutdown and staging to the SM. In summary, then, the abort modes may be classified according to the stage under consideration as follows:

- SIC burn: - Abort using LES
- SII burn: - Abort using LES
  - Engine shutdown and stage to SIVB
  - Engine shutdown and stage to SM.
- SIVB burn: - Engine shutdown and stage to SM.

It should be noted that abort during SIC boost could be accomplished at some point in time after liftoff by engine shutdown and staging to either SII or SIVB. This procedure could only take place late in the SIC burn after certain altitude and velocity requirements have been fulfilled. These possibilities are being investigated by NASA at the present time.

A premature staging operation will usually, although not always, result in loss of prime mission capability. The time during the mission at which engine shutdown and staging occur determines which of the alternate missions can be achieved. This is shown by the Stage Abort and Crew Risk Models, figures 3-1 and 3-2. The models summarize the following information for each stage:

- The malfunction effect which leads to abort
- The method of abort
- The alternate mission achievable after abort.

3.3 CREW RISK

3.3.1 GENERAL

In order to determine the reduction in crew risk derived from a READI decision to abort, as compared with the no-action case, it is necessary to evaluate the relative risks to the crew associated with the various abort modes considered in subsection 3.2. First, however, the closely related concept of "escape" should be examined briefly. The Escape Model, which is discussed in subsection 3.4, determines the lead time required to escape safely from an explosion, breakup, or other hazardous condition, given an abort decision. The lead time and method of abort are used to estimate the probability of safe escape which is needed for READI system evaluation. The Escape Model is the principal factor in determining whether or not an abort will result in a catastrophic loss. Once the "escape" period has passed, the crew risk is dependent primarily

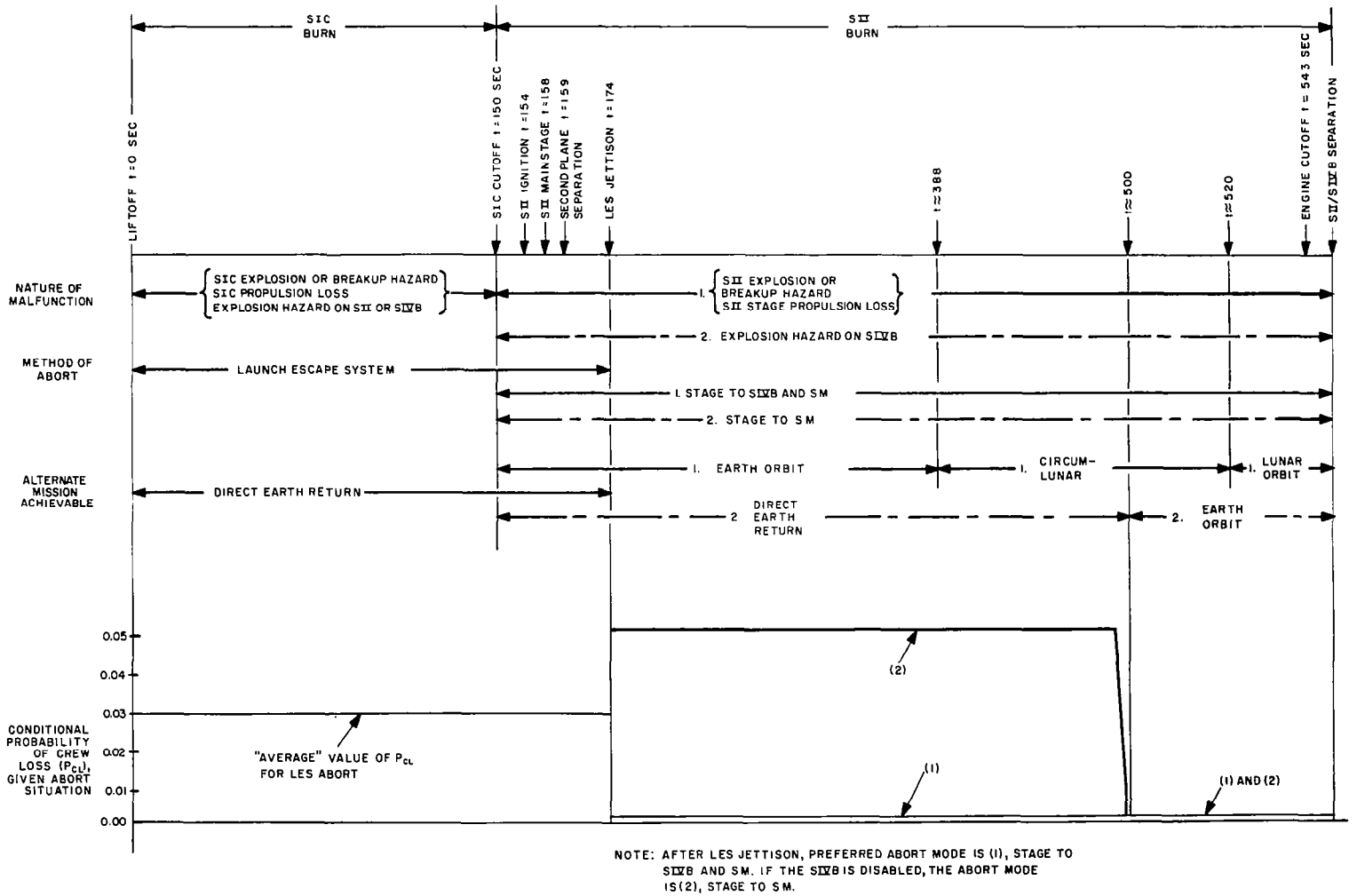

NOTE: AFTER LES JETTISON, PREFERRED ABORT MODE IS (1), STAGE TO S IV B AND SM. IF THE S IV B IS DISABLED, THE ABORT MODE IS (2), STAGE TO SM.

FIGURE 3-1. SIC, SII STAGE ABORT AND CREW RISK MODEL

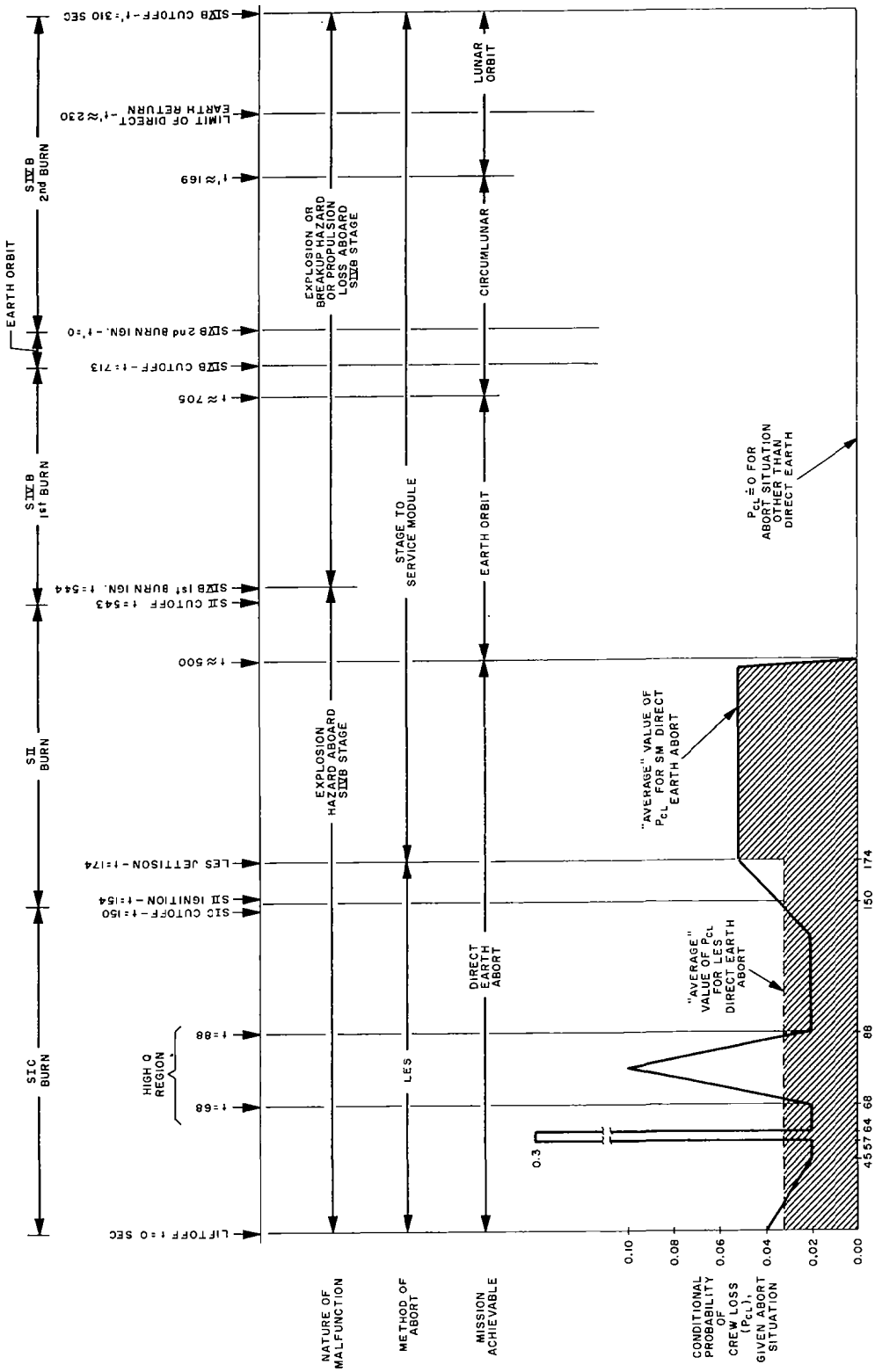

FIGURE 3-2. SIVB ABORT AND CREW RISK MODEL

upon the vehicle unreliability and the surrounding environment. A safe escape will lead to one of two situations:

- An abort mode in which an earth or lunar orbit is achievable
- An abort mode which results in a direct earth return.

A sharp distinction can be drawn between these two situations so far as crew risk is concerned. In the former case, assuming a safe escape has already occurred, the risk to the crew is essentially the same as would exist during a normal boost. Once earth orbit is achieved, the crew is afforded the opportunity to maximize mission value by choosing an alternate mission or, if this is not possible, to descend to earth at a preferred landing site.

If, on the other hand, the abort results in a direct return to earth, the probability of safe crew return is substantially reduced. In order to assign crew risk values during abort for the purpose of READI system evaluation, the following ground rules have been established:

- For an abort which permits an earth or lunar orbit to be achieved, no increase in crew risk over that normally encountered is incurred.
- For an abort which results in a direct earth return, an additional crew risk is assigned.

3.3.2 DIRECT EARTH ABORT

The additional crew risk incurred during a direct earth abort is determined primarily by the time during the flight profile at which the abort takes place. The SIC and SII Abort and Crew Risk Model, figure 3-1, shows that a direct earth return may be required any time after launch up to approximately 500 seconds. For the interval between SIC ignition and 174 seconds after liftoff, the LES is used for direct earth abort. This interval contains several periods which are especially critical for abort because of the surrounding environment, as indicated below.

3.3.2.1 Liftoff and Shortly Afterwards - Assuming there is sufficient lead time to effect a safe escape, an abort during this period is still subjected to the following hazardous conditions:

- Unsuccessful separation due to vehicle or LES collision with launch umbilical tower.
- Minimum altitude (4000 ft) required for parachute deployment not attained by LES.
- Proper orientation of Command Module (CM) not achieved because of drogue parachute assembly failure.

3.3.2.2 Maximum Dynamic Pressure (Max Q) and Transonic Regions - The greatest hazard during the Max Q period is the possibility of exceeding the structural limits of the LES or the spacecraft itself due to excessive angle of attack. During the relatively short transonic period the acceleration of the launch vehicle exceeds that of the LES, and SIC engine shutdown is mandatory.

3.3.2.3 High Altitude Region - During this period the normal abort hazards are increased due to the high velocity already achieved, crew acceleration limits, and spacecraft heating considerations. A further hazard results from having to

recover the spacecraft several hundred miles downrange in a non-preferred landing area.

During these high risk periods, the probability of crew loss is greater than it would be for a "normal" LES abort. This is indicated by figures 3-1 and 3-2, where the conditional probability of crew loss (P_{CL}) is plotted as a function of flight time. The value of P_{CL} for an LES abort during a non-critical period is taken as 0.02. It should be kept in mind that the value is conditional upon an abort situation, which has a relatively low probability of occurrence, and on successful escape. The average value of P_{CL} for a direct earth abort using the LES is seen to be about 0.03. This average value is used in the effectiveness evaluation when the abort causing malfunction occurs with equal probability throughout the time interval.

After the LES is jettisoned, the SM is used for a direct earth return. Following a safe escape, this abort mode is subjected to the following hazards:

- Crew accelerations and spacecraft heating
- Stability and control of the CM
- Unplanned landing site up to thousands of miles downrange.

Immediately following LES jettison, the conditional probability of crew loss, P_{CL} resulting from a SM abort is essentially the same as that which existed just before LES jettison. At approximately 500 seconds after launch, P_{CL} decreases to zero, since earth orbit is achievable. Between these two limits P_{CL} is assumed to remain constant. The increase in velocity and range to landing site due to longer flight times is offset by the extra time available for crew control of the CM. The value of P_{CL} for SM abort is shown on the Abort and Crew Risk Models, figures 3-1 and 3-2.

3.4 ESCAPE MODEL

3.4.1 INTRODUCTION

The purpose of this subsection is to illustrate several of the approaches which may be used in the development of escape models, and to provide an insight into some of the factors which must be taken into consideration. The primary objective of the models is to provide a measure of the warning, or lead time, required to safely escape from a hazardous condition aboard a launch vehicle. This information can then be applied to an evaluation of READI system effectiveness, by comparing the lead time required for escape with READI's capability to detect a hazardous condition and initiate an abort.

So far as most vehicles including Saturn V are concerned, the escape problem can be divided into atmospheric and exo-atmospheric conditions. In the following paragraphs escape models are discussed for several representative types of hazardous conditions. These models are by no means inclusive, and the analysis is not strictly rigorous. They are presented simply as examples of the type of work which must be carried out for the particular situation under investigation.

3.4.2 ATMOSPHERIC ESCAPE (SIC BOOST)

3.4.2.1 General - It is assumed for the purpose of the model that escape during SIC boost will be accomplished using the LES. Although it may be possible to shut

down engines prematurely and stage to SII late in the boost, this method of abort will not be considered at this time. The two conditions requiring an escape attempt which were investigated are the following:

- Imminent explosion hazard
- Imminent vehicle break-up due to loss of thrust vector control.

3.4.2.2 Explosion Hazard - A "safe escape" from an explosion hazard means that the crew and spacecraft have been removed sufficiently far from the center of the explosion to avoid any of its harmful effects. In many respects the explosion due to the propellants aboard Saturn V may be likened to a TNT explosion. Because of these similarities, and because of the lack of specific data on propellant explosions, TNT equivalencies have been used in the explosion hazard analysis.

Of the several effects produced by an explosion, including fireball, debris, etc., the one which is of primary concern is the accompanying blast (or shock) wave. It is generally accepted that an overpressure of about 5 psi is the maximum which can be withstood by a structure such as the CM[3]. Therefore, the LES must have sufficient warning time to accelerate and outdistance the shock wave as it travels outward from the center of the explosion. The required warning time can be determined from a comparison of the distance-versus-time plots of the LES and the shock wave for a given set of conditions.

For the purpose of the model, the following assumptions were made:

(1) An explosion aboard Saturn V will encompass the fuel aboard all three stages. This assumption effectively sets up a "worst case" condition.

(2) The equivalent TNT yield of SIC propellant (RP-1) is taken as 10 percent, the equivalent TNT yields of SII and SIVB propellant (LOX, LH_2) is assumed to be 60 percent.[3]

(3) Using the above, the explosive yield prior to liftoff is equivalent to about 0.56 kiloton of TNT, centered at a point approximately 150 feet below the LES.

The path of the shock wave due to an explosion with the equivalent TNT yield of (3) above is shown in figure 3-3.[4] It can be seen that an overpressure of 5 psi extends to a distance of over 1200 feet and arrives at that point approximately 0.65 second after the explosion has occurred. The LES flight path is also shown on figure 3-3. It is evident that a lead time of about 2.5 seconds is needed if the LES is to escape the 5 psi overpressure shock wave caused by an explosion on the launch pad. The time required for the LES engine to reach 90-percent thrust after the abort command has been initiated (reaction time) is assumed to be 200 milliseconds. The READI system will make a decision to abort within a negligible time (about 10 milliseconds) after sensing the malfunction. The LES flight path is approximate, being calculated simply from the expression:

$$d = d_o + 1/2 \ \frac{Tg}{W} t^2$$

- - - - - - -

(3)Refer to reference 3, Appendix C.

- - - - - - -

(4)Refer to reference 4, Appendix C.

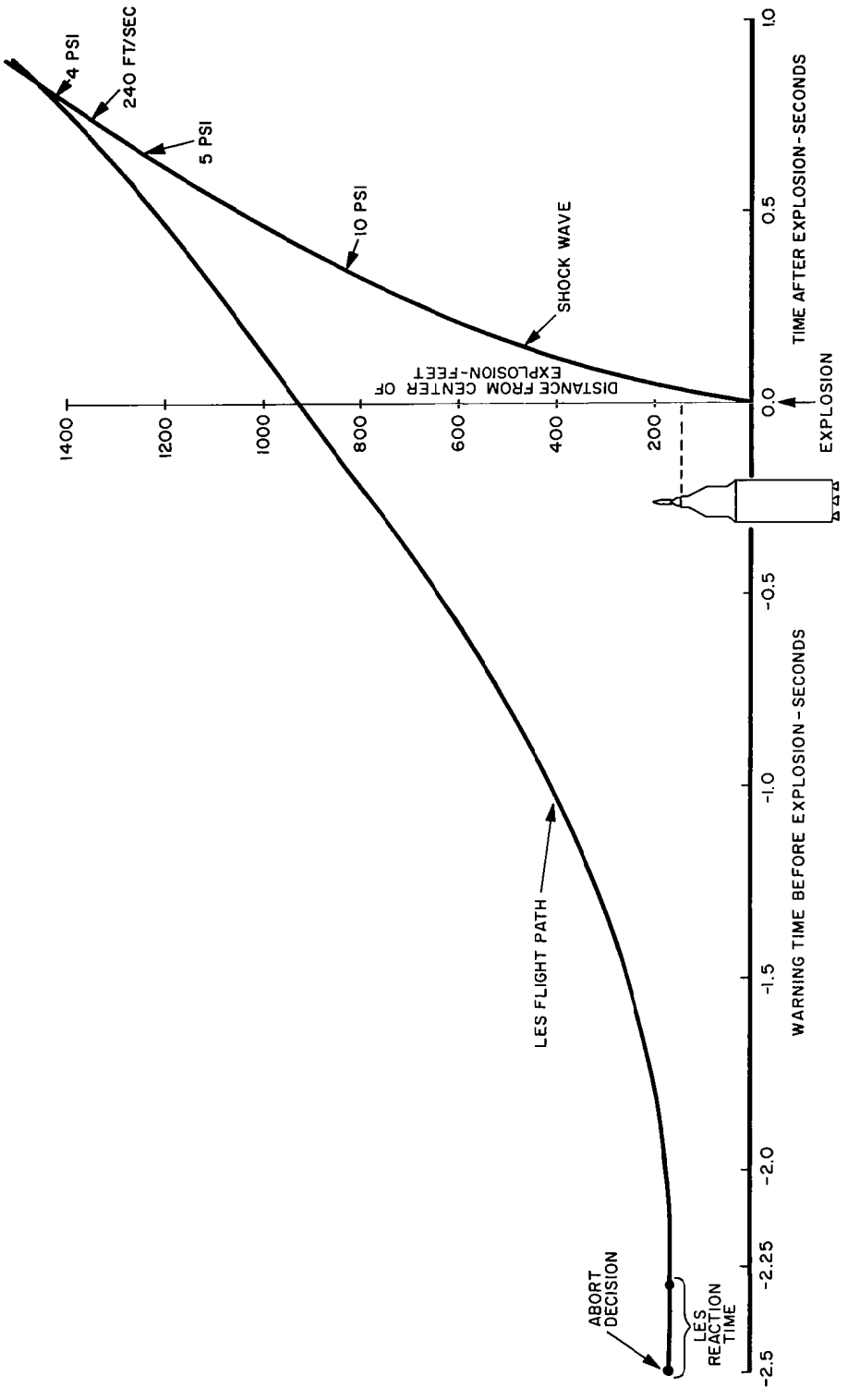

FIGURE 3-3. LES ESCAPE FROM SATURN V
EXPLOSION ON PAD

where

d = straight line distance from the center of the explosion

d_o = initial separation (150 feet)

t = time after 90% thrust is reached

g = gravitational constant

W = weight of the LES, CM, and crew, assumed to be 16,700 lbs

T = thrust of LES motor, assumed to average 155,000 lbs for the first 1.5 seconds of burn, 65,700 lbs for the remaining 6.5 seconds.

The effect of gravity was neglected because of the extremely high thrust-to-weight ratio of the LES.

Figure 3-3 shows that a lead time of 2.5 seconds is required to escape from an explosion on the launch pad. This lead time is reduced if the explosion occurs some time after launch, so that the chance of escaping the overpressure hazard is increased. However, this does not necessarily mean that the probability of crew survival is greater, since other factors such as vehicle stability and orientation must be taken into account.

As the flight time of the vehicle increases, several factors act to reduce the blast hazard from which the spacecraft must escape. The most obvious is that the potential explosive yield is being reduced as the propellants are consumed. A second factor is that the altitude of the vehicle is continually increasing. The resulting decrease in ambient pressure effectively reduces the range to which the critical 5 psi overpressure extends. Another effect of increased altitude is to reduce the velocity of the shock wave front, thereby increasing the arrival time of the damaging overpressure. A third factor which aids the escape from an explosion is the increase in vehicle velocity after launch. If it is assumed that the exploding mass and the resulting shock wave have no forward velocity at the instant of detonation, the LES will be moving away from the explosion with the velocity it had attained the instant before detonation. (This of course requires separation prior to the explosion.) At some point in time after launch, the vehicle velocity will equal the velocity of the expanding shock wave, and will therefore remain safely ahead of it.

The results of the above discussion are summarized in figure 3-4, which shows the decrease in lead time required for safe escape as a function of increasing flight time. The minimum value of warning time is seen to be 0.8 second, which is the time required to separate and accelerate the LES so that a 50-foot separation "safety factor" exists between the LES and the Saturn V vehicle at the instant of explosion.

3.4.2.3 Vehicle Breakup - In the example discussed below, vehicle breakup is considered to be the result of a four engine hardover condition during SIC boost. Although the probability of occurrence of such a malfunction is admittedly small, it is worthy of consideration because of the ensuing catastrophic-type failure. The four engine hardover condition could be caused by a saturated error signal from either a rate gyro, control accelerometer, or attitude control signal. It is the intent of this discussion to determine the lead time required to escape from such a

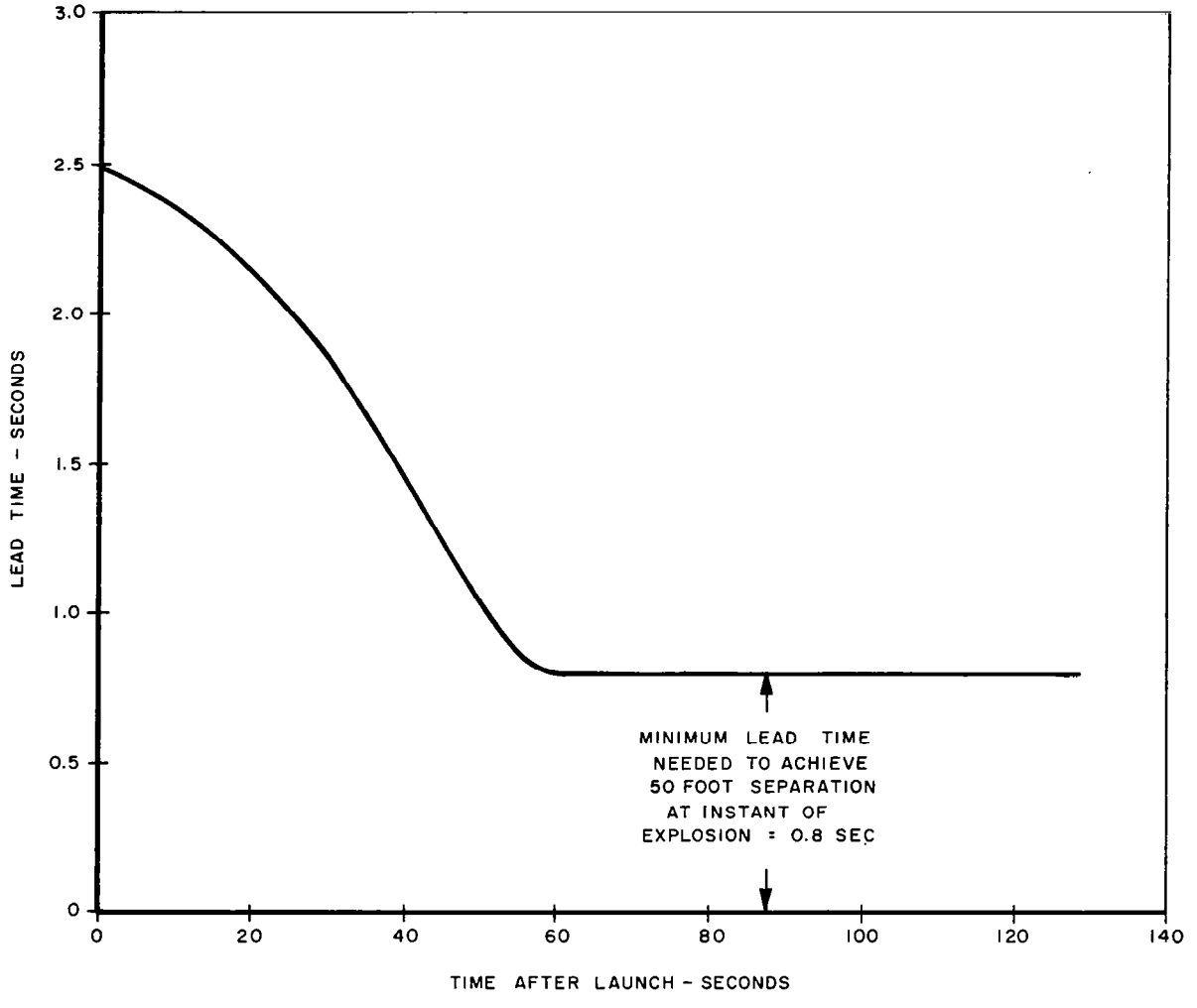

FIGURE 3-4. LEAD TIME REQUIRED FOR SAFE LES ESCAPE FROM EXPLOSION

condition, and to investigate methods of increasing the margin of safety.

A study of the Saturn V vehicle dynamics following a four engine hardover malfunction indicates an extremely rapid divergence of attitude rate and angle of attack. This is illustrated by figure 3-5, in which engine deflection angle (β), pitch rate ($\dot{\phi}$), and angle of attack (α) are plotted as a function of time following the malfunction. For illustrative purposes, the time of occurrence of the malfunction was chosen to be about 78 seconds after launch. Since the vehicle is passing through the region of maximum dynamic pressure (Max Q) at this time, a worst case condition is established so far as the structural limits of the vehicle are concerned. For the purpose of constructing the model, the maximum allowable angle of attack in the Max Q region is taken as 10 degrees; this value of α is based on the NASA Crew Safety Panel studies[3] and other documentation.[2]

The warning time available for escape depends upon the method used to sense the effects of the four engine hardover malfunction. One method of accomplishing this might be measurements of the engine deflection angle, β, and its derivative. As shown by figure 3-5, these quantities could be measured accurately within a very short time of the malfunction. (It should be noted at this point that although the malfunction occurs at $t = 0$, the engine gimbal system has an inherent time lag of about 100 milliseconds due to fluid compressibility.) This method of detecting the hardover condition could provide a warning time of approximately 0.7 second before the critical angle of attack is exceeded. This warning time is reduced to about 0.5 second if the pitch angle rate is used as an indication of the malfunction, and further reduced to 0.13 second if an angle of attack sensor is employed.

It is evident that, regardless of the quantity being sensed, the red-line limits of the malfunction detector must be set above the normal operating range of the variable in order to reduce the possibility of a false alarm. However, the longer one waits to insure that the four engine hardover condition actually exists, the shorter the warning time becomes. Thus, tradeoffs must be made between the time available for an escape attempt and the probability of a false alarm. It should be noted that the false alarm probability can be reduced substantially by the judicious use of signal and information redundancy. Also, processing circuitry can be used to filter out the effects produced by non-hazardous transient conditions.

One of the possible remedial actions which READI might take in the event of a four engine hardover condition would be to shut down all engines and initiate abort. In order to evaluate the effectiveness of various READI detection techniques and decisions, it is necessary to establish a relationship between SIC engine shut down and the resulting increase in warning time. Referring to figure 3-5, it may be seen that, following a hardover signal, the engine deflection angle (β) increases to its limit of 5 degrees at the rate of 10 degrees/second. This of course applies a continually increasing turning moment to the vehicle, as shown by the dashed line of figure 3-6. This moment can be reduced and consequently the turning rate of the

(2) and (3) Refer to references 2 and 3, Appendix C.

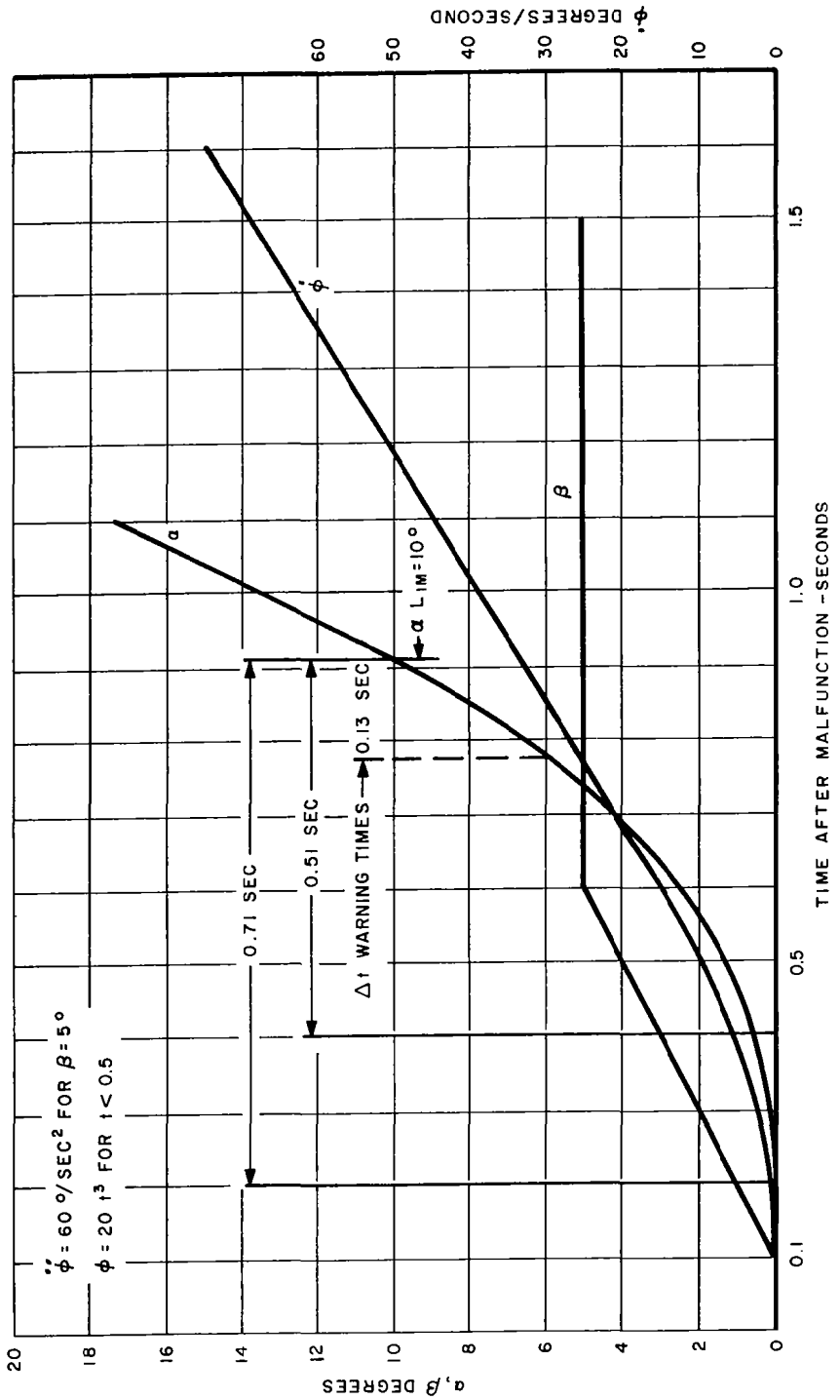

FIGURE 3-5. SATURN V VEHICLE CHARACTERISTICS FOLLOWING 4-ENGINE HARDOVER AT MAXIMUM Q

vehicle lessened, by shutting down the engines. Curve A on figure 3-6 shows the decrease in the moment if the engine cutoff command is given 0.6 second after the malfunction has occurred. The shape of this curve is essentially the F-1 engine thrust decay characteristic. By reducing the delay time between the occurrence of the malfunction and the engine cutoff command, the curves of B, C, and D result. Curve D indicates a delay of zero time. Although this is not physically realizable, it may be possible to initiate engine cutoff with very little delay. As mentioned previously, the cause of the four engine hardover malfunction is electrical in nature. Therefore, it may be possible to sense the saturated gyro or accelerometer error signal directly rather than waiting to detect its effect on pitch rate or angle of attack.

The areas under the curves of figure 3-6 are proportional to the integrated moment acting to turn the vehicle and increase the angle of attack. As the area decreases, a longer time is required to reach the critical value of α, thereby increasing the available lead time. This is shown by the curves of figure 3-7, in which the helpful results of engine shutdown are clearly evident. If the hardover condition can be detected almost immediately and the engines shut down, several seconds are available for escape before the critical angle of attack is reached. As the delay time for engine shutdown increases, the available warning time decreases accordingly. If it is assumed that an explosion occurs at the instant of breakup, then the maximum delay which could be tolerated in shutting down the engines is about 0.3 second. This would provide a warning time of approximately 0.8 second, which is the minimum required to escape from an explosion.

3.4.3 EXO-ATMOSPHERIC ESCAPE

The escape model is significantly affected by the different conditions which exist during atmospheric and exo-atmospheric flight. It is instructive to examine some of these differences briefly at the outset. One of the more important factors is that the LES is jettisoned early during exo-atmospheric flight, and therefore is not available for use as an escape vehicle. As a result, escape during most of the SII boost, for example, must be accomplished by staging to either the SIVB or the SM. Unlike escape with the LES, staging requires engine shutdown and separation before the engines of the SIVB or SM can be ignited. This will be discussed more fully in the following paragraphs.

A second important difference is that once the vehicle is "outside" the atmosphere (above 150,000 ft), the very low air density precludes the propagation of a shock wave. Therefore, the danger of a damaging overpressure exists only in the immediate vicinity of the explosion. Because of the lower air density, the thermal energy which is radiated is deposited over a much larger volume than would be the case had the explosion occurred in the atmosphere. As a result, the hazard due to destructive fireball temperatures can be neglected a short distance from the explosion.

A third distinction between atmospheric and exo-atmospheric escape conditions is that once outside the atmosphere,

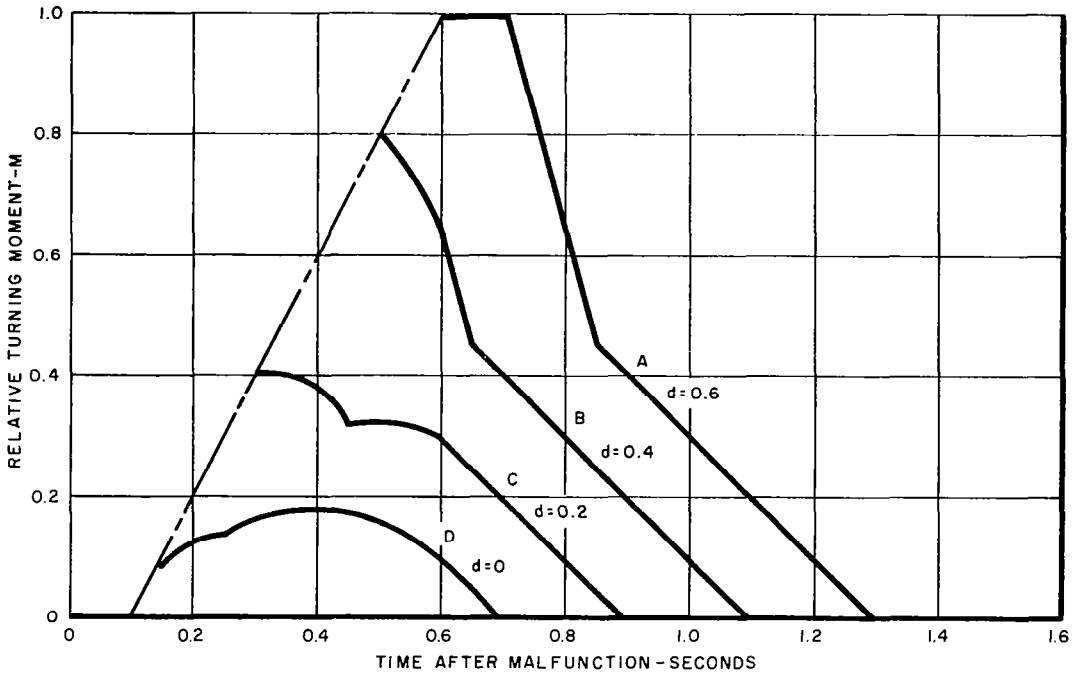

FIGURE 3-6. RELATIVE TURNING MOMENT FOLLOWING 4-ENGINE HARDOVER AND ENGINE SHUTDOWN AT MAXIMUM Q

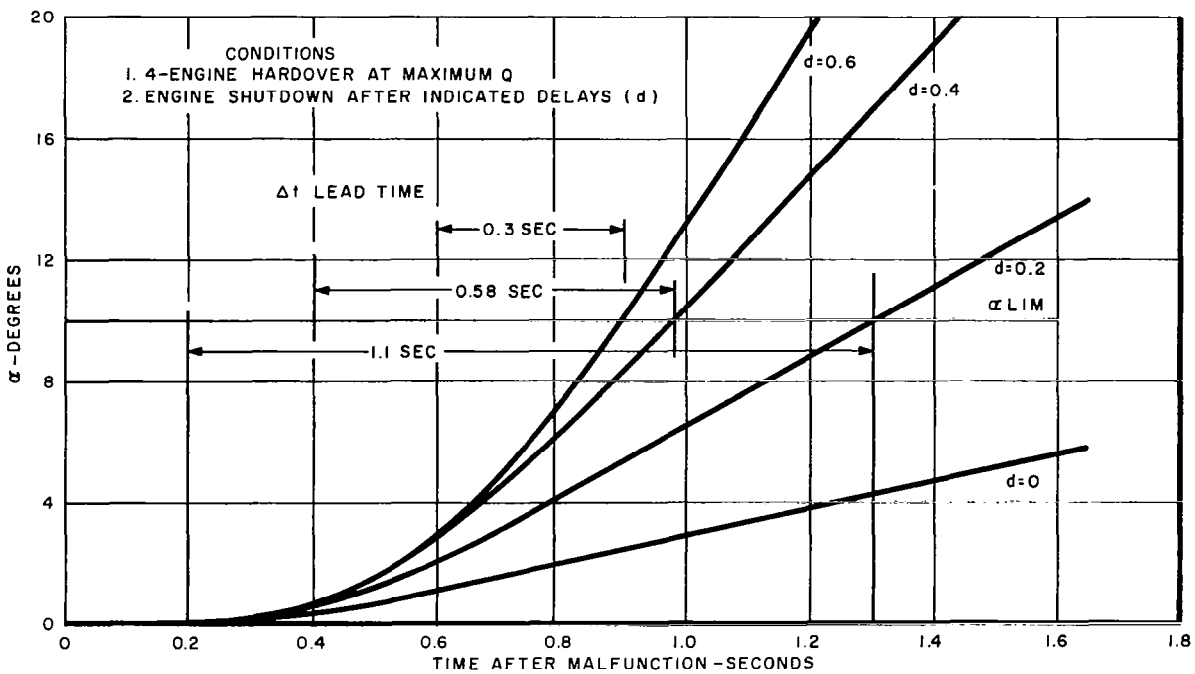

FIGURE 3-7. LEAD TIMES PRIOR TO REACHING CRITICAL ANGLE OF ATTACK

the vehicle is not subjected to such high dynamic pressures, so that the danger of structural breakup is reduced.

From the above, the following criterion may be established to define safe escape under exo-atmospheric conditions. If, at the instant of catastrophic failure, the escape vehicle has separated a distance of 100 feet from the boost stage, a high probability of successful escape exists. The value of 100 feet is somewhat arbitrary, and was chosen primarily for the purpose of illustrating the Escape Model. Having established the above criterion, the required lead times may be determined, using escape during SII boost as an example.

Figure 3-8 shows the normal SII and SIVB separation sequence which was used in construction of the model. It can be seen that a delay of about 1.3 seconds exists between the abort decision and the SIVB engine start signal. A straight line approximation was used to represent the J-2 engine thrust buildup characteristic. For the first second after the start signal no appreciable thrust is generated. During the next 2.5 seconds the thrust increases linearly to the rated value. Since virtually no thrust is produced for the first second following the start signal, a delay of 2.3 seconds exists during which there is no separation of escape vehicle and booster except for that produced by ullage and retrorocket firing. The buildup of separation distance following J-2 engine ignition is shown in figure 3-9. The figure shows that nearly four seconds have elapsed before the J-2 engine reaches mainstage, at that point more than five seconds are required to achieve a separation of 100 feet. The escape path using the SM as the escape vehicle is also shown on figure 3-9. Although the SM engine reaches full thrust within 100 milliseconds of the start signal, the lower thrust-to-weight ratio prevents much of a reduction in the required warning time.

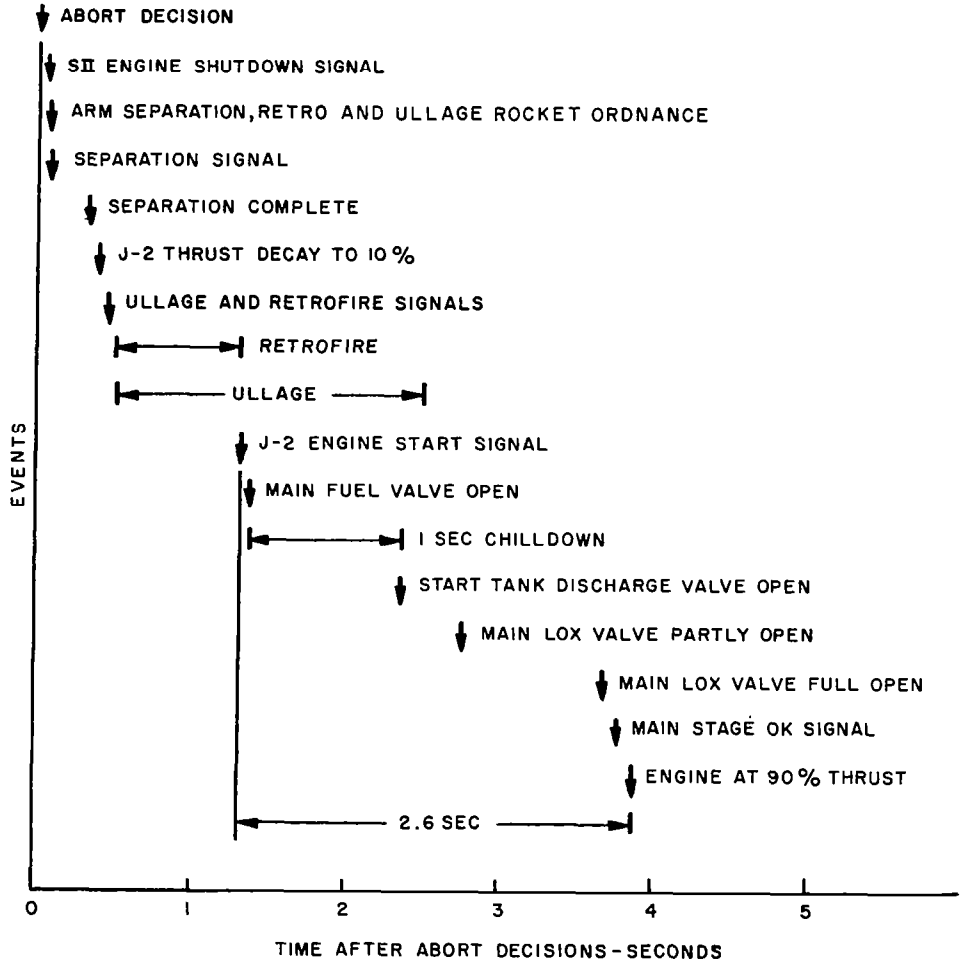

FIGURE 3-8. SII/SIVB SEPARATION SEQUENCE

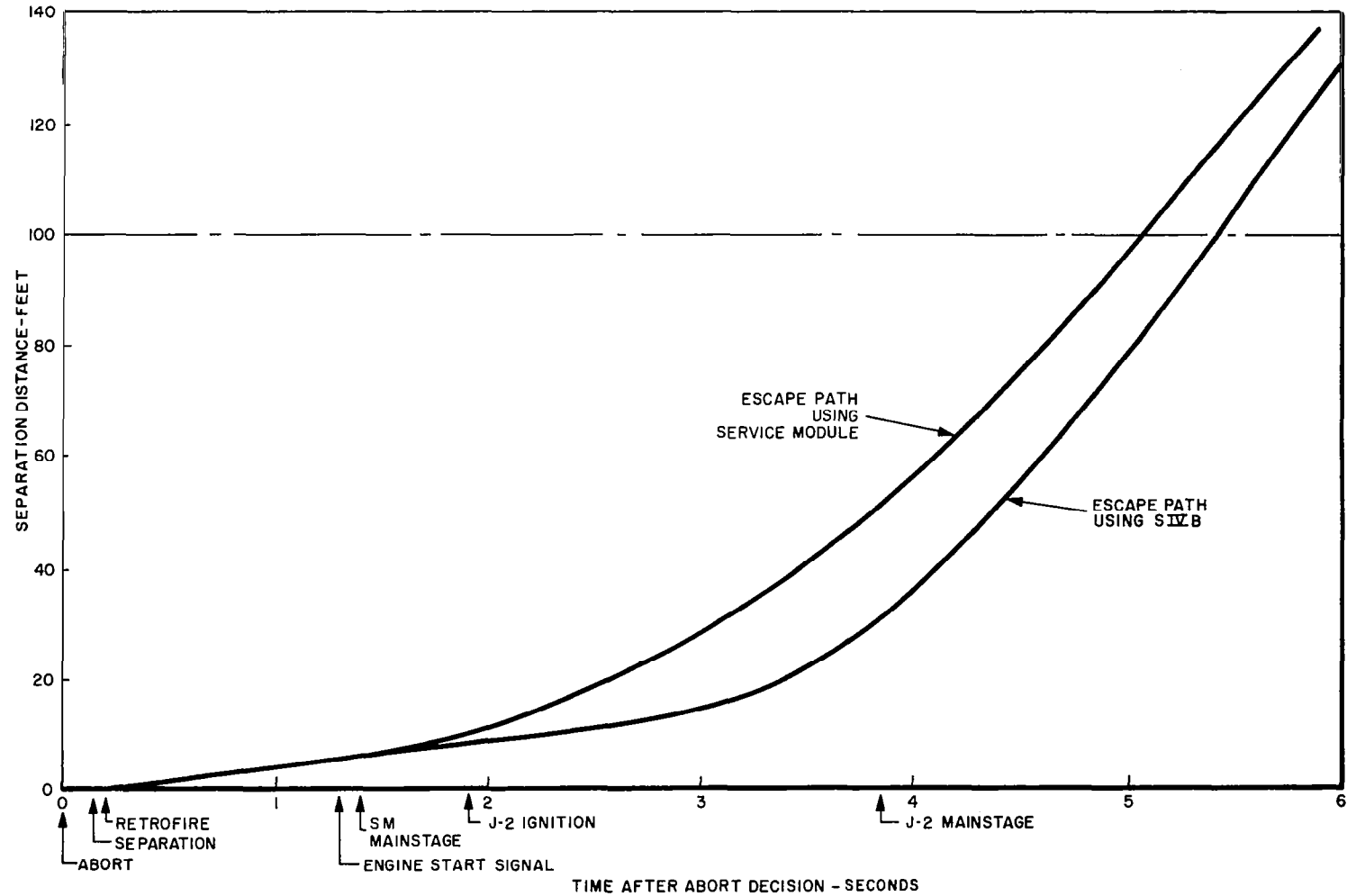

FIGURE 3-9. ESCAPE DURING SII BOOST

SECTION IV

STAGE PERFORMANCE DEGRADATION MODELS

4.1 INTRODUCTION AND SUMMARY

As discussed in subsection 2.3, alternate mission capability, of Section II, non-catastrophic propulsion failures may result in degraded but useful mission performance. The propulsion failure effects can be related to mission performance through a set of performance curves or "maps". Typically, one set of performance curves is developed for each stage of a multistage vehicle. These curves are plots of one specific performance parameter versus time-of-occurence of the given malfunction. The performance model serves to convert the various failure effects into equivalent variations of the basic parameter. For this study, the normalized usable residual propellant in 100 nm orbit (M_{PRN}) was taken as the basic parameter. The performance models can, therefore, be used in conjunction with figure 2-2, which shows the alternate mission capability as a function of M_{PRN}. The effect of various malfunctions upon stage performance is summarized by the stage performance maps, figure 4-1 and figures 4-3 through 4-7.

The three stages of the Saturn V vehicle present the same problems, with varying degrees of complexity, to the development of Stage Performance Degradation Models. This makes the Saturn V particularly amenable to model solution, since a single approach can be developed and then modified and expanded, where necessary, to account for the problems of the individual stages. This method will become evident in the following subsections.

4.2 SIVB STAGE PERFORMANCE DEGRADATION

The SIVB flight takes place outside the atmosphere in near-orbital conditions. Because of this, it was possible to use a simplified set of equations to represent the SIVB flight path and to determine the effect of various malfunctions upon the residual propellant in 100 nm orbit. Unlike the SII and SIC performance degradation models, the equations used in the SIVB model do not require iterative integration techniques for their solution when malfunction disturbances are introduced. The normalization processes used in the model development tended to cancel the majority of error introduced by the simplifying assumptions, since the value of normal residual propellant was calculated using the same techniques and assumptions.

Since the SIVB flight is exo-atmospheric and nearly horizontal (assuming nominal SIC and SII boost), the gravity component loss was neglected and the single ΔV relation shown below was used to describe the flight characteristics of interest:

$$\Delta V = Vex \, \ell n \left[\frac{M_o}{M_f} \right] \quad \dagger$$

- - - - - - -

† See Appendix B for an explanation of terms.

The use of this simplified equation yields an error of about 5 percent over the full SIVB trajectory, compared to the nominal trajectory computed by NASA.(5) This error is partially compensated for by using the same relation for normal as well as malfunction computations, and by dividing to obtain the desired ratio of M_{PR} to M_{PRN}.

The following three types of malfunctions were investigated using the SIVB model to determine their effect upon the residual propellant in 100 nm orbit:

(1) Engine out during second burn

(2) Propellant utilization system locked at ± 10 percent

  (a) During first and second burn

  (b) During second burn only

*(3) Leaks (oxidizer or fuel) - 3%, 12%, 36% of normal tankage flow

  (a) From launch to start of first burn

  (b) During first burn

  (c) During second burn.

The effects of these malfunctions are shown in figure 4-1, SIVB Performance Maps, where the time-of-occurrence of the malfunction is plotted against M_{PR} and M_{PRN}, the ratio of the residual propellant under malfunction conditions to the normal residual propellant. As an example, consider the effect of a 12-percent oxidizer leak which occurs halfway through first burn. The performance map shows that the residual propellant M_{PR} available in 100 nm orbit will be 91 percent of the normal value. An examination of figure 2-2, Alternate Mission Capability, indicates that although the prime mission is not achievable under these conditions, a lunar orbit mission can be accomplished. This example illustrates how the Stage Performance and Mission Models are used to relate the effect of a specific malfunction to a relative mission loss value to be used in READI evaluation.

Since the malfunctions under consideration fall into three different time periods - launch to first burn, first burn, and second burn, the basic ΔV equation for the SIVB stage was modified accordingly. The equations and definitions of the terms used in them are presented in Appendix B.

4.3 SII STAGE PERFORMANCE DEGRADATION MODEL

The SII Performance Degradation Model is comprised of a set of integral equations of motion, together with mass flow and control equations. These equations are integrated by a simple stepwise iteration technique, with the appropriate malfunction effects being introduced at the selected time of occurrence, t*. The performance data for the SII (and SIC) stage was obtained from a computer simulation of the stage dynamics described by the equation set. The flow chart used for the computer program is shown in figure 4-2. The program itself was run on a UNIVAC 1107.®

The SII equations are integrated from the nominal starting conditions of altitude (H_o), altitude rate ($\dot{H}_o$), and velocity ($V\psi_o$) which correspond to the nominal SIC cutoff conditions, until either fuel or oxidizer depletion is achieved. The

- - - - - - - -

(5) Refer to reference 5, Appendix C.

*The leak is assumed to be trivial during the orbital coast period. If this is not the case, M_{PRN} is zero for all leaks greater than 2.0 percent.

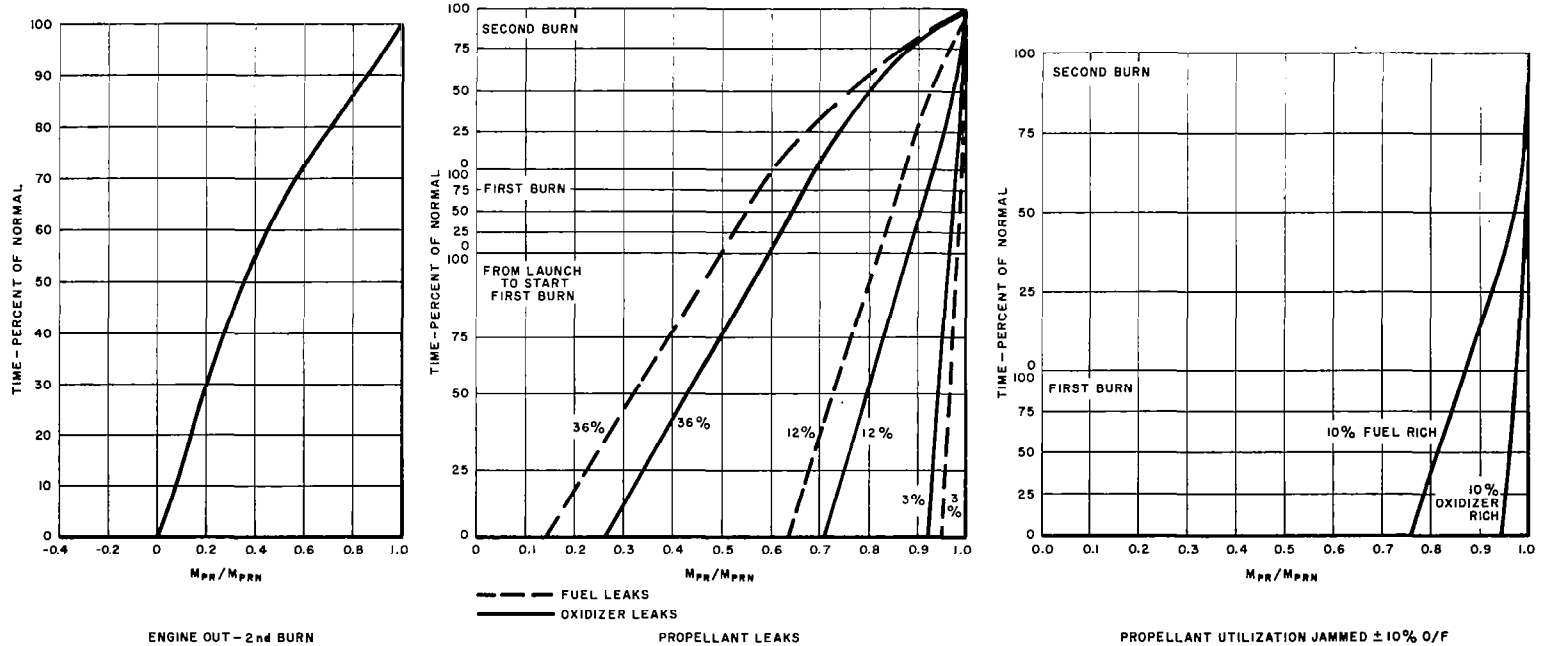

FIGURE 4-1. S IVB PERFORMANCE MAPS

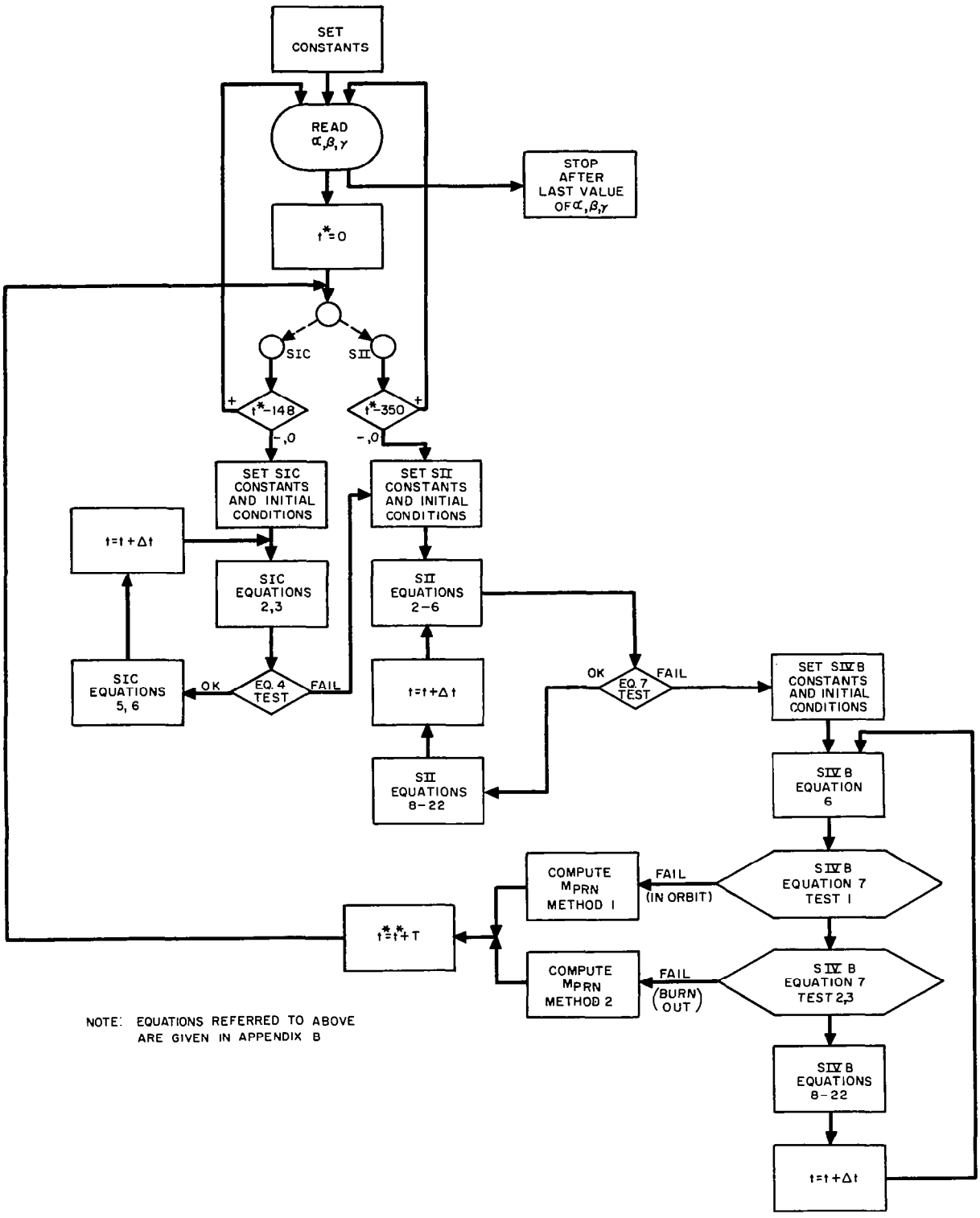

FIGURE 4-2. FLOW CHART OF SII, SIC PERFORMANCE DATA COMPUTATION

program then "stages" to SIVB, using the end points of SII as the initial conditions, and integrates the SIVB equations until either orbital velocity or propellant depletion is reached. The residual propellant so obtained is then divided by the nominal value of propellant in orbit (obtained from a similar integration process, with no failure in SII) to derive M_{PR}/M_{PRN}.

In order to obtain sufficient data points for curve plotting, the equations were solved for the malfunction occurring at 40-second intervals. A four-second iteration interval was used.

The SII equation set contains an approximation to the propellant utilization system. The SII stage is biased oxidizer rich at the start to obtain a high thrust condition at the beginning of stage burn. The propellant utilization equations act to maintain a high oxidizer/fuel (O/F) ratio in order to reduce the oxidizer bias and achieve the nominal O/F ratio required for simultaneous propellant depletion. At some point during stage burn this ratio is attained, resulting in a high specific impulse condition until the end of the burn. The guidance program is an heuristic approximation to the normal trajectory. The main approximation is that the program tries to attain the normal altitude-time trajectory at the expense of the velocity-time trajectory.

For the purpose of the model, the effect of a malfunction such as leakage in the lox bootstrap line, for example, is expressed in terms of changes to three basic parameters:

- Change in oxidizer flow (α)
- Change in fuel flow (β)
- Change in thrust (γ).

The magnitude of the changes to these parameters is based upon the results of the J-2 engine analog computer simulation studies which are described in detail in Section V of this report. Thus, the performance characteristics of the SII stage were investigated for parameter variations which represent realistic malfunctions having a relatively high probability of occurrence. The combinations of parameter variations utilized in the SII stage computer program are given in table 4-1.

Table 4-1. SII PERFORMANCE DEGRADATION INPUT DATA

Run No.	Effect of Malfunction	Change in Oxidizer Flow (α)	Change in Fuel Flow (β)	Change in Thrust (γ)
1	1 engine out	-0.2	-0.2	-0.2
2	45% loss in fuel turbopump efficiency	-0.02	-0.08	-0.05
3	35% loss in engine thrust	-0.07	-0.07	-0.07
4	50% engine leak (fuel)	0	+0.1	0

Table 4-1. SII PERFORMANCE DEGRADATION INPUT DATA (Cont)

Run No.	Effect of Malfunction	Change in Oxidizer Flow (α)	Change in Fuel Flow (β)	Change in Thrust (γ)
5	50% engine leak (oxidizer)	+0.1	0	0
6	20% engine leak (oxidizer)	+0.04	0	0
7	20% engine leak (fuel)	0	+0.04	0
8	15% loss in engine thrust	0	0	-0.03

The results of the computer runs are plotted on the SII Performance Maps, figures 4-3 and 4-4. For reference, the fraction of normal residual propellant needed to achieve prime mission is indicated. This can be used as a measure of the relative sensitivity of stage performance to different combinations of parameter variations.

The equations and terms used in the SII Stage Performance Model are included in Appendix B.

4.4 SIC STAGE PERFORMANCE DEGRADATION MODEL

The SIC Performance Degradation Model is a modification of the one used for the SII stage. Since the SIC trajectory is almost completely within the atmosphere, an extensive section has been added to compute approximations to the drag terms and the variation of thrust with altitude. A fairly simple exponential relation was used for thrust variation which gives a good match to the F-1 thrust-time curve for normal flight. Some form of hold or delay on the turning rate was required for longer-than-normal SIC burns (1 engine out) to prevent complete turnover. A proportional angular rate guidance technique was used which slows the turning rate proportional to variations in the predicted burn time, which in turn is computed from the remaining propellant mass. The propellant utilization system approximation is not carried over from SII, since this type of system is not used by the SIC stage.

Malfunctions were entered into the model by the same three parameters (α, β, γ) as were used in SII. Data points were taken for malfunctions introduced during successive runs at 24-second intervals after launch. The computation technique for deriving M_{PRN} is the same as used in SII, but at the end of SIC burn (propellant depletion), a malfunction-free run is made on the SII and SIVB stages to obtain the residual propellant in orbit. The end point of the malfunctioned SIC burn is taken as the starting point of the SII burn, that is,

$$\dot{H}o_{SII} = \dot{H}co_{SIC}$$

$$Ho_{SII} = Hco_{SIC}$$

$$V_{o_{SII}} = V_{co_{SIC}}$$

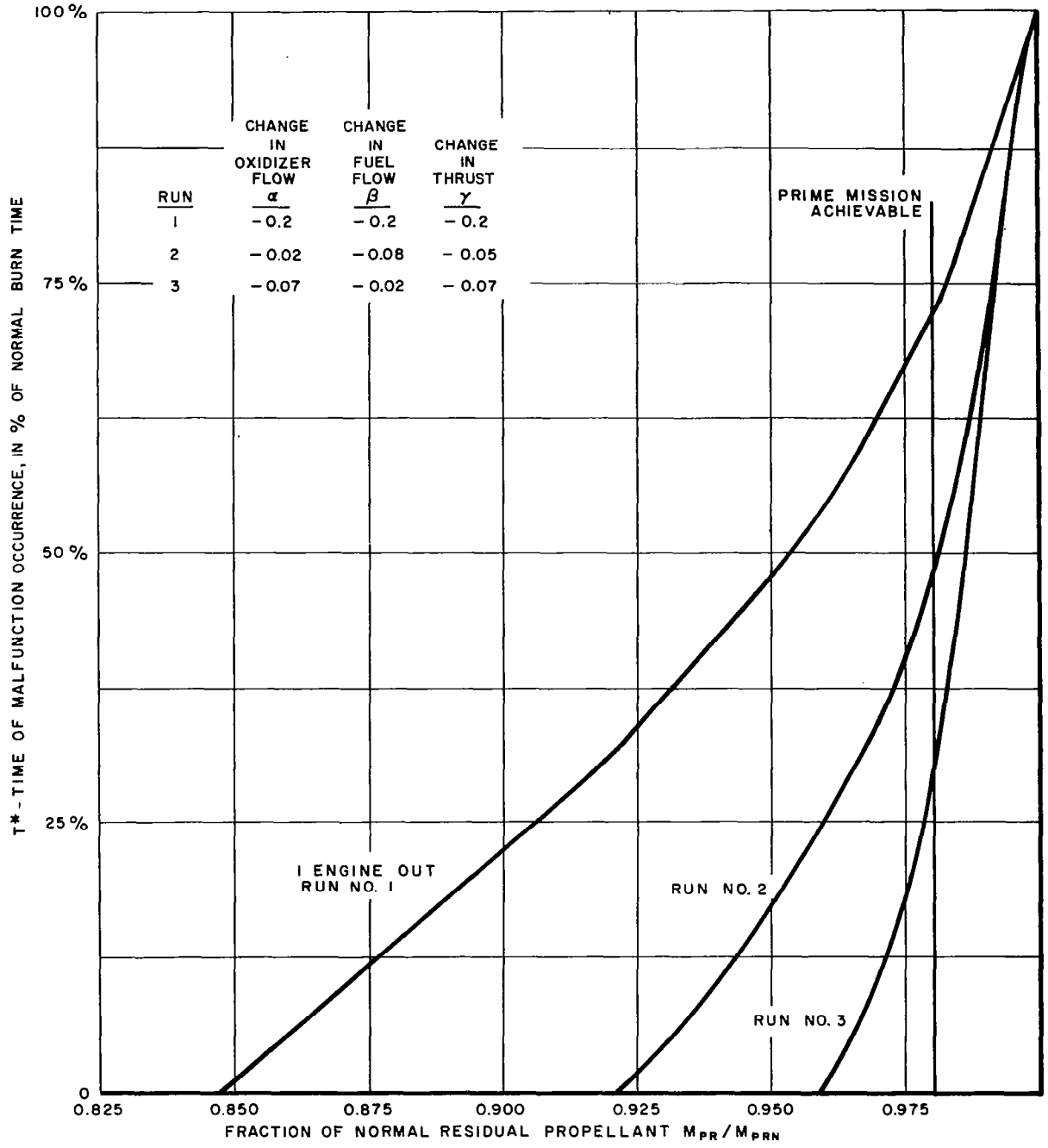

FIGURE 4-3. S II PERFORMANCE MAP
FOR COMPUTER RUNS 1-3

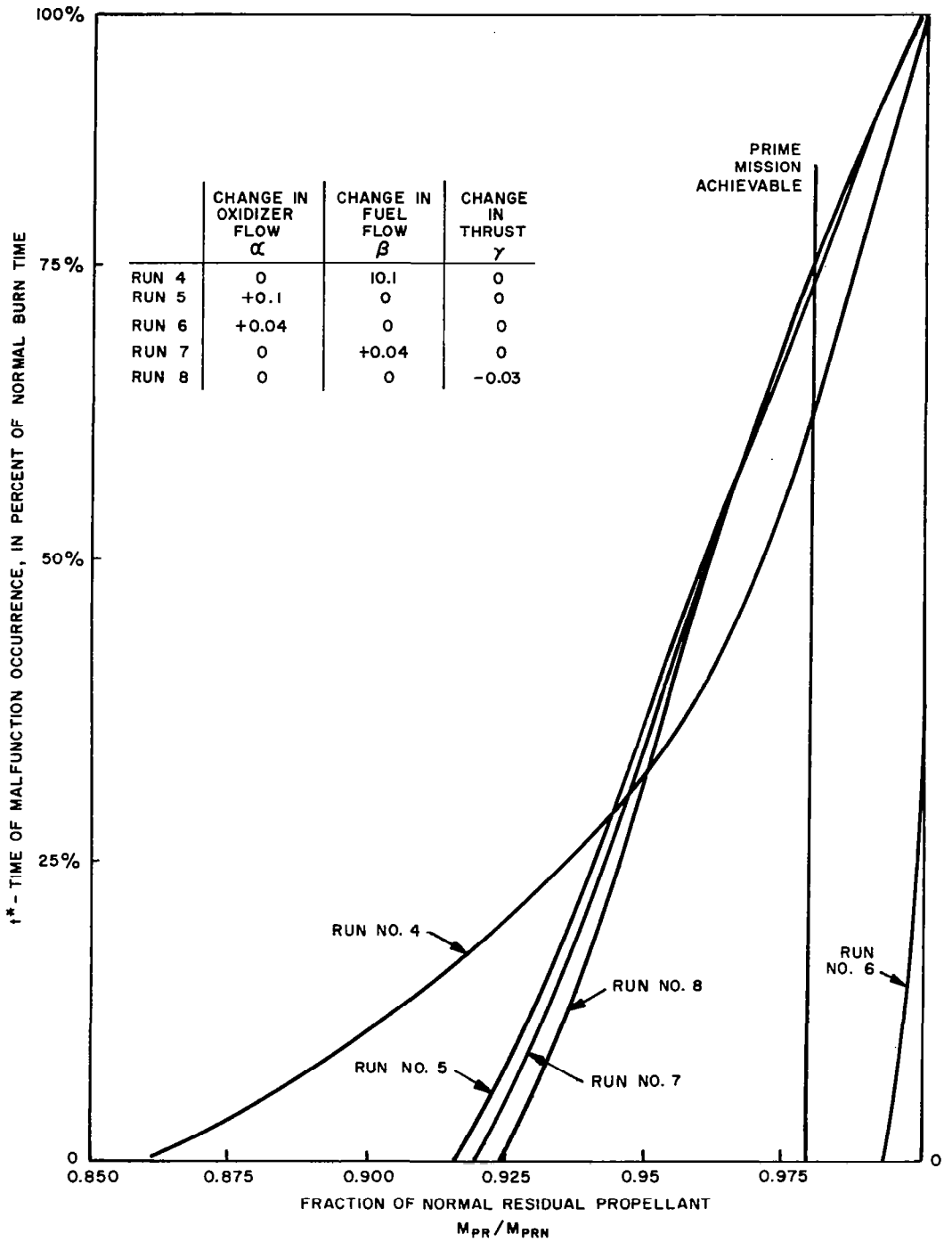

FIGURE 4-4. SII PERFORMANCE MAP FOR COMPUTER RUNS 4-8

where

Aco_{SIC} = cutoff value of variable A from SIC

Ao_{SII} = starting value of variable A for SII.

The input data set used with this model is given in table 4-2.

Table 4-2. SIC PERFORMANCE INPUT DATA SET

Run No.	Effect of Malfunction	Change in Oxidizer Flow (α)	Change in Fuel Flow (β)	Change in Thrust (γ)
1	1/2 engine out	-0.1	-0.1	-0.1
2	1 engine out	-0.2	-0.2	-0.2
3	2 engines out	-0.4	-0.4	-0.4
4	50% engine leak (ox)	+0.1	0	0
5	25% engine leak (ox)	+0.05	0	0
6	50% engine leak (fuel)	0	+0.1	0
7	25% engine leak (fuel)	0	+0.05	0
8	50% engine thrust loss	0	0	-0.1
9	25% engine thrust loss	0	0	-0.05

The effect of these malfunctions upon the SIC stage performance is summarized in the Stage Performance Maps. Figure 4-5 shows the effect on M_{PR} of various engine out conditions. Figure 4-6 indicates how M_{PR} is affected by different propellant leaks, and figure 4-7 relates thrust losses to M_{PR}. The equations used in the SIC Stage Performance Model are given in Appendix B.

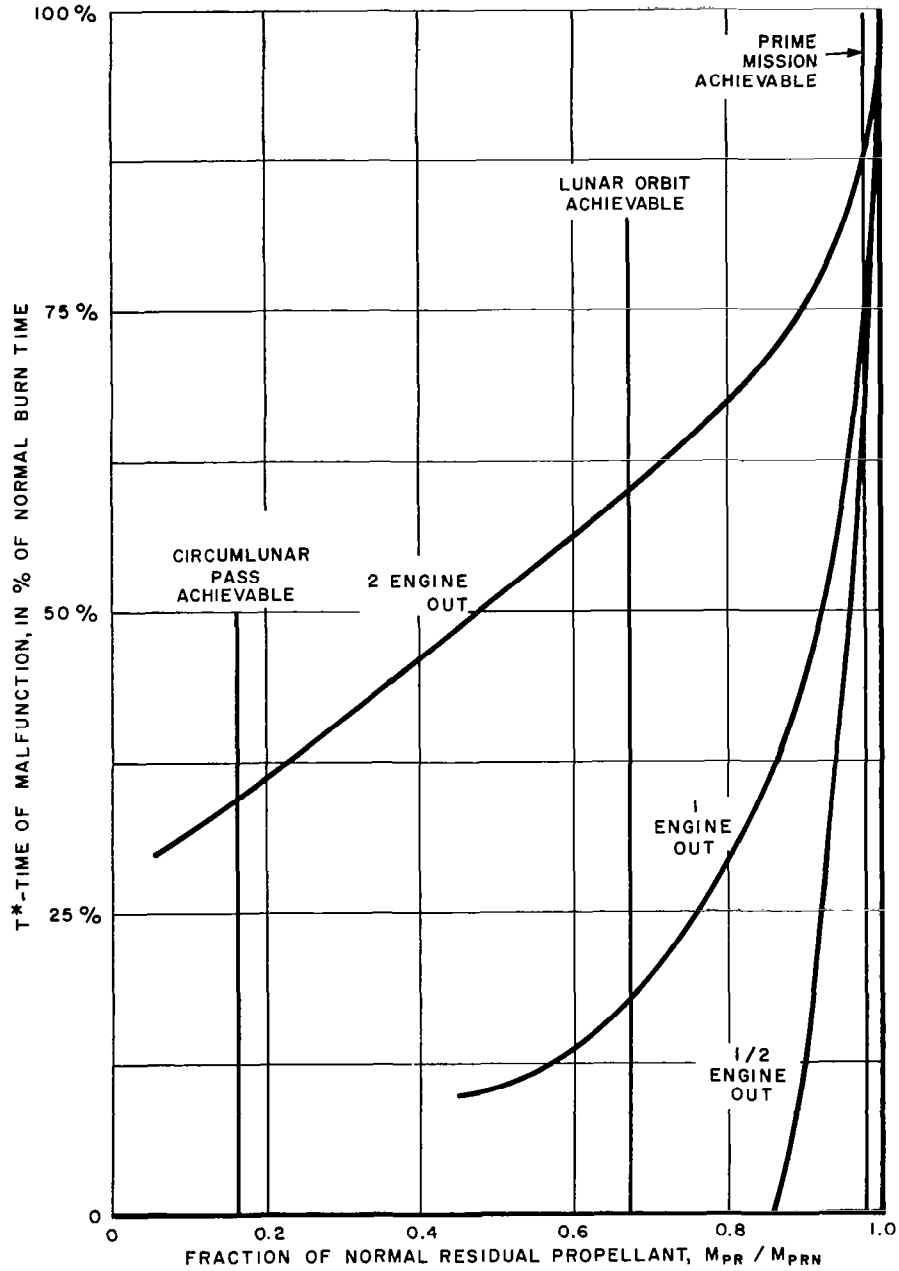

FIGURE 4-5. TIME OF MALFUNCTION VERSUS PERFORMANCE FOR SIC (THEORETICAL ENGINE OUT CAPABILITY)

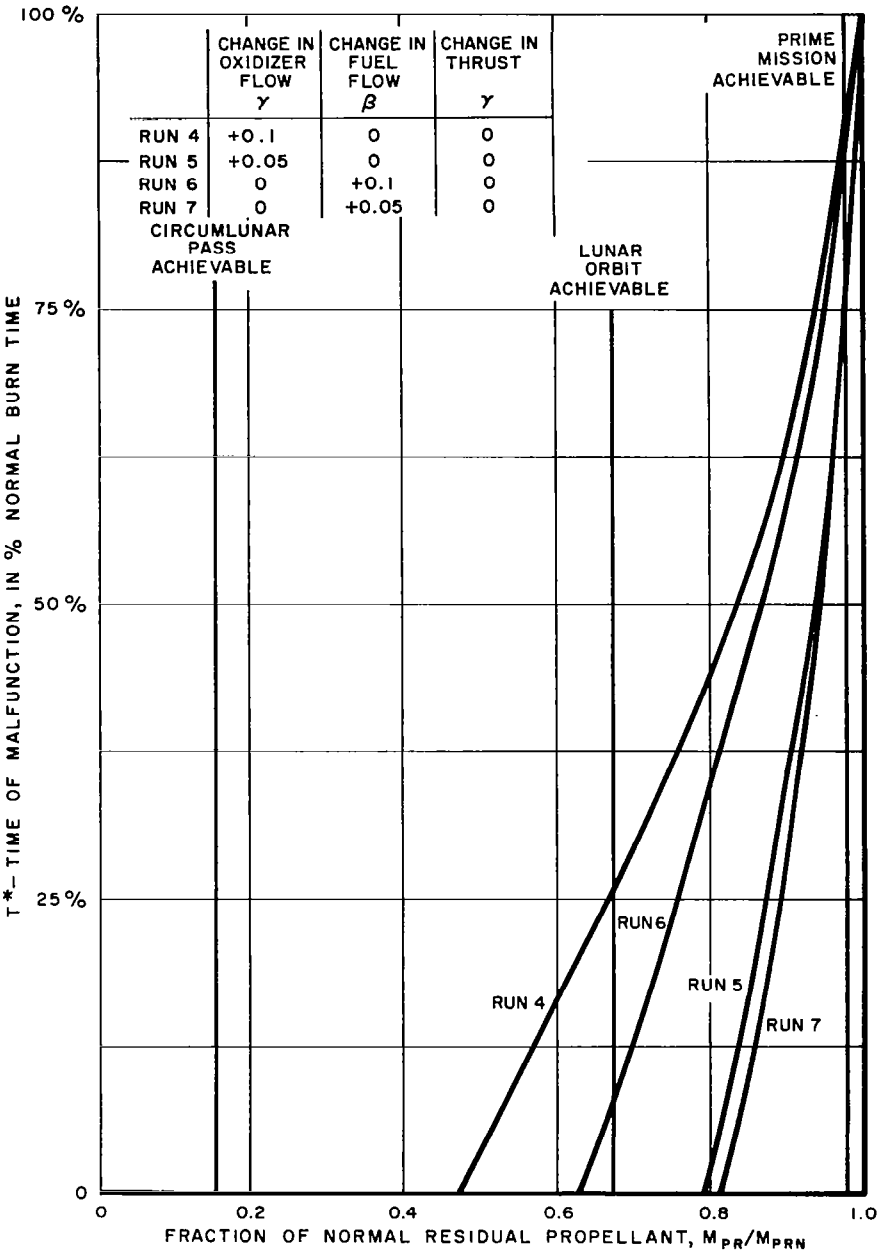

FIGURE 4-6. TIME OF MALFUNCTION VERSUS PERFORMANCE FOR SIC (PROPELLANT LEAKS)

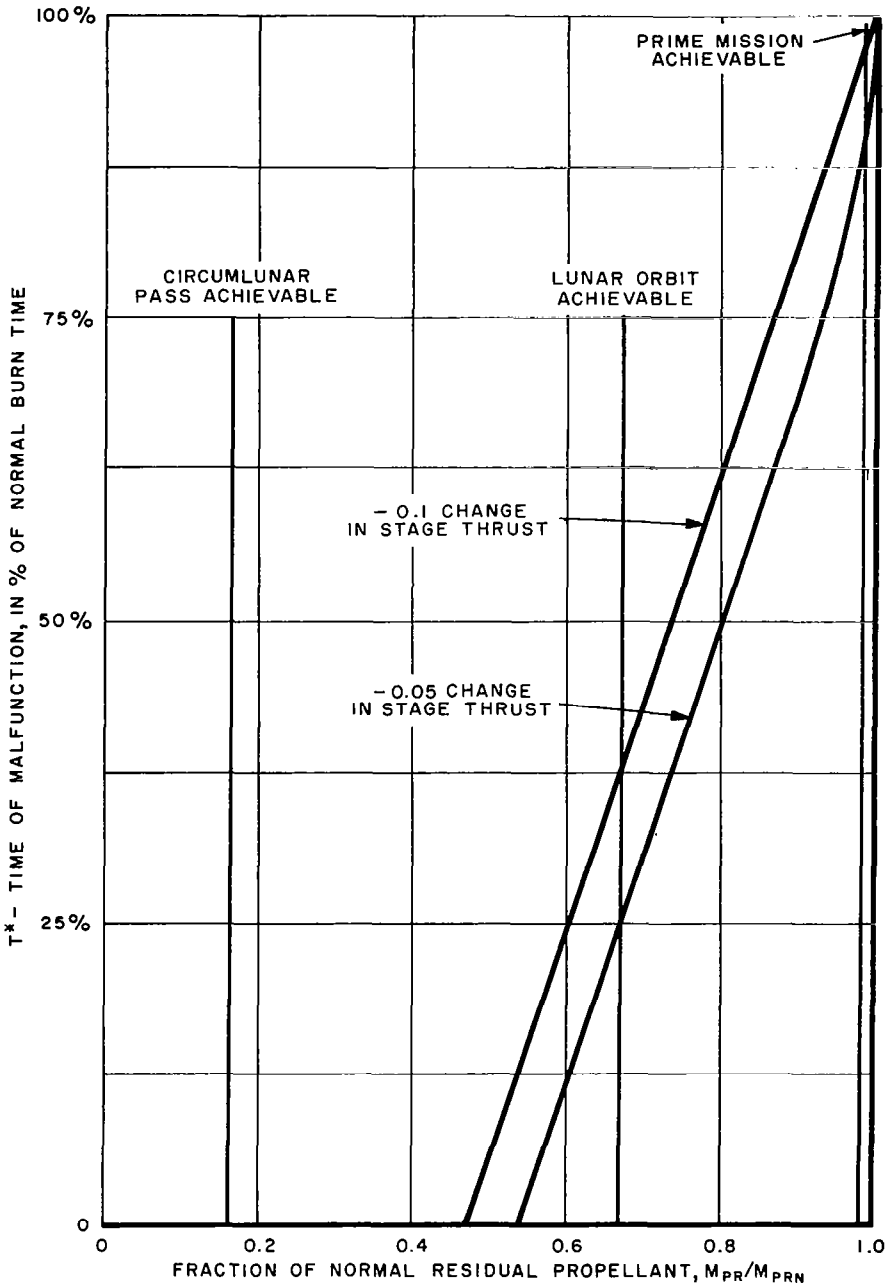

NOTE:
NO CHANGE IN OXIDIZER OR FUEL FLOW OCCURS

FIGURE 4-7. TIME OF MALFUNCTION VERSUS PERFORMANCE FOR SIC (THRUST LOSS)

SECTION V

ENGINE AND SUBSYSTEM MALFUNCTION MODEL

5.1 INTRODUCTION AND SUMMARY

There are several Saturn V vehicle subsystems that are of interest to this READI investigation. The J-2 engine was selected as the most appropriate of these for intensive study and development of a malfunction model. This choice was based upon two primary factors:

- Relative complexity of S-2 engine as compared to other subsystem: The J-2 engine is employed in both SII and SIVB stages. Although the basic engine is the same, there are variations in interface and environmental details that affect the READI system design. In addition, the engine restart requirement in the SIVB stage contributes additional failure modes and increases overall criticality.
- Availability of mathematical model: The development of a dynamic model of the J-2 engine was in progress by the Propulsion and Vehicle Engineering Laboratory of the George C. Marshall Space Flight Center. Modification of this model, which was designed for analog computer simulation, permitted study of both transient and steady-state malfunctions in considerable depth.

This section contains details of the dynamic model and discusses the results of an extensive analog computer simulation program that was undertaken to evaluate the utility of this type of model to the READI design procedure. The analog computer simulation approach was chosen because the engine mathematical model is too complex for rigorous theoretical analyses of malfunctions.

The results of this analog computer simulation program have been of great value in the following areas of interest:

- Determination of the effects of steady-state malfunctions on mission model input variables
- Study of remedial actions for steady-state and transient malfunctions
- Investigation of malfunction detection methods
- Evaluation of stochastic variations in parameters.

5.2 J-2 ENGINE MODEL

The mathematical model of the J-2 engine that is described here was used for analog computer simulation of malfunction effects and remedies. It was developed by the Marshall Space Flight Center for studies of the J-2 engine start transient and has been modified to permit its use for malfunction analysis. Figure 5-1 is a simplified engine schematic diagram that shows the relationship of the engine components that are represented by the model. It also shows the locations of the various types of leaks that are included in the subsequent discussion of steady-state malfunctions.

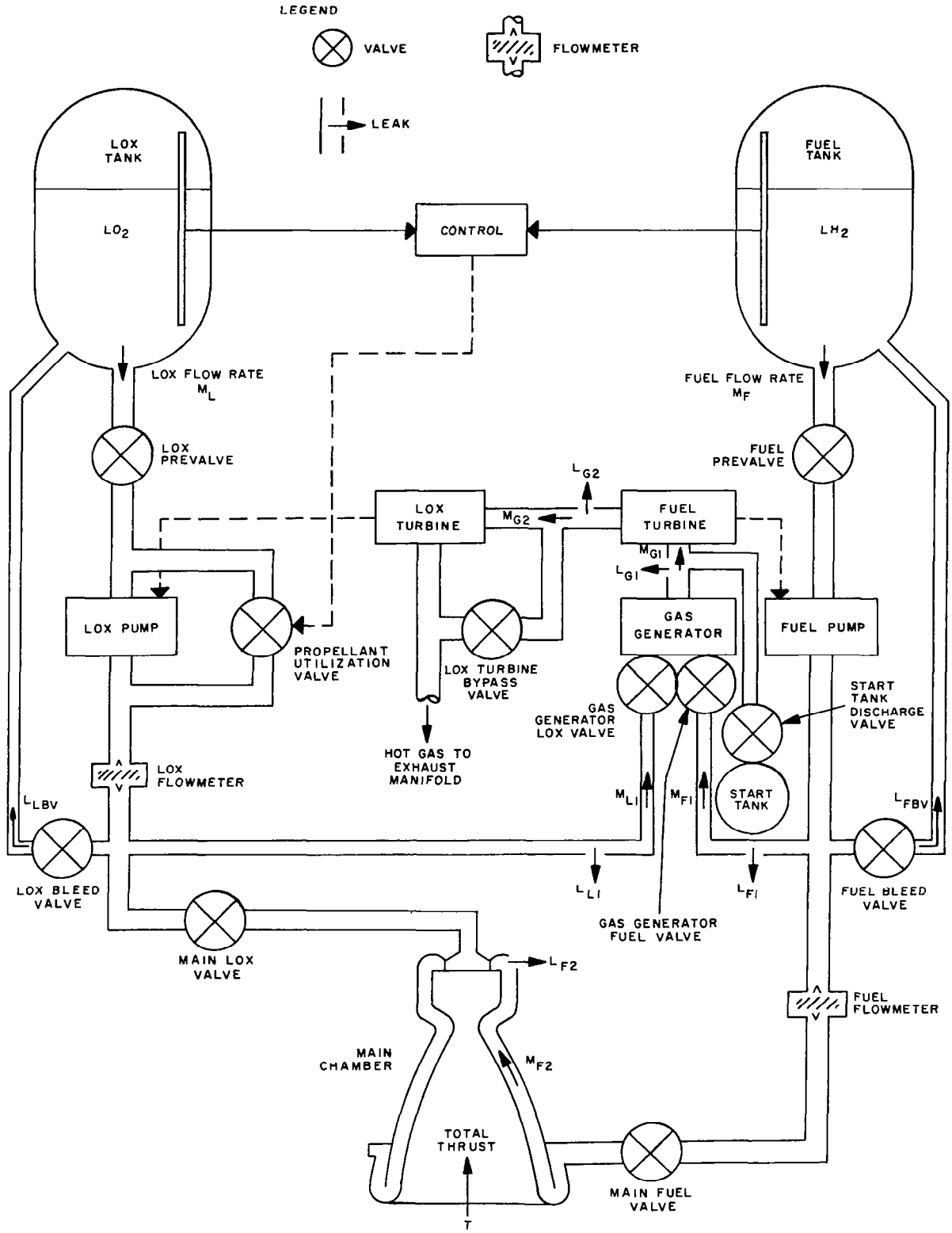

FIGURE 5-1. SIMPLIFIED ENGINE SCHEMATIC DIAGRAM

The complete set of model equations and functions is contained in Appendix A. This model defines the dynamic behavior of the propellant pressures and flow rates and the turbopump speeds as functions of the engine valve positions and propellant tank pressures. Valve control and vehicle dynamics are not included in the model. In the simulation work, the engine valve positions were treated as arbitrary functions of time. Propellant tank pressures and temperatures were assumed to be constant. Figure A-2 of Appendix A shows what was considered to be the normal valve operation sequence.

The modifications that were introduced into the original start transient model have been chiefly concerned with improving the capability of simulating off-nominal conditions. These modifications have included such items as low O/F mixture ratio limits on gas generator ignition and combustion, the alternative methods of computing turbine flows and the inclusion of the propellant prevalves in the shutdown sequence. It was, of course, also necessary to use various methods of introducing the perturbing malfunctions into the model. These can generally be categorized as liquid leaks, gas leaks, decreased pump efficiencies, or discrete changes in the valve sequences.

There are limitations associated with this model, chiefly stemming from the fact that it was developed to approximate the performance of a normal engine. In principle, the constant coefficients of the model could be replaced by nonlinear functions wherever necessary for simulation of off-design operation. In practice, lack of test data for these conditions has rendered this impractical.

5.3 STEADY-STATE MALFUNCTION EFFECTS

The effects of various steady-state malfunctions on engine performance were studied in order to determine values of engine performance degradation parameters that should be used as inputs for the Stage Performance Degradation Model discussed in Section IV. The general procedure was to introduce a malfunction of variable magnitude into the engine simulation and increase its size until some critical effect was produced. Steady-state engine performance was recorded for several malfunction amplitudes. From these data, the performance degradation parameters corresponding to the critical level of the malfunction were computed.

The performance degradation is expressed by a set of three normalized parameters, which represent changes in propellant consumption and thrust; these parameters are defined as follows:

$$\alpha = \frac{\text{Net change in oxidizer flow}}{\text{Normal oxidizer flow}}$$

$$\beta = \frac{\text{Net change in fuel flow}}{\text{Normal fuel flow}}$$

$$\gamma = \frac{\text{Change in thrust}}{\text{Normal thrust}}, \text{ which is}$$

$$\approx \frac{\text{Change in main chamber pressure}}{\text{Normal main chamber pressure}}$$

The malfunctions that were examined are tabulated in table 5-1, which shows the critical size of the malfunction, the nature of the critical effect and the values of the three performance parameters that correspond to the critical size.

Table 5-1. STEADY-STATE MALFUNCTION EFFECTS

Malfunction	Figure	Critical Size	Critical Effect	Performance Parameters for Malfunction of Critical Size		
				α (Lox Flow)	β (Fuel Flow)	γ (Thrust)
Lox Turbopump; Loss of Efficiency	5-2	$\Delta\eta_L = 0.54\ \eta_L$	Low gas generator mixture ratio	-0.495	+0.040	-0.392
Fuel Turbopump; Loss of Efficiency	5-3	$\Delta\eta_F = 0.302\ \eta_F$	High gas generator temperature and fuel pump stall	-0.080	-0.360	-0.195
Lox Bleed Valve Leakage to Lox Tank	5-4	No critical effects for maximum flow through valve.	-	-	-	-
Fuel Bleed Valve Leakage to Fuel Tank	5-5	$L_{FBv} = 0.415\ M_F$	High gas generator temperature	-0.078	-0.370	-0.195
Lox Bootstrap Line Leakage	5-6	$L_{L1} = 1.07\ M_{L1}$	Low gas generator mixture ratio	-0.025	-0.030	-0.035
Fuel Bootstrap Line Leakage	5-7	$L_{F1} = 1.42\ M_{F1}$	High gas generator temperature	-0.065	-0.065	-0.085
Gaseous Fuel Leakage from Injector Manifold	5-8	$L_{F2} = 0.395\ M_{F2}$	High main chamber mixture ratio	-0.030	+0.025	-0.165
Hot Gas Leakage from Gas Generator	5-9	$L_{G1} = 0.54\ M_{G1}$	Fuel pump stall	-0.380	-0.420	-0.400
Hot Gas Leakage from Manifold between Turbines	5-10	$L_{G2} = 0.47\ M_{G2}$	Low gas generator mixture ratio	-0.490	+0.035	-0.400

Two general types of malfunctions are included. One type is a loss of turbopump efficiency, which might be due to increased axial loads resulting from abnormal balance-cavity pressures. In these cases, the critical sizes are expressed as functions of the normal turbopump efficiencies. The second type of malfunction is leakage from the various locations indicated in figure 5-1. Here, the critical sizes are expressed as functions of the normal flows through the ducts or lines from which the leakage emanates. Table 5-1 also indicates a reference illustration, figures 5-2 through 5-10, for each malfunction. These illustrations show the variation of the three performance parameters and the critical variable for each malfunction.

In figures 5-4 and 5-5, which show the effects of lox and fuel bleed valve leakage, the leakage size corresponding to full valve opening is indicated. In figure 5-10, which shows the effects of hot gas leakage from the manifold that connects the fuel turbine exhaust with the lox turbine inlet, the leakage equivalent to a fully opened lox turbine bypass valve is noted.

5.4 REMEDIAL ACTION DEVELOPMENT

The analog simulation of the engine was employed in studying remedial actions for various types of malfunctions. A number of these are listed in table 5-2, with comments on the effectiveness of the attempted action. For the most part, this group of malfunctions is composed of various valve failures, and the appropriate remedies consist of modifying the operation of other valves in order to mitigate the effects of the malfunction. In the case of fuel pump stall, the requirement is to anticipate the malfunction and take action to avoid it. Since this is primarily a measurement problem, it is discussed in greater detail in subsection 5.5 Malfunction Detection Techniques. Figure 5-11 illustrates the effectiveness of the remedial action.

In table 5-2, the critical effects noted for starting with either the lox or fuel bleed valves open do not include the probable structural failure of the recirculation lines that lead back to the tanks (in the SII and SIVB stages of the Saturn V), due to exposing them to abnormally high pressures. These lines were excluded from the engine model since they are part of the stage. Any remedial actions considered for these malfunctions must take the structural considerations into account.

Table 5-2 is not, of course, a complete listing of all the engine malfunctions for which remedial actions are available, but includes those cases where the simulation of the engine dynamics was of importance in evaluating the effects of the remedies.

5.5 MALFUNCTION DETECTION TECHNIQUES

The analog simulation of the engine has been used to considerable advantage in determining methods of sensing malfunctions. One evidence of this is in the anticipation of fuel pump stall, the results of which are shown in figure 5-11. Since the engine model defined the stall region as that where the ratio of volumetric flow through the fuel pump to fuel pump speed was too low, this ratio was chosen as the basis for the detection system. It had

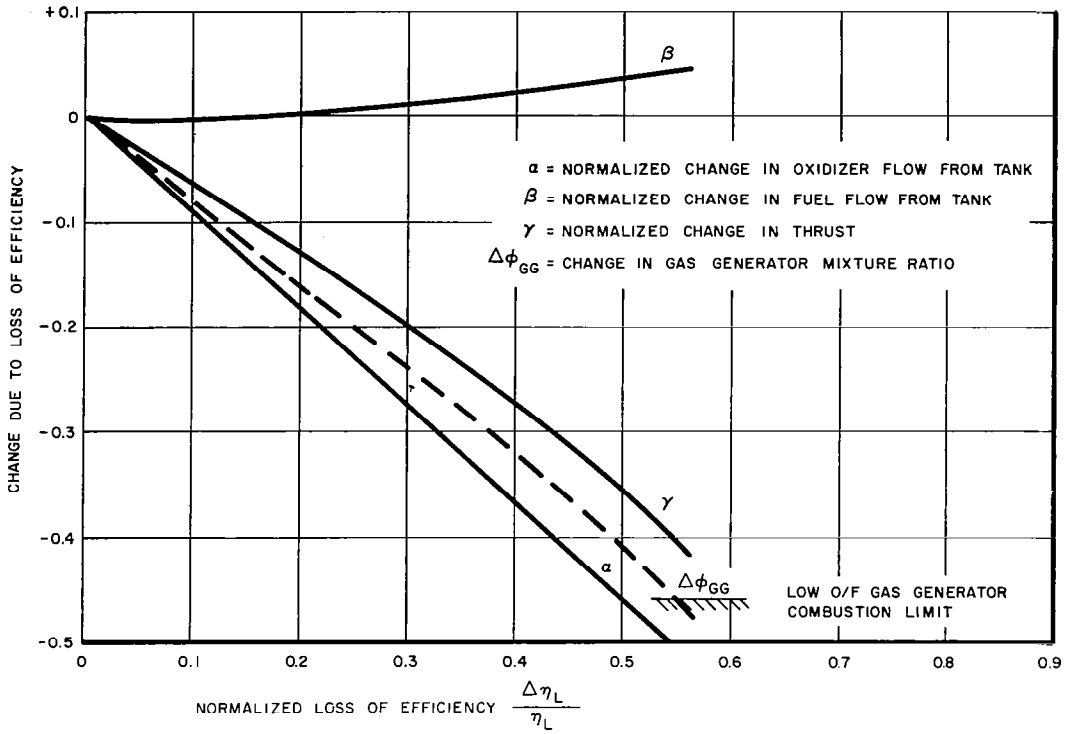

FIGURE 5-2. PERFORMANCE DEGRADATION DUE TO LOX TURBOPUMP LOSS OF EFFICIENCY

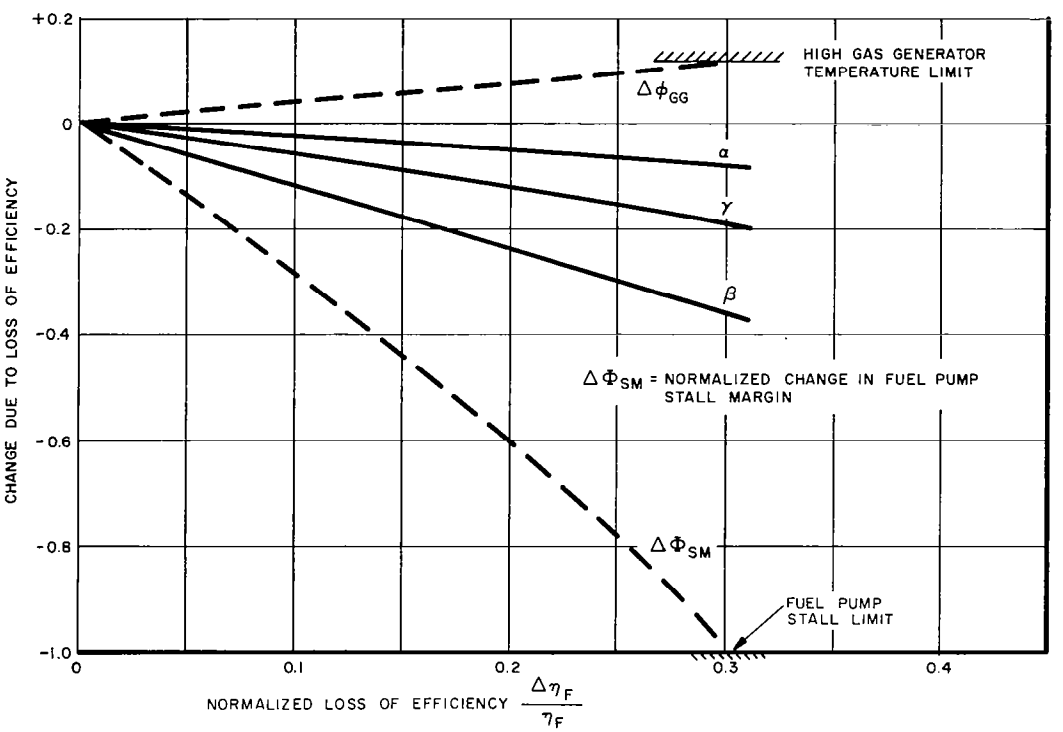

FIGURE 5-3. PERFORMANCE DEGRADATION DUE TO FUEL TURBOPUMP LOSS OF EFFICIENCY

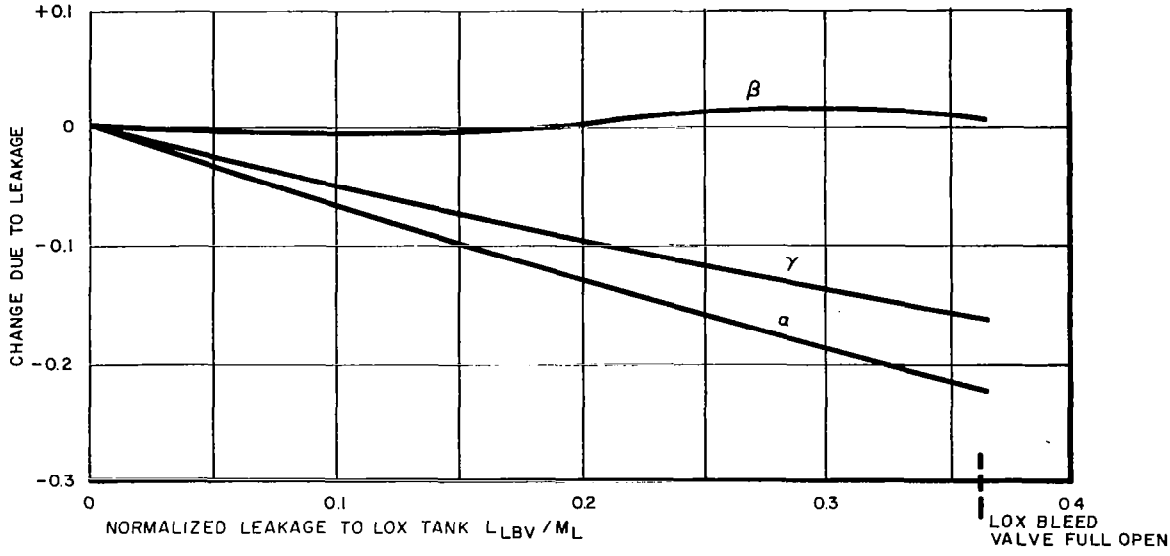

FIGURE 5-4. PERFORMANCE DEGRADATION DUE TO LOX BLEED VALVE LEAKAGE TO LOX TANK

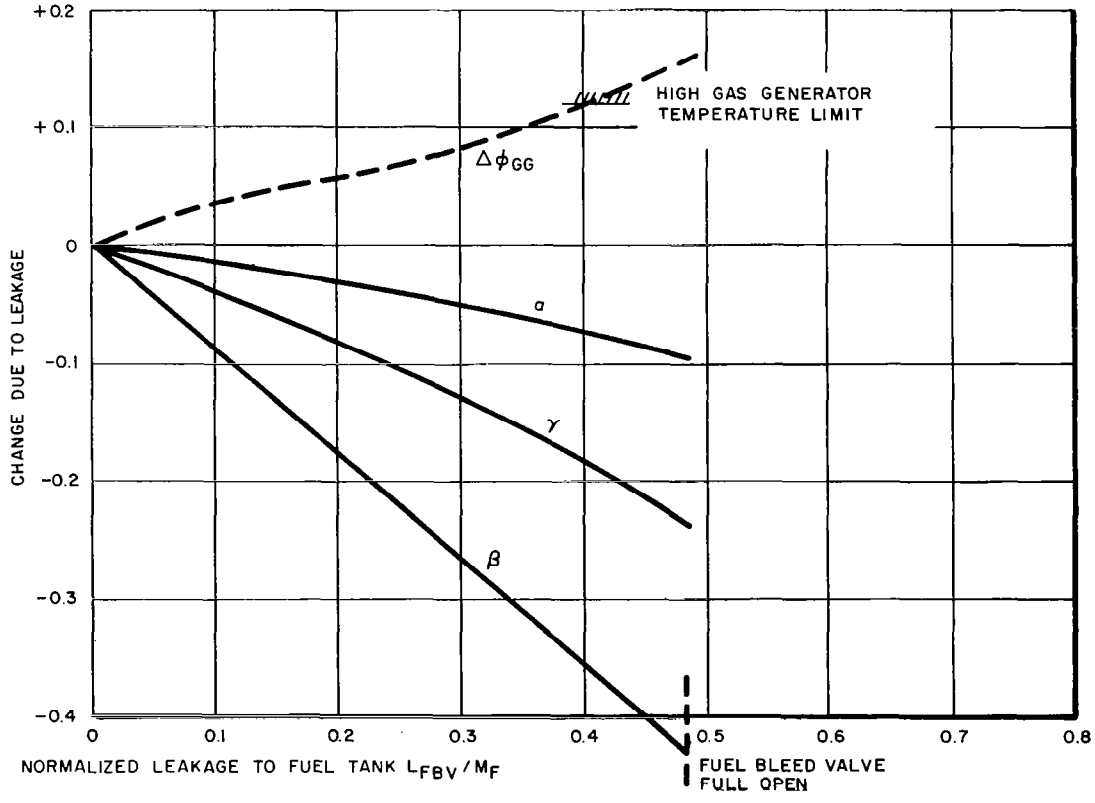

FIGURE 5-5. PERFORMANCE DEGRADATION DUE TO FUEL BLEED VALVE LEAKAGE TO FUEL TANK

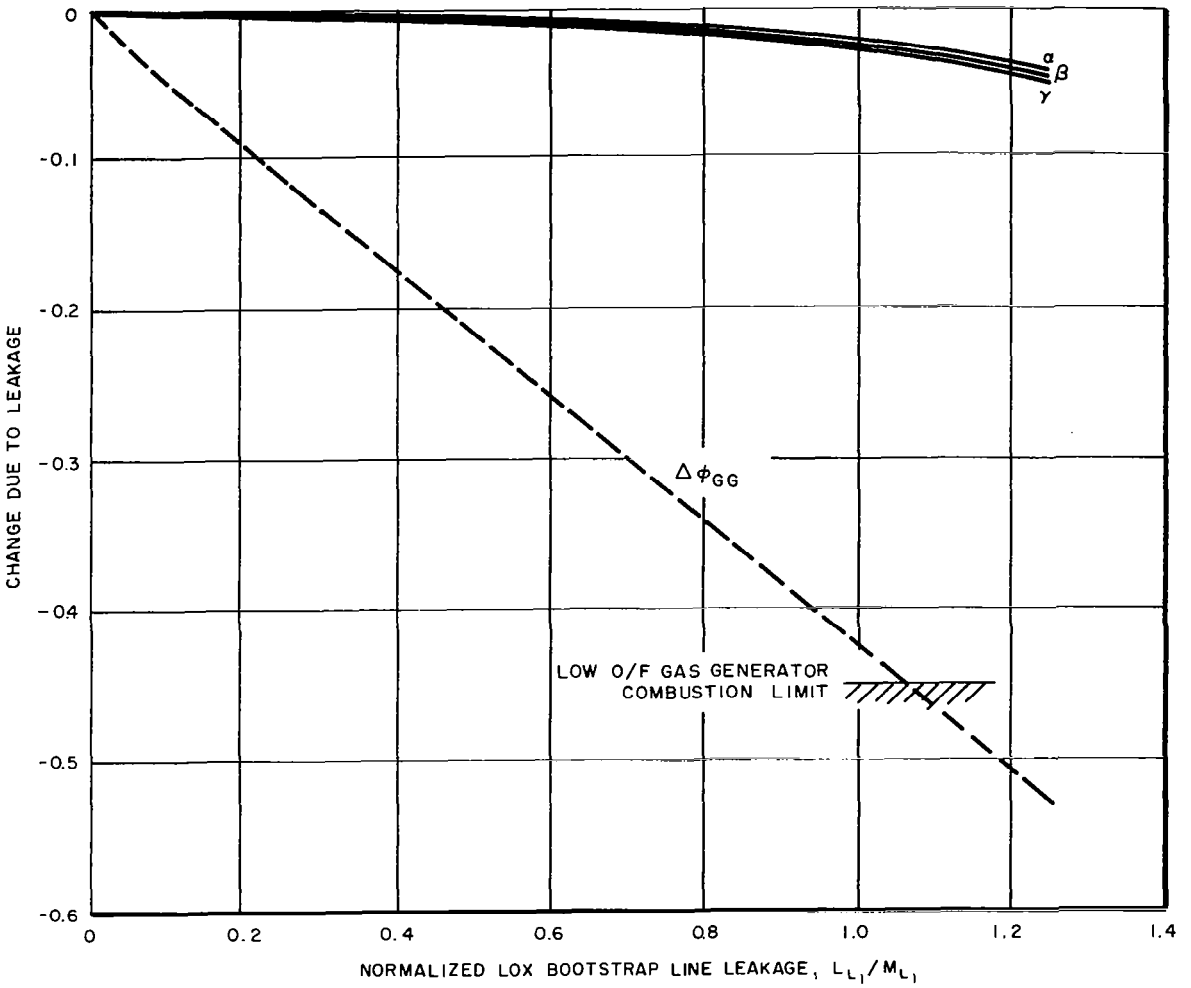

FIGURE 5-6. PERFORMANCE DEGRADATION DUE TO LOX BOOTSTRAP LINE LEAKAGE

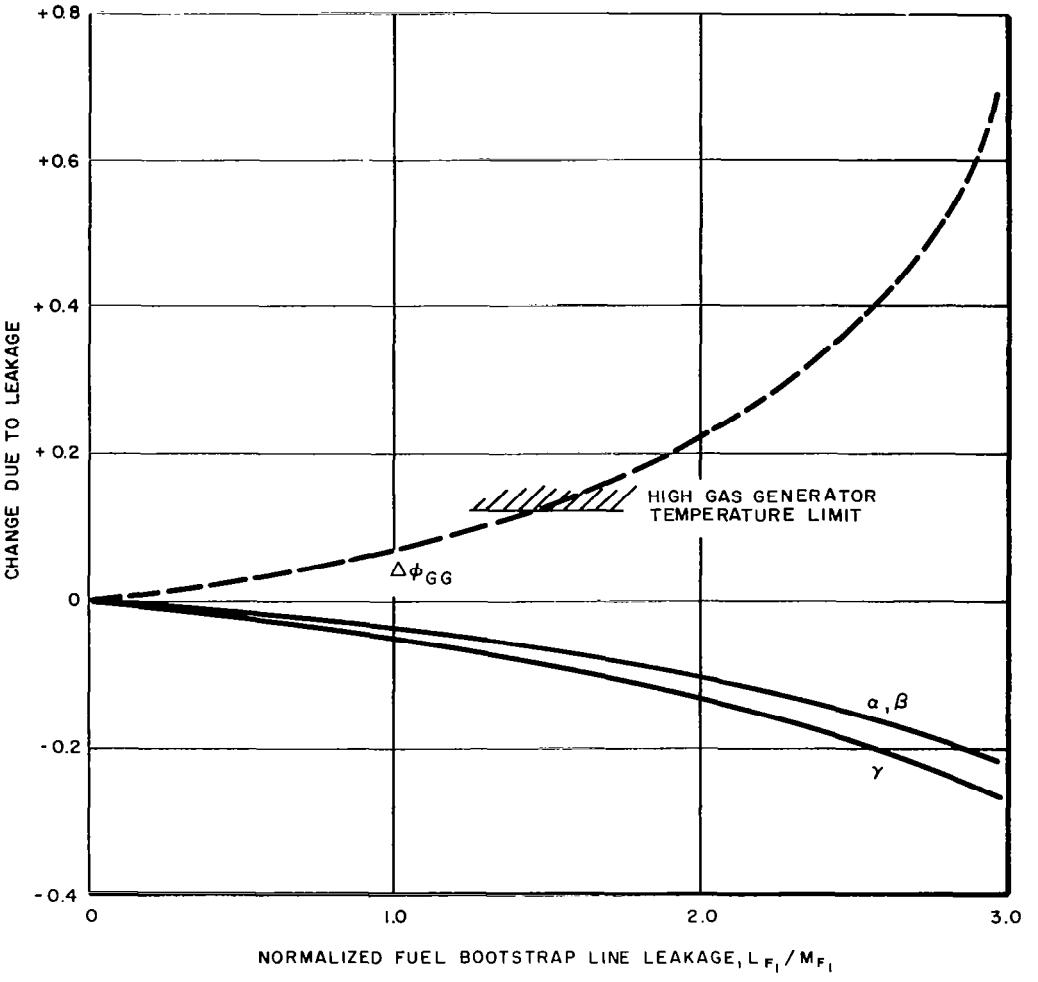

FIGURE 5-7. PERFORMANCE DEGRADATION DUE TO FUEL BOOTSTRAP LINE LEAKAGE

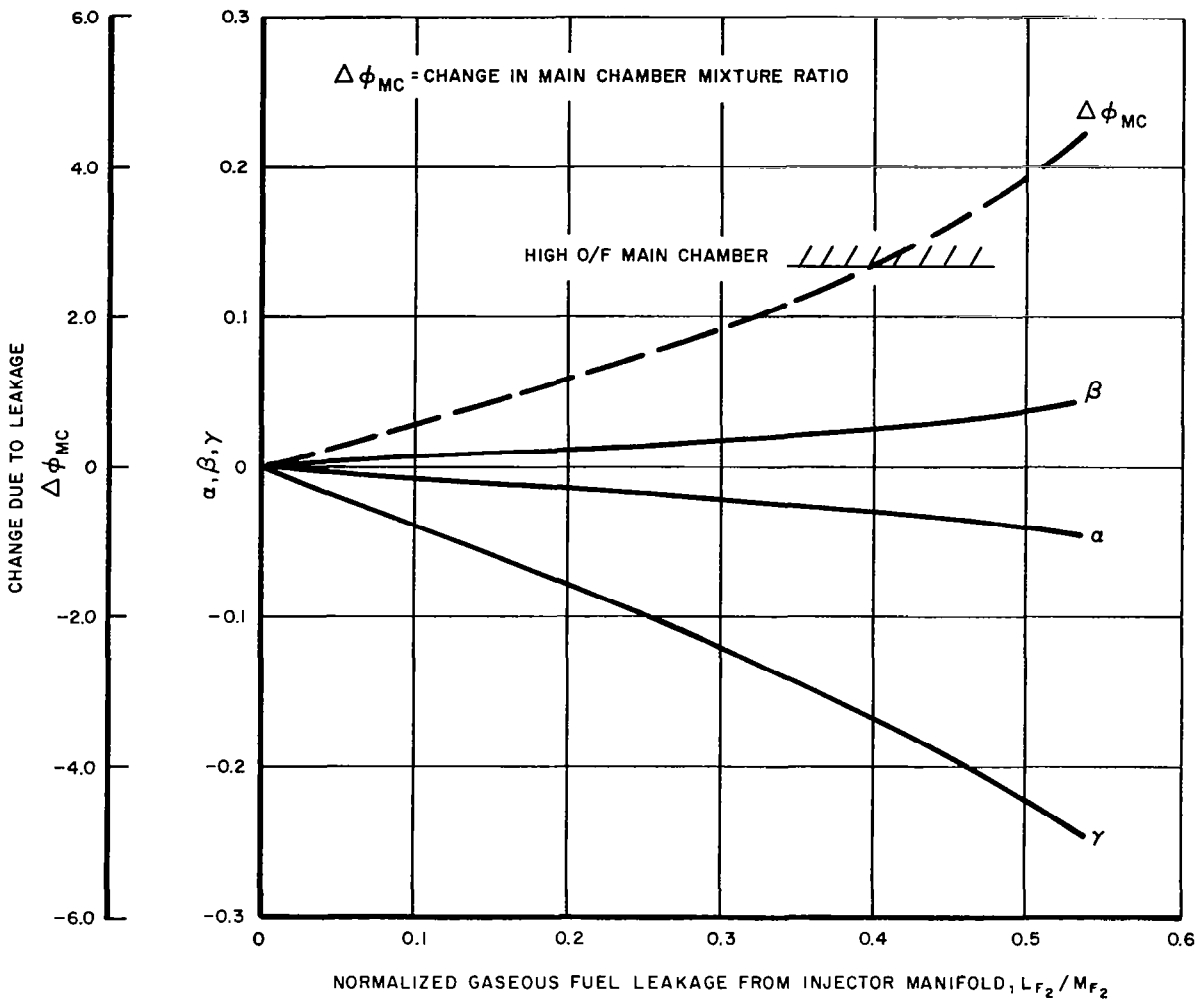

FIGURE 5-8. PERFORMANCE DEGRADATION DUE TO GASEOUS FUEL LEAKAGE FROM INJECTOR MANIFOLD

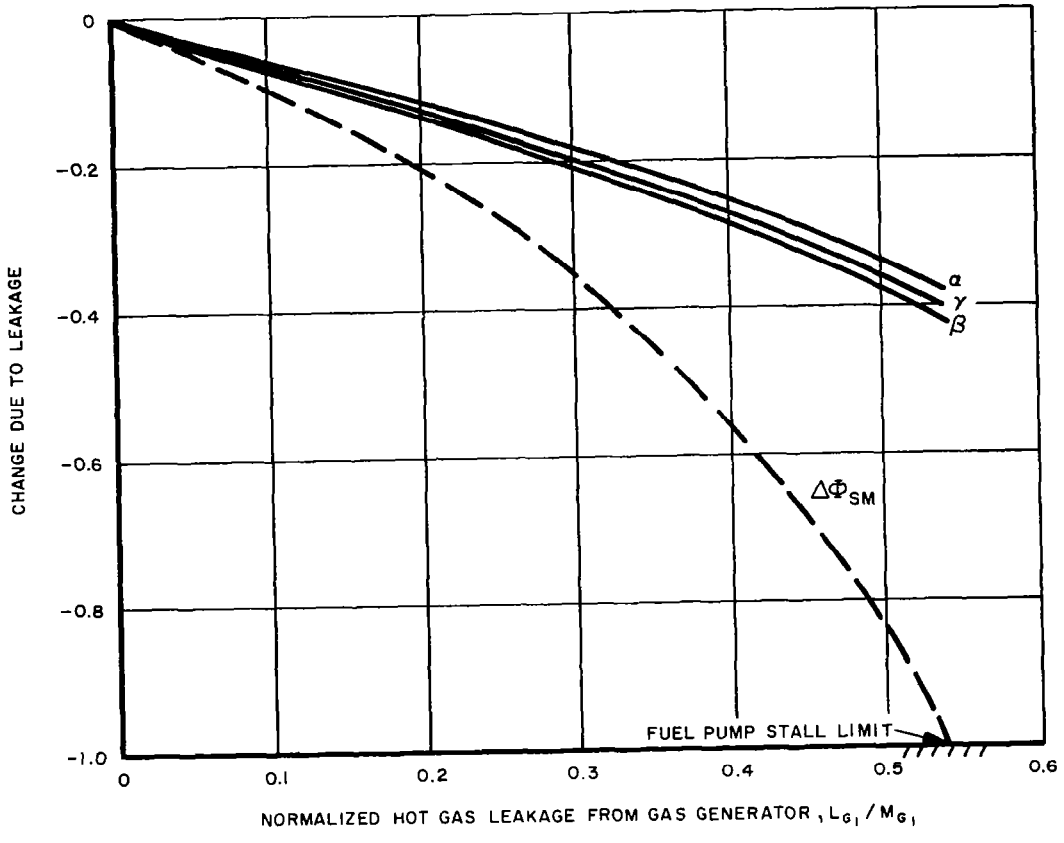

FIGURE 5-9. PERFORMANCE DEGRADATION DUE TO HOT GAS LEAKAGE FROM GAS GENERATOR

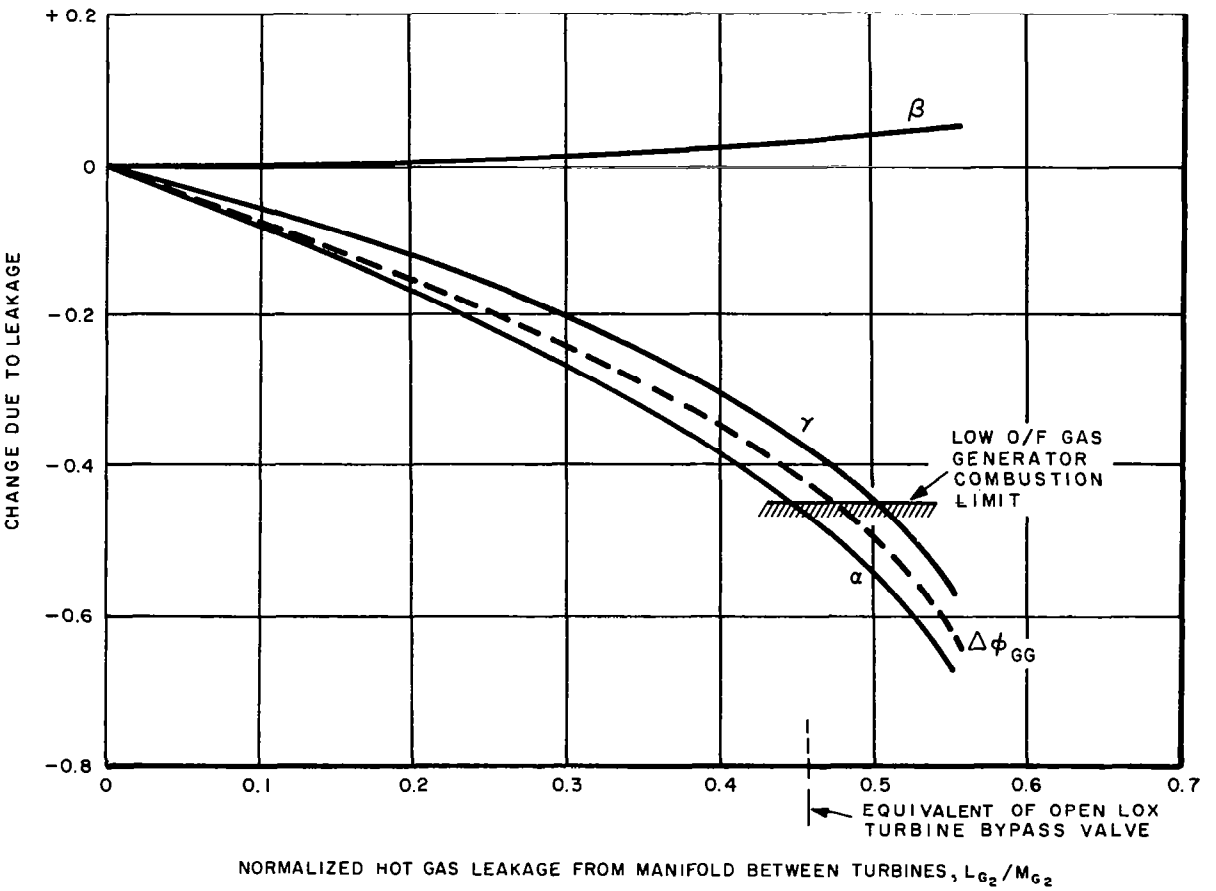

FIGURE 5-10. PERFORMANCE DEGRADATION DUE TO HOT GAS LEAKAGE FROM MANIFOLD BETWEEN TURBINES

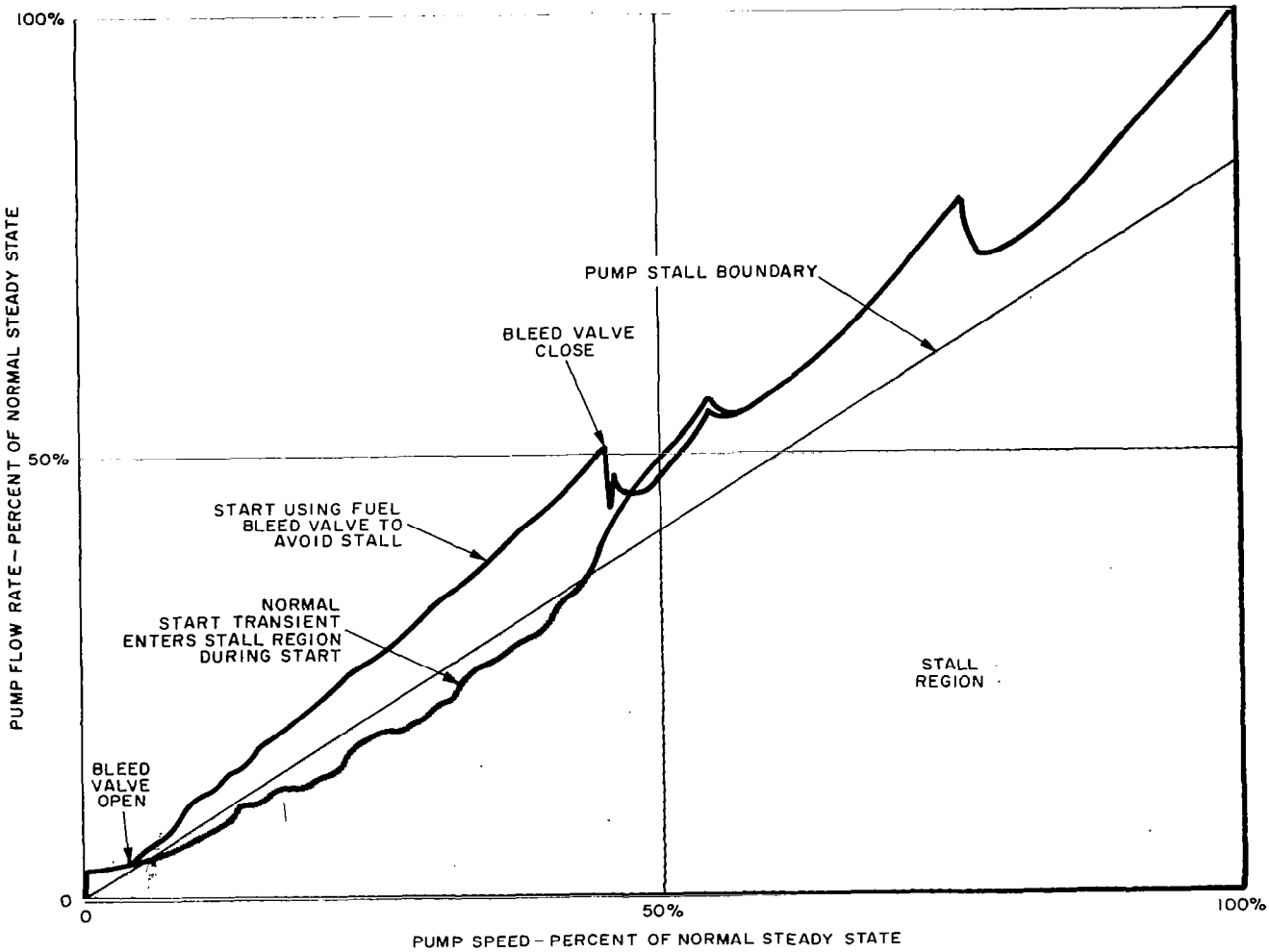

FIGURE 5-11. FUEL PUMP FLOW RATE VERSUS PUMP SPEED CHARACTERISTICS DURING ENGINE START

Table 5-2. REMEDIAL ACTIONS INVESTIGATED FOR VARIOUS TRANSIENT MALFUNCTIONS

Malfunction	Critical Effect	Remedial Action Attempted	Assessment of Remedial Action
Stalling of Fuel Turbopump during Normal Engine Start Transient	Lox rich combustion due to loss of fuel flow	Modulation of fuel bleed valve as a function of fuel flow and pump speed	Effective in avoiding stall region during start. See figure 5-11
		Modulation of fuel bleed valve as a function of fuel pump discharge pressure and pump speed	Equally effective
Start with Lox Bleed Valve Open	Engine will not bootstrap due to low lox pump pressure	Delay opening of main lox valve to aid build-up of lox pressure	Undesirable. Causes excessively lox rich combustion in gas generator
Start with Fuel Bleed Valve Open	Lox rich combustion in gas generator due to low fuel pump pressure	Do not open main lox valve beyond first step. Introduce flow restrictor in lox bootstrap line	Can achieve low thrust (40% of normal) operating condition
Start with Lox Turbine Bypass Valve in Closed (Mainstage) Position	Lox rich combustion due to rapid acceleration of lox turbopump	Delay second step opening of main lox valve. Temporarily restrict flow in lox bootstrap line	Effective in avoiding lox rich combustion during start. Main lox valve must be opened and flow restrictor removed when lox turbopump speed reaches normal operating level or overspeed will result
Failure of Lox Turbine Bypass Valve to go from Open (Start) to Close (Mainstage) Position During Start	Marginally low O/F mixture ratio in gas generator	Close propellant utilization valve after lox turbine bypass valve fail to operate normally	Gas generator mixture ratio somewhat improved. (Effect of malfunction is reduced by approximately 25%)
Failure of Main Lox Valve to Open Beyond First Step	Lox rich combustion in gas operator due to high lox pump discharge pressure	Keep lox turbine bypass valve in open (start) position	Gas generator mixture ratio near normal. Main chamber mixture ratio very low. Thrust approximately 45% of normal
Main Lox Valve Goes Full Open at Once Instead of Stopping at First Step	Fuel pump stall due to increased main chamber pressure	Modulation of fuel bleed valve as a function of fuel flow and pump speed	Stall is avoided, but gas generator O/F mixture ratio becomes critically low, main chamber mixture ratio is excessively lox rich, engine will not bootstrap

Table 5-2. REMEDIAL ACTIONS INVESTIGATED FOR VARIOUS TRANSIENT MALFUNCTIONS (Cont)

Malfunction	Critical Effect	Remedial Action Attempted	Assessment of Remedial Action
Main Lox Valve Fails to Close at Cutoff	Lox rich combustion after main fuel valve closes	Reopen main fuel valve, then shut down with prevalues	Effective if closure of main fuel valve is arrested and reversed before it closes more than halfway - otherwise fuel pump stalls
Loss of Start Tank Pressure	No turbopump starting flow	Tank head start	Undesirable. Causes excessively lox rich combustion in the gas generator

to be assumed that the ratio could not be directly calculated, since the fuel flowmeter location is such that it does not measure the fuel that flows to the gas generator or through the fuel bleed valve. Consequently, the detection scheme shown in figure 5-12 was adopted. The fuel bleed valve position was used to modify the decision computation and a smoothing network was introduced to avoid instability due to high frequency overshoots in the measured flow when the bleed valve operated.

As noted in the list of remedial actions in table 5-2, an alternative fuel pump stall anticipation method was developed. This was based upon the fact that the stall region could equally well be defined as a high ratio of fuel pump pressure head to the square of pump speed. By using techniques similar to those described above, an equally effective system was synthesized from measurements of the pump pressures and speed.

Another illustration of detection techniques is the comparison of the fuel and lox turbopump speeds to determine the position of the lox turbine bypass valve during the start transient. This determination is required as an independent check on the valve position switch indication. If the valve has malfunctioned so that it is in the closed (mainstage) position during the start, the lox turbine will accelerate too rapidly and cause excessively lox rich combustion. Figure 5-13 shows how the fuel and lox turbopump speeds compare during the discharge of the start tank, with the lox turbine bypass valve either opened or closed. There is a brief period in which the relative speeds of the two pumps may be used to decide whether to continue with the start or to shutdown the engine.

Steady-state leakage conditions can usually be most readily distinguished by pressure drop measurements. Figure 5-14 shows how several fuel measurements vary as a function of gaseous fuel leakage from the fuel injector manifold. The fuel injector pressure drop is more sensitive to the leakage than any other parameter. Normal or slightly increased fuel flowmeter output can be utilized in conjunction with the low injector pressure drop to provide a unique indication of a leak. Reference to figure 5-8 shows that this leakage may be considered critical at a rate of 39 percent of normal flow. This criticality is based upon a high main chamber mixture ratio, rather than any attendant fire hazard which was not considered in the model. The appropriate remedial action is to open the propellant utilization valve at the lowest practical detection level, in order to keep the main chamber mixture ratio as near normal as possible. If the leakage approaches the critical level, engine shutdown is required.

5.6 STOCHASTIC EFFECTS ON MEASURED PARAMETERS

The engine operation parameters that would be measured for purposes of malfunction detection are subject to some variations during normal engine running. The influence of these variations on the detection problem is treated in Section VII, Malfunction Sensing Model. A knowledge of the magnitude of these variations is desirable in order to completely

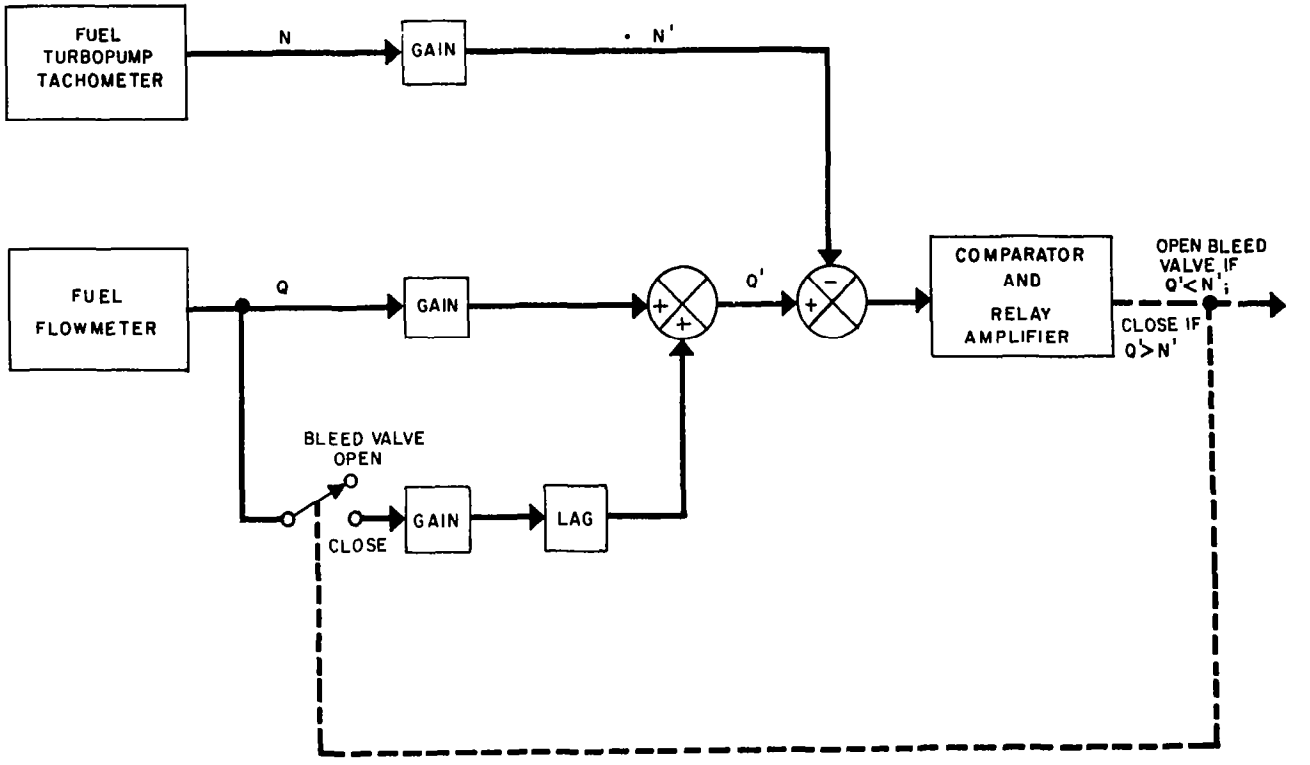

FIGURE 5-12. FUEL PUMP STALL ANTICIPATION AND REMEDIAL ACTION

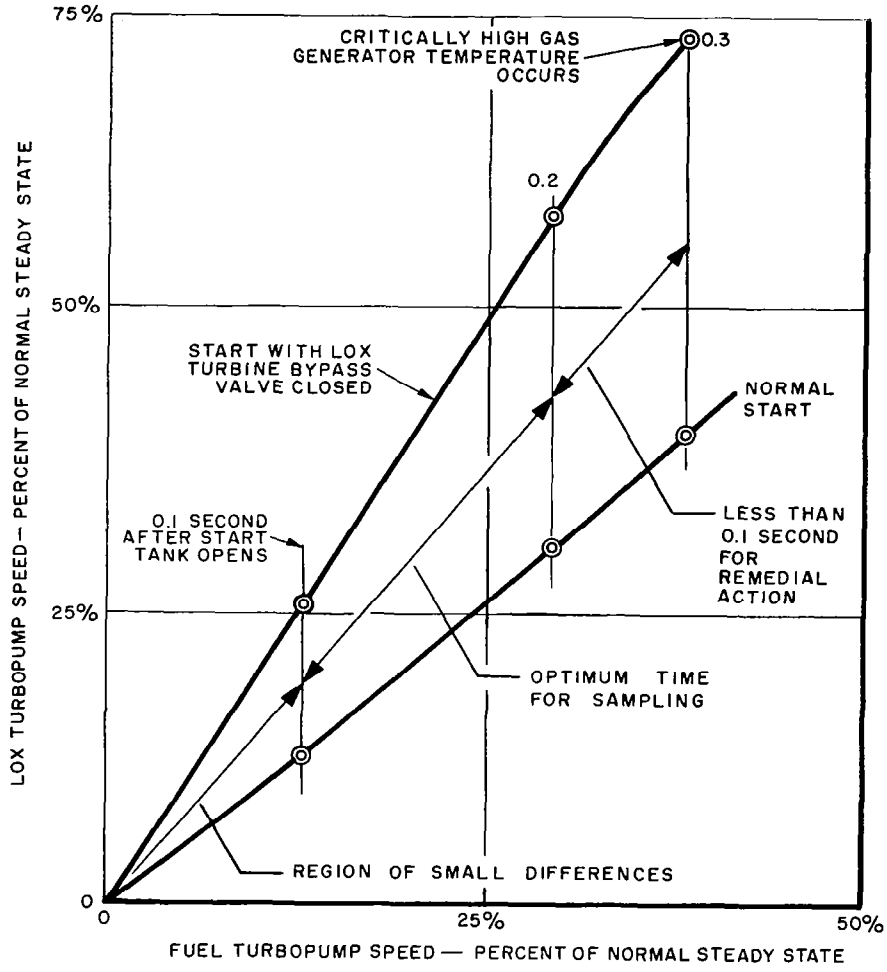

FIGURE 5-13. EFFECT OF CLOSED LOX TURBINE BYPASS VALVE ON INITIAL TURBOPUMP SPEED RELATIONS

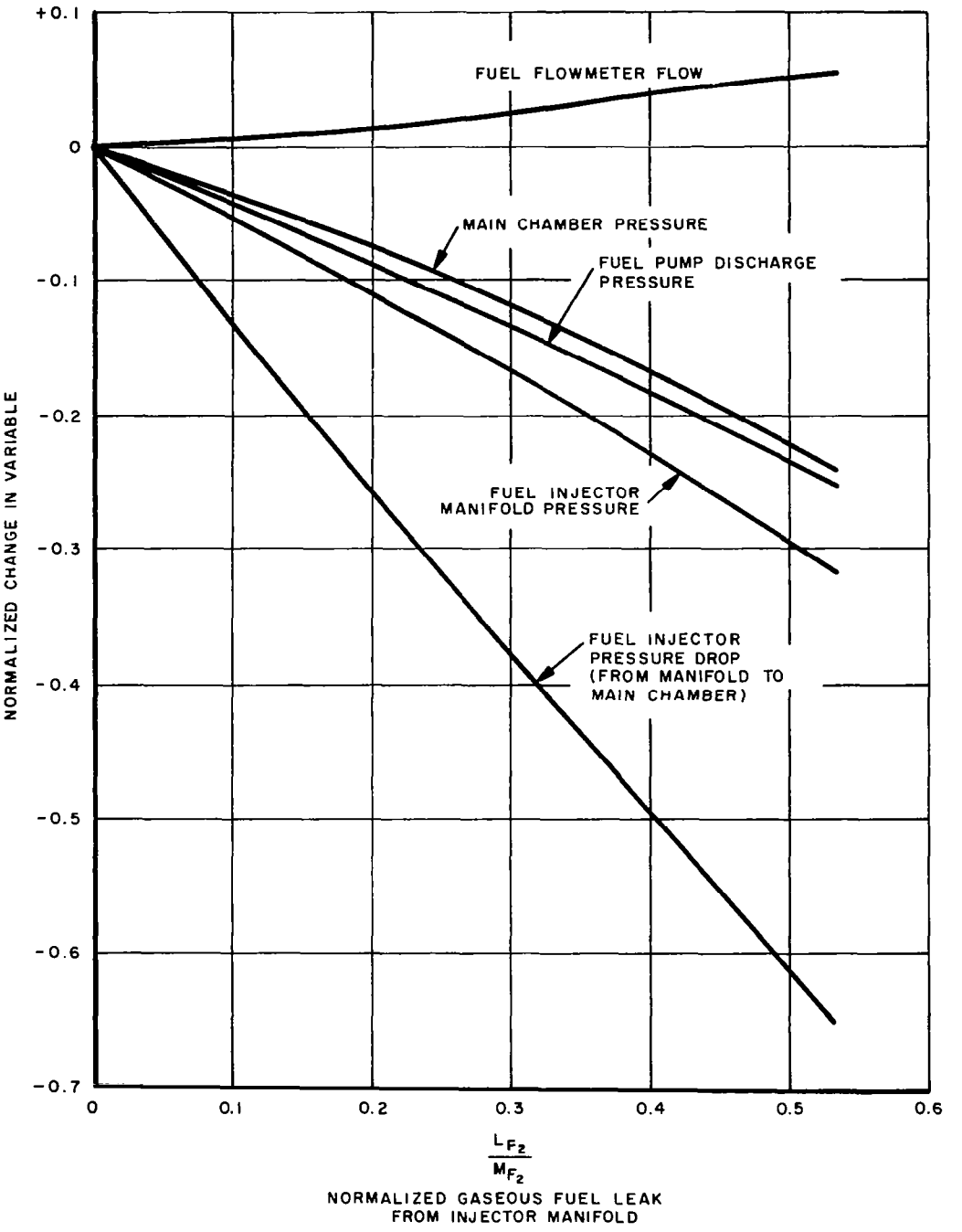

FIGURE 5-14. SENSITIVITY OF SEVERAL FUEL MEASUREMENTS TO FUEL INJECTOR MANIFOLD LEAKAGE

define a detection system; however, no statistical data on the J-2 engine performance have been available during this study.

Variations in engine operation may either be due to external conditions such as propellant tank temperatures and pressures and the ambient atmospheric pressure, or they may result internally from differences in the physical parameters of the engines. Examples of these differences might be variations in the areas of valves and ducts, or in the geometry of turbine blades. The engine manufacturer publishes influence coefficients that define the effects of the external conditions, but there is no similar information on the influence of the internal parameters. Consequently, various constants in the engine analog model were perturbed, one at a time, in order to obtain a set of influence coefficients. These are presented in table 5-3 and represent the values derived from perturbations that affected the most sensitive engine measurements by approximately 10 percent. Since the engine model equations are nonlinear, these influence coefficients may be expected to vary with the size of the perturbation.

In order to provide some indication of the magnitude of J-2 engine performance variations, the qualification test logbook data for three production engines were examined. Since each set of test data included engine performance measurements that were corrected to standard environmental conditions, a comparison of these measurements should be indicative of the effects of internal engine variations. One-sigma variances for a number of measurements were therefore computed and normalized as ratios of the average measurement. These are listed in table 5-4. As a comparison, this table includes some similar data on the RL-10 engine.* These RL-10 data were based on measurements that had been corrected to standard environmental conditions and also to standard engine mixture ratio.

Table 5-4 also shows normalized variances in the analog computer simulation of various engine measurements. These indicate that the simulation was more consistent than the actual engines.

- - - - - - -

*The RL-10 engine data were taken from "Tables I, II, and III, Flight Instrumentation Corrected Data, Average and Three Sigma, for RL10A-3S, RL10A-3C, and RL10A-3-1 Delivery Engines", issued by Pratt and Whitney, and supplied by NASA.

Table 5-3. INFLUENCE COEFFICIENTS FOR THE EFFECTS OF ENGINE PARAMETERS ON PERFORMANCE MEASUREMENTS

Engine Parameter Perturbed	Percentage Change in Engine Measurements Due to a 1% Perturbation in Engine Parameter							
	Pump Discharge Pressures		Fuel Injector Pressure Drop	Flowmeter Flows		Turbopump Speeds		Gas Generator Mixture Ratio (O/F)
	Lox	Fuel		Lox	Fuel	Lox	Fuel	
High Pressure Lox Duct Area	-0.01	0.14	-0.08	0.23	0.07	0.04	0.07	0.21
High Pressure Fuel Duct Area	-0.03	-0.15	0.06	-0.05	0.09	-0.03	-0.01	0.17
Lox Bootstrap Line Area	0.24	0.21	0.03	0.20	0.24	0.14	0.16	0.62
Fuel Bootstrap Line Area	0.07	0.06	-0.01	0.06	0.06	0.04	0.05	-0.23
Lox Injector Area	-0.13	-0.02	-0.05	0.05	-0.08	-0.04	-0.04	-0.20
Fuel Injector Area	-0.07	-0.54	-4.06	-0.18	0.31	-0.07	-0.07	0.52
Lox Turbine Efficiency	1.15	0.66	-0.38	1.12	0.33	0.72	0.34	1.01
Fuel Turbine Efficiency	0.48	0.76	0.50	0.19	1.17	0.23	0.68	-0.48
Gas Generator Nozzle Area	0.72	0.63	0.04	0.59	0.64	0.43	0.46	0.53
Main Chamber Nozzle Area	-0.60	-0.44	0.98	0.08	-0.13	-0.23	-0.19	-0.47
Lox Turbine Bypass Valve Area	-0.09	-0.06	0.04	-0.09	-0.03	-0.06	-0.03	-0.08
Effect of Main Chamber Combustion Temperature on Cooling Jacket Temperature (K120)	0.03	0.13	0.96	0.05	-0.08	0.02	0.01	-0.21

Table 5-4. NORMALIZED ONE-SIGMA VARIANCES IN ENGINE PERFORMANCE MEASUREMENTS

	Combustion Chamber Pressures		Pump Discharge Pressures		Flowmeter Flows		Turbopump Speeds		Fuel Turbine Inlet Temperature
	Main Chamber	Gas Generator	Lox	Fuel	Lox	Fuel	Lox	Fuel	
4 J-2 Engine Qualification Test Runs (3 different engines, corrected to standard environment)	0.0103	0.0386	0.0242	0.0259	0.0153	0.0103	0.0087	0.00354	0.0591
56 RL10A-3S Engines	0.0052		0.0176	0.0167			0.0089		
24 RL10A-3C Engines	0.0058		0.0246	0.0237					
12 RL10A-3-1 Engines	0.0025		0.0174	0.0163			0.0086		
(All RL10 data corrected to standard environment and standard mixture ratio)									
10 J-2 Analog Simulation Runs	0.0036	0.0024	0.0033	0.0026	0.0017	0.0008	0.0013	0.0012	0.0111
6 J-2 Analog Simulation Runs	0.0022	0.0018	0.0018	0.0017	0.0015	0.0021	0.0009	0.0009	0.0018

SECTION VI

MALFUNCTION AND DECISION PAIR ANALYSIS COMPILATION (MADPAC)

6.1 INTRODUCTION AND SUMMARY

The Malfunction and Decision Pair Analysis Compilation (MADPAC) is a tabulation of component malfunctions with remedial action decisions and their effect on mission and crew loss. The data contained in MADPAC form the basic input for the READI design. From these data various combinations of malfunction sensors and remedial actions can be evaluated in terms of their effectiveness in reducing mission and crew losses. It is obvious that in a real mission-vehicle complex such as Saturn V the volume of data which must be assembled and operated upon is extremely large. The use of hand computations would be a cumbersome and time-consuming task. For this reason, the MADPAC data are stored on a computer tape, and various printouts have been programmed to meet the requirements of the READI synthesis and evaluation procedures. In addition to the time savings, this approach affords a great deal of flexibility. The computer program can easily be modified to permit re-evaluation of a candidate READI system in the event a weighting factor or other variable is changed. The basic input and output formats used in MADPAC are described in subsections 6.2 and 6.3.

6.2 DEFINITION AND FORMAT OF INPUTS

The MADPAC input format is typified by the computer printout shown in figure 6-1. The column headings that have been included in figure 6-1 are defined in table 6-1.

The first line of the input data contains the coded definition of the particular component malfunction. In the example, figure 6-1, the malfunction of stalling of the fuel pump of the J-2 engine in the SIVB stage of the Saturn V vehicle is shown.

The following lines of input data define the probability of component failure during a particular mission phase, the conditional probability of the failure causing a loss of the prime mission with the assumption that a particular remedial action has been taken, and the conditional probabilities of the various mission alternates that may result if the prime mission is lost.

The input data on figure 6-1 represents three different possible READI systems, identified by the entry numbers in the last column. Each entry number includes a set of data that defines the system operation over the various mission phases. For the example shown, there are two significant phases - SIVB first and second engine start periods. The system identified as Entry Number 1 is the basic system with no READI remedial actions. The data show that occurrence of the malfunction will always result in the loss of the prime mission (β=1) and that approximately one-third of these losses will be

A1 = LUNAR ORBITAL ALTERNATE
A2 = CIRCUMLUNAR ALTERNATE
A3 = EARTH ORBITAL ALTERNATE
A4 = DIRECT EARTH ABORT
A5 = CATASTROPHIC LOSS

SYS	SUBS ST	S SUBS EN	COMP REM	FUNC F MODE UNREL	VENO BETA	P(A1)	P(A2)	P(A3)	P(A4)	P(A5)	ENTRY NO
2132	24	20	2	0 189	501				GROUP NO.		112
	1	130	-0	.000	-.000	-.000	-.000	-.000	-.000	-.000	1
	130	31	-0	1938.000	1.000	-.000	-.000	.680	-.000	.320	1
	31	32	-0	.000	.000	-.000	-.000	.000	-.000	.000	1
	32	143	-0	.000	-.000	-.000	-.000	-.000	-.000	-.000	1
	143	44	-0	1323.000	1.000	.230	.450	-.000	-.000	.320	1
	44	46	-0	.000	.000	.000	.000	-.000	-.000	.000	1
	1	130	300	.000	-.000	-.000	-.000	-.000	-.000	-.000	2
	130	31	333	1938.000	.200	-.000	-.000	.998	-.000	.002	2
	31	32	333	.000	-.000	-.000	-.000	-.000	-.000	-.000	2
	32	143	300	-.000	-.000	-.000	-.000	-.000	-.000	-.000	2
	143	44	333	1323.000	.200	.333	.665	-.000	-.000	.002	2
	44	46	333	.000	-.000	-.000	-.000	-.000	-.000	-.000	2
	1	130	300	.000	-.000	-.000	-.000	-.000	-.000	-.000	3
	130	31	301	1938.000	1.000	-.000	-.000	.991	-.000	.009	3
	31	32	301	.000	-.000	-.000	-.000	-.000	-.000	-.000	3
	32	143	300	.000	-.000	-.000	-.000	-.000	-.000	-.000	3
	143	44	301	1323.000	1.000	.331	.660	-.000	-.000	.009	3
	44	46	301	.000	-.000	-.000	-.000	-.000	-.000	-.000	3
	-0	-0	-0	-.000	-.000	-.000	-.000	-.000	-.000	-.000	-0

FIGURE 6-1. TYPICAL MADPAC INPUT FORMAT

catastrophic [P(A5) = 0.32]. If they are catastrophic, a successful separation of the control and service modules will lead to the possibility of an earth orbital, a lunar orbital, or a circumlunar mission, depending on when the malfunction occurs.

Entry Number 2 identifies a system that provides a stall anticipation and corrective remedial action (identified by number 333 in the REM column). In this case, only 20 percent of the malfunctions result in the loss of the prime mission (β=0.2) and a very small fraction of these losses are catastrophic since the system provides additional warning time for escape.

Entry Number 3 identifies a system that contains stall detection and provides an engine shutdown remedial action (301). Occurrence of the malfunction always leads to the loss of the prime mission, but most of the time this loss is due to deliberate shutdown rather than physical damage; therefore about one percent of the losses are catastrophic.

6.3 DEFINITION AND FORMAT OF OUTPUTS

The basic MADPAC output format is illustrated in figure 6-2, which contains the criticalities computed from the input data of figure 6-1. The various column headings are defined in table 6-1. For each input entry number there is an output line that sums the criticalities over the mission phases for that particular system.

The data in figure 6-2 indicate that the stall alleviation system (remedial action number 333) results in a substantial reduction of prime mission criticality and almost complete elimination of crew risk. The alternative system, with detection and shutdown (remedial action number 301) is almost as effective in reducing crew risk, but cannot save any prime mission losses.

Figure 6-3 illustrates a slightly different output format which shows how the prime mission criticality is divided among the various possible mission alternates.

Table 6-1. DEFINITION OF MADPAC PRINTOUT HEADINGS

Heading	Description
SYS	System
SUBS	Subsystem
SSUBS	Sub-subsystem
COMP	Component
FUNC	Function
FMODE	Failure Mode
VENO	Vehicle Number
ST	Event which marks start of phase
EN	Event which marks end of phase
REM	Remedial Action
UNREL	The number of components which fail in the phase and mode per million
BETA	The probability that existing failure will cause loss of prime mission
$P(A_i)$	Mission alternate transition probability; the conditional probability that having lost the prime mission, alternate A_i results.
PMAL	Number of missions per million which fly in the phase with the malfunction. $\text{PMAL } j = \sum_{k=1}^{j} \text{UNREL}_k - \sum_{k=1}^{j-1} \text{CRIT}_k$

SYS 2132 SUBS 24 SSUBS 20 COMP 2 FUNC 0 FMODE 189 VENO 501 GROUP NO. 112

ST	EN	REM	UNREL	BETA	PMAL	CRIT	GAMA	CCRIT	ALMF	MCRIT	TCRIT	DCRIT	DCCRIT	DMCRIT	DTCRIT
1	130	-0	.00	-.000	.00	-.00	.000	-.00	.000	-.00	-.00	.00	.00	.00	.00
130	31	-0	1938.00	1.000	1938.00	1938.00	.320	620.16	.966	1872.11	8073.71	.00	.00	.00	.00
31	32	-0	.00	.000	.00	.00	.000	.00	.000	.00	.00	.00	.00	.00	.00
32	143	-0	.00	-.000	.00	-.00	.000	-.00	.000	-.00	-.00	.00	.00	.00	.00
143	44	-0	1323.00	1.000	1323.00	1323.00	.320	423.36	.773	1022.68	5256.28	.00	.00	.00	.00
44	46	-0	.00	-.000	.00	.00	.000	.00	.000	.00	.00	.00	.00	.00	.00
SUMS						3261.00		1043.52		2894.79	13329.99	.00	.00	.00	.00
1	130	300	.00	-.000	.00	-.00	.000	-.00	.000	-.00	-.00	-.00	-.00	-.00	-.00
130	31	333	1938.00	.200	1938.00	387.60	.002	.78	.950	368.26	376.01	1550.40	619.38	1503.85	7697.70
31	32	333	.00	-.000	1550.40	-.00	.000	-.00	.000	-.00	-.00	.00	.00	.00	.00
32	143	300	-.00	-.000	1550.40	-.00	.000	-.00	.000	-.00	-.00	-.00	-.00	-.00	-.00
143	44	333	1323.00	.200	2873.40	574.68	.002	1.15	.667	383.48	394.98	748.32	422.21	639.20	4861.30
44	46	333	.00	-.000	2298.72	-.00	.000	-.00	.000	-.00	-.00	.00	.00	.00	.00
SUMS						962.28		1.92		751.74	770.99	2298.72	1041.60	2143.04	12559.00
1	130	300	.00	-.000	.00	-.00	.000	-.00	.000	-.00	-.00	-.00	-.00	-.00	-.00
130	31	301	1938.00	1.000	1938.00	1938.00	.009	17.44	.950	1841.97	2016.39	-.00	602.72	30.14	6057.32
31	32	301	.00	-.000	.00	-.00	.000	-.00	.000	-.00	-.00	.00	.00	.00	.00
32	143	300	.00	-.000	.00	-.00	.000	-.00	.000	-.00	-.00	-.00	-.00	-.00	-.00
143	44	301	1323.00	1.000	1323.00	1323.00	.009	11.91	.670	885.88	1004.95	-.00	411.45	136.80	4251.33
44	46	301	.00	-.000	.00	-.00	.000	-.00	.000	-.00	-.00	.00	.00	.00	.00
SUMS						3261.00		29.35		2727.85	3021.34	.00	1014.17	166.93	10308.64

FIGURE 6-2. TYPICAL MADPAC CRITICALITY OUTPUT FORMAT

SYS 2132 SUBS 24 SSUBS 20 COMP 2 FUNC 0 FMODE 189 VENO 501 GROUP NO. 112

ST	EN	REM	UNREL	BETA	M1	M2	M3	M4	M5	MCRIT	TCRIT	DCRIT	DCCRIT	DMCRIT	DTCRIT
1	130	-0	.00	-.000	.00	.00	.00	.00	.00	-.00	-.00	.00	.00	.00	.00
130	31	-01938	.00	1.000	-.00	-.00	1317.84	-.00	620.16	1872.11	8073.71	.00	.00	.00	.00
31	32	-0	.00	.000	-.00	-.00	.00	-.00	.00	.00	.00	.00	.00	.00	.00
32	143	-0	.00	-.000	.00	.00	.00	.00	.00	-.00	-.00	.00	.00	.00	.00
143	44	-01323	.00	1.000	304.29	595.35	-.00	-.00	423.36	1022.62	5256.28	.00	.00	.00	.00
44	46	-0	.00	.000	.00	.00	-.00	-.00	.00	.00	.00	.00	.00	.00	.00
SUMS					304.29	595.35	1317.84	.00	1043.52	2894.79	13329.99	.00	.00	.00	.00
1	130	300	.00	-.000	.00	.00	.00	.00	.00	-.00	-.00	-.00	-.00	-.00	-.00
130	31	3331938	.00	.200	-.00	-.00	386.82	-.00	.78	368.26	376.01	1550.40	619.38	1503.85	7697.70
31	32	333	.00	-.000	.00	.00	.00	.00	.00	-.00	-.00	.00	.00	.00	.00
32	143	300	-.00	-.000	.00	.00	.00	.00	.00	-.00	-.00	-.00	-.00	-.00	-.00
143	44	3331323	.00	.200	191.37	382.16	-.00	-.00	1.15	383.48	394.98	748.32	422.21	639.20	4861.30
44	46	333	.00	-.000	.00	.00	.00	.00	.00	-.00	-.00	.00	.00	.00	.00
SUMS					191.37	382.16	386.82	.00	1.92	751.74	770.99	2298.72	1041.60	2143.04	12559.00
1	130	300	.00	-.000	.00	.00	.00	.00	.00	-.00	-.00	-.00	-.00	-.00	-.00
130	31	3011938	.00	1.000	-.00	-.00	1920.56	-.00	17.44	1841.97	2016.39	-.00	602.72	30.14	6057.32
31	32	301	.00	-.000	.00	.00	.00	.00	.00	-.00	-.00	.00	.00	.00	.00
32	143	300	.00	-.000	.00	.00	.00	.00	.00	-.00	-.00	-.00	-.00	-.00	-.00
143	44	3011323	.00	1.000	437.91	873.18	-.00	-.00	11.91	885.88	1004.95	-.00	411.45	136.80	4251.33
44	46	301	.00	-.000	.00	.00	.00	.00	.00	-.00	-.00	.00	.00	.00	.00
SUMS					437.91	873.18	1920.56	.00	29.35	2727.85	3021.34	.00	1014.17	166.93	10308.64

FIGURE 6-3. TYPICAL MADPAC ALTERNATE MISSION PROBABILITY OUTPUT FORMAT

Table 6-1. DEFINITION OF MADPAC PRINTOUT HEADINGS (Cont'd)

Heading	Description
CRIT	Criticality - the number of prime missions per million which are lost in the phase $CRIT_j = (PMAL\ j)\ (BETA\ j)$
GAMA	The conditional probability that the prime mission loss will result in the loss of the crew $GAMA = \sum_{i=1}^{N} P\ (A_i)\ L_C\ (A_i)$ $L_c\ (A_i)$ = Crew loss associated with alternate A_i
CCRIT	Crew criticality - the probability of crew loss X 10^6 CCRIT = (CRIT) (GAMA)
ALMF	Alternate mission factor - the ratio of mission value loss when alternates have value to mission value loss when alternates have no value $ALMF = \sum_{i=1}^{N} P\ (A_i)\ L_m\ (A_i)$ $L_m\ (A_i)$ = Mission loss associated with alternate A_i

Table 6-1. DEFINITION OF MADPAC PRINTOUT HEADINGS (Cont'd)

Heading	Description
MCRIT	Mission criticality - the normalized mission value lost per million based on the concept of alternate missions MCRIT = (CRIT) (ALMF)
TCRIT	Total criticality - the combined criticality of mission and crew TCRIT = MCRIT + λ (CCRIT) (λ = 10 for the example shown)
DCRIT	CRIT (no remedial action) - CRIT (with remedial action)
DCCRIT	CCRIT (no remedial action) - CCRIT (with remedial action)
DMCRIT	MCRIT (no remedial action) - MCRIT (with remedial action)
DTCRIT	TCRIT (no remedial action) - TCRIT (with remedial action)
M_i	The number of missions per million which will result in alternate A_i rather than in the prime mission.

SECTION VII

MALFUNCTION SENSING MODEL

7.1 INTRODUCTION

The effectiveness of a READI system or a particular function of READI is dependent on its ability to sense the existence of malfunctions that require remedial action. An understanding of the available malfunction sensing processes is therefore necessary for preliminary design and effectiveness estimating purposes as well as for detailed equipment design phases.

The situations that are of most interest are the malfunctions that fullfill the following conditions:

- The malfunctions lead to extremely hazardous end effects involving structural failures;
- The remedial action itself is costly, usually involving sacrifice of prime mission, but not as costly as a structural failure;
- A decision on the remedial action must be made before the final structural failure occurs.

The fact that the remedial action decision must be made before structural failure has occurred introduces the possibility of unnecessary aborts or the need to accept the risk of an unnecessary abort to prevent a catastrophic loss. READI system value therefore is dependent on how accurately the malfunction can be assessed so that unnecessary aborts can be minimized while still preventing catastrophic failures.

The mechanism of the structural failure of an engine usually involves a cause and effect chain that begins with some discrete failure such as a leak, a frozen valve, or a broken wire, and eventually results in overstressing some structural members. The sensing of the initial, intermediate, and final effects of a discrete failure provides many possibilities for design of malfunctions sensing.

Since there are usually a great many more initial malfunctions than possible structural failures, the effects of the malfunctions can be drawn in the form of a tree that converges to the final catastrophic failures. A simplified example of such a failure effects tree is shown in figure 7-1.

Sensing effects near the end of this converging network have the advantage that relatively few variables need be sensed to pick up many malfunctions. Also, the effect on the stress parameters that cause structural failures can be accurately assessed. In fact, the stress variable itself can be measured. The sensing of these relatively final effects has the disadvantage that the lead time provided is often inadequate to permit effective remedial action before the catastrophic failure occurs. Furthermore, the originating

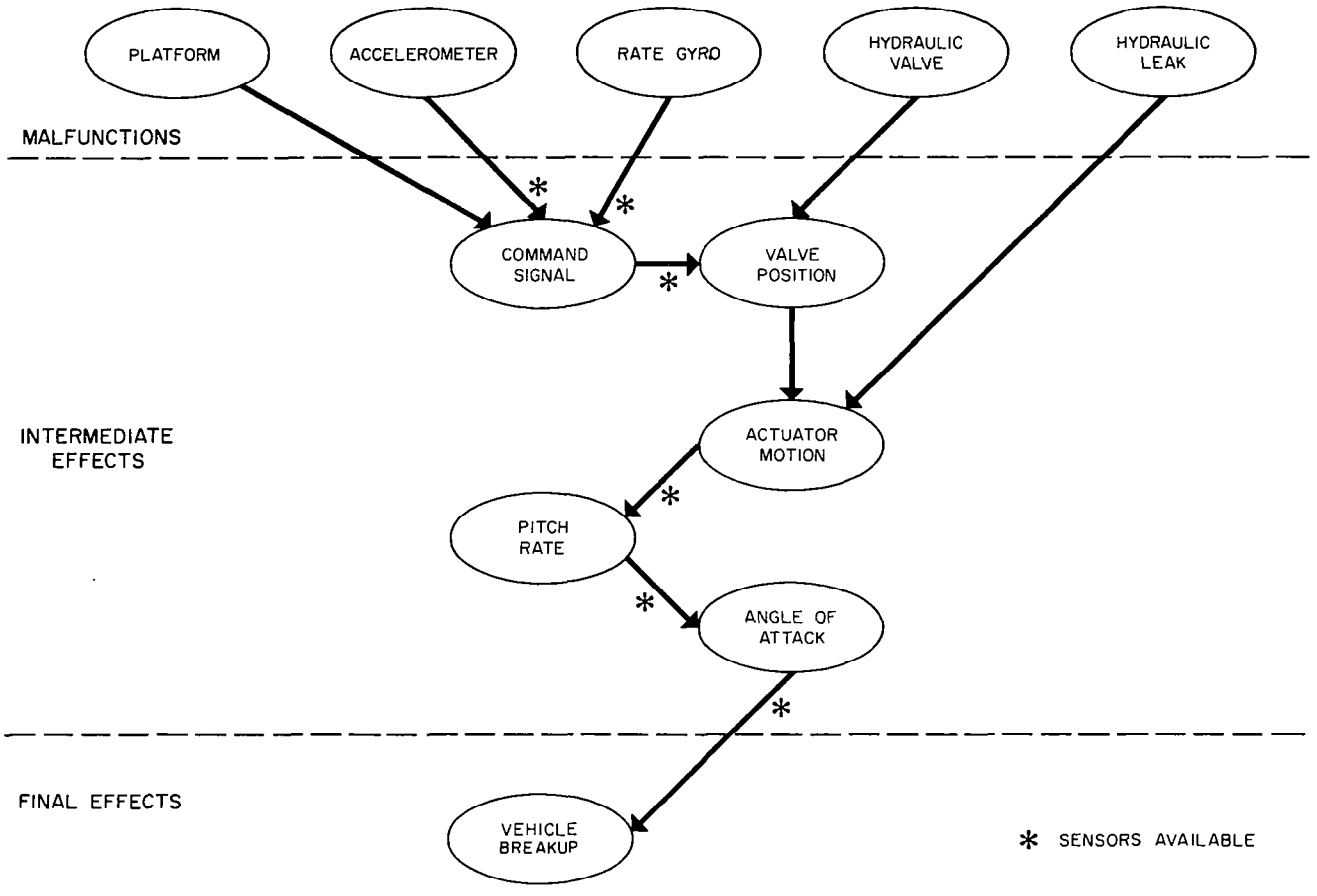

FIGURE 7-1. FAILURE EFFECTS TREE (ACTUATOR HARDOVER)

malfunction may not be localized sufficiently to allow the choice of the most appropriate remedial action.

Sensing of the initial or intermediate effects, on the other hand, does provide greater lead time and more accurate localization but has the disadvantage of requiring more transducers.

The optimum design of a READI system requires the sensing of both initial and intermediate effects. In fact, it is usually desirable to utilize more than one set of measurements for each malfunction group to prevent the possibility of false alarms due to a single defective transducer.

This section does not treat the problem of optimizing the design of READI with fallible equipment which is subject to random failure, since this problem has been analyzed in detail in previous READI reports listed in the Foreword. The particular problem treated here is the design of the malfunction detection network, taking into account the stochastic nature of the operating parameters and malfunction induced stresses.

7.2 MODEL OF PROCESS

A random failure occurrence initiates a chain of effects that may terminate in catastrophic failure. This is illustrated in figure 7-2, which also indicates the processes involved in malfunction sensing.

READI may sense any or all of the four possible effects shown in figure 7-2. In most cases, sensing of the final catastrophic effect is too late. Adequate warning time must be provided to allow crew escape to a distance sufficient to withstand any ensueing explosion if these effects are not prevented by timely shutdown.

Use of direct initial sensing of the failed component is also feasible only when the component is already equipped with the sensing device. Otherwise, too many transducers are required to implement the system.

The sensing of intermediate effects on the stress variables are of particular interest and are discussed in the following subsections.

7.3 SENSING THE INTERMEDIATE VARIABLE

By far, the most desirable measurements to employ for malfunction sensing are those associated with intermediate effects. Intermediate measurements are a good compromise between the enormous number of measurements required to pinpoint every malfunction and the high risk associated with looking at only the final effects.

The prime condition for the use of intermediate measurements is a knowledge of the deterministic chain of events from initial to final effects, hence the ability to predict the final effect. Such knowledge is derived from detailed analytical treatment of the subsystems, computer simulation, surveys of subsystem development tests, results, and special test - to - failure and failure inducing tests on the subject hardware.

Numerous examples of the use of intermediate measurements are found in the design of a typical READI system. Figure 7-1 indicates that the thrust vector actuator command signal may be a suitable

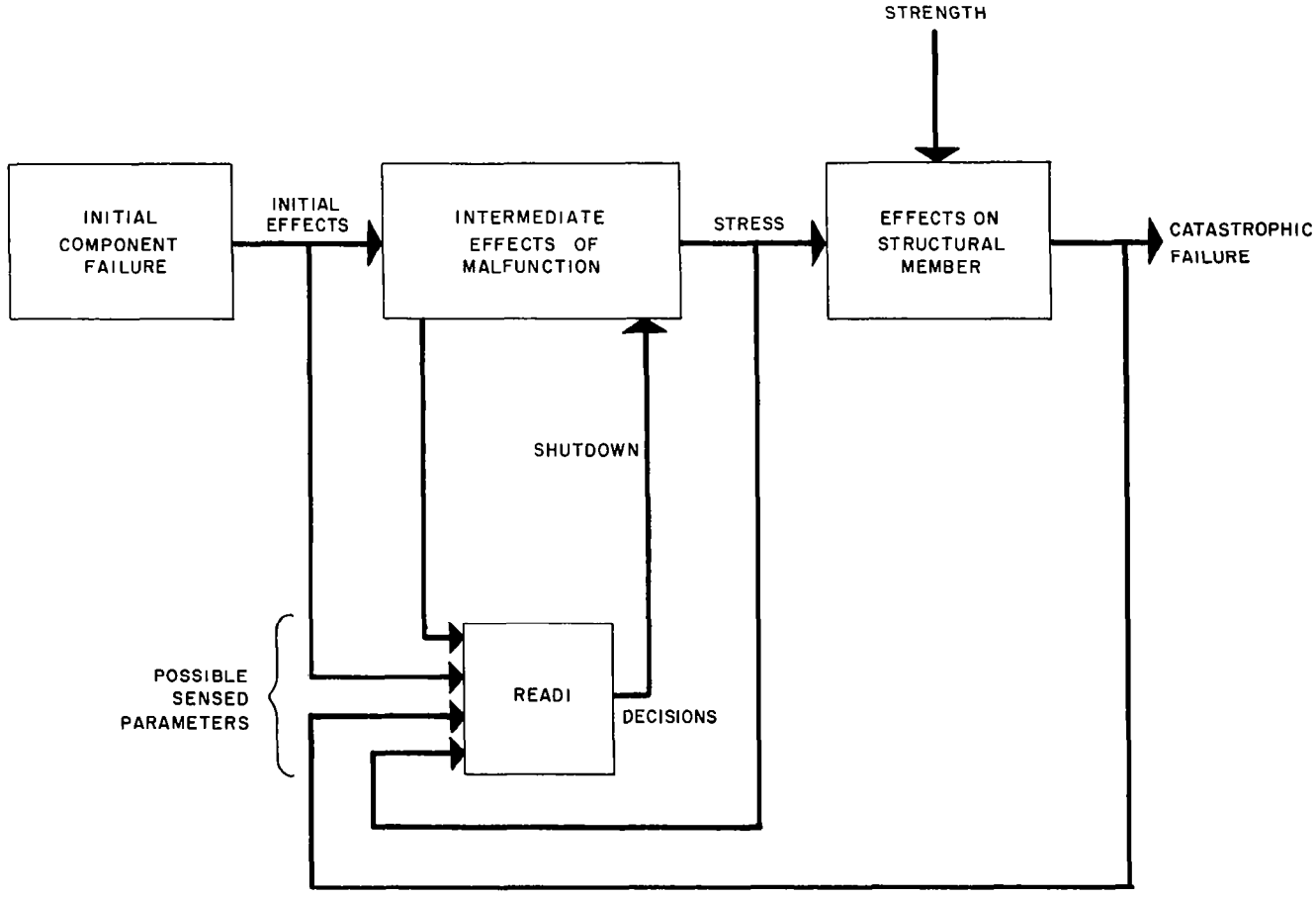

FIGURE 7-2. MODEL OF PROCESS

input to predict an all engines hardover failure, which results eventually in vehicle breakup. Measurements of pitch rate and angle of attack will provide less lead time since the vehicle response lag is introduced in the computation.

Cryogenic engines such as J-2 require chilldown of the lox and fuel pumps before starting. Overboard or tank return flow through bleed valves is employed to accomplish the chilling operation. If the bleed valve fails to close at start, a very hazardous condition may result because of lox rich combustion in the gas generator and main chamber. For this situation the following measurements are available, for malfunction sensing:

Initial Measurements	• Bleed valve position • Bleed flow • Bleed valve pressure drop	Before main start signal (Discharge start tank valve signal in the case of the J-2 engine)
	• Bleed flow • Bleed valve pressure drop • Pump flow, pressure, and speed	After main start signal
Stress Measurements	• Gas generator temperature • Fuel injection temperature	After main start signal
Final Effects	• Gas generator burn-through* • Main chamber burn-through* • Loss of pump speed • Loss of thrust	After main start signal

If the bleed valve is signaled to close and fails to do so, the flow through the chilldown system will continue. If there is a delay between the signal to close the bleed valve and the signal to start the engine, the indication of flow during this interval will be an indication of valve failure. After the start signal is given, the open bleed valve can be detected from the resulting abnormality in the pump performance in terms of main flow, pressure rise, and speed.

*Possible hazardous effects.

The measurement of gas generator temperature is associated directly with the failure mechanism. This type of measurement is discussed in the following subsection.

7.4 SENSING THE STRESS VARIABLE

Figure 7-3 illustrates some typical structural failure modes of a rocket engine and the associated stress variables that can cause the failures.

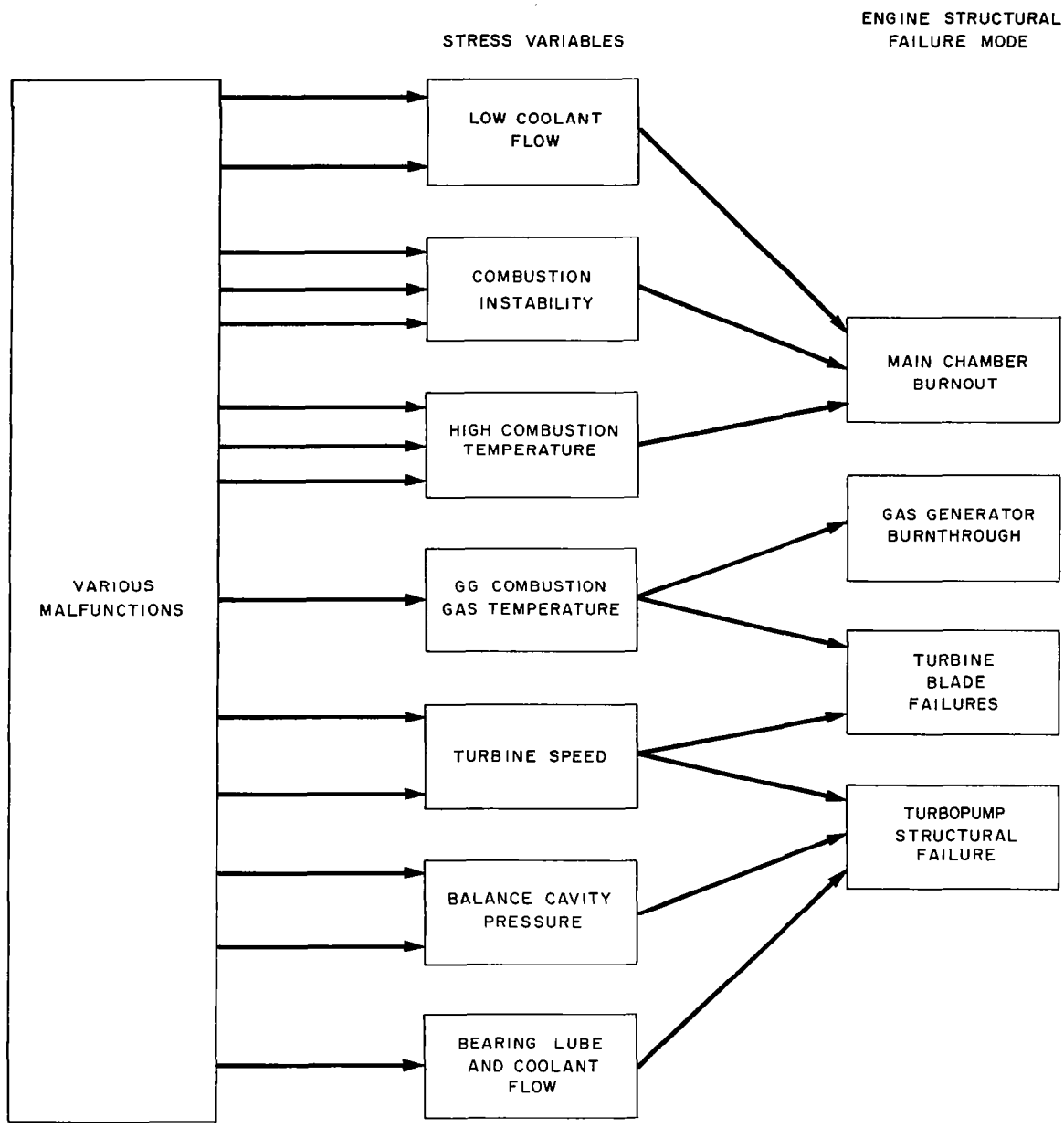

FIGURE 7-3. POSSIBLE ENGINE FAILURE MODES

The engine will normally be designed so that the structural members can withstand normal variations in engine operating parameters with a very low probability of failure. However, when a malfunction is present in the engine, much larger excursions of the stress parameters are experienced and a higher probability of failure can be expected.

The variations of stress and strength of a normal engine are usually represented as random variables having a normal distribution. Likewise, the stress variable under malfunction conditions can be assumed to be normally distributed since it is the net effect of many possible different malfunctions of varying amplitudes.

A typical example is shown in figure 7-4. The stress on a particular structural member under normal conditions has a mean deviation, σ_o, and the strength of the member has mean a deviation, σ_f. The mean values of the two parameters are separated by a sufficient margin,

$$\left(\bar{X}_f - \bar{X}_o\right) = 4\sqrt{\sigma_f^2 + \sigma_o^2} ,$$

so that the chance of random failure is very small. For the no-malfunction condition, shown in figure 7-4, the chance of a random failure is only 32×10^{-6}.

Under malfunction conditions the mean deviation of stress is increased to

$$\left(\bar{X}_f - \bar{X}_o\right) = 4\sqrt{\sigma_f^2 + \sigma_m^2}$$

to yield a conditional probability of 0.16 for a catastrophic structural failure, given a malfunction.

A sensor threshold can be interposed between the strength and stress distributions so that when the stress exceeds the threshold, the engine is shutdown and catastrophic loss is prevented at the expense of an engine shutdown and the consequent effect on mission capability. However, since the stress and strength distributions overlap there is no sensor setting for which there will be no unnecessary shutdowns (when the engine would not have failed) and there will always be come possibility of not shutting down when engine failure will result.

Figure 7-4 illustrates the four possible end states:

- Normal: No malfunction has occurred, hence the probability of failure or shutdown is negligible.
- Safe Off-Design: A malfunction has occurred, but the engine continues to run safely in an off-design condition, and no shutdown occurs.
- Safe Shutdown: A malfunction has occurred, but the condition has been sensed and the engine safely shutdown.
- Explosion: A malfunction has occurred, but the sensor was not actuated and failure occurred.

The optimum setting of the sensor is the setting that minimizes the total expected risk due to these four end states. In figure 7-4, the sensor setting balances the false and missed alarm rates to optimize the system for the assigned loss values shown in the figure. The resulting distribution of probabilities for the four end states and expected loss are tabulated in figure 7-4 with comparison value figures

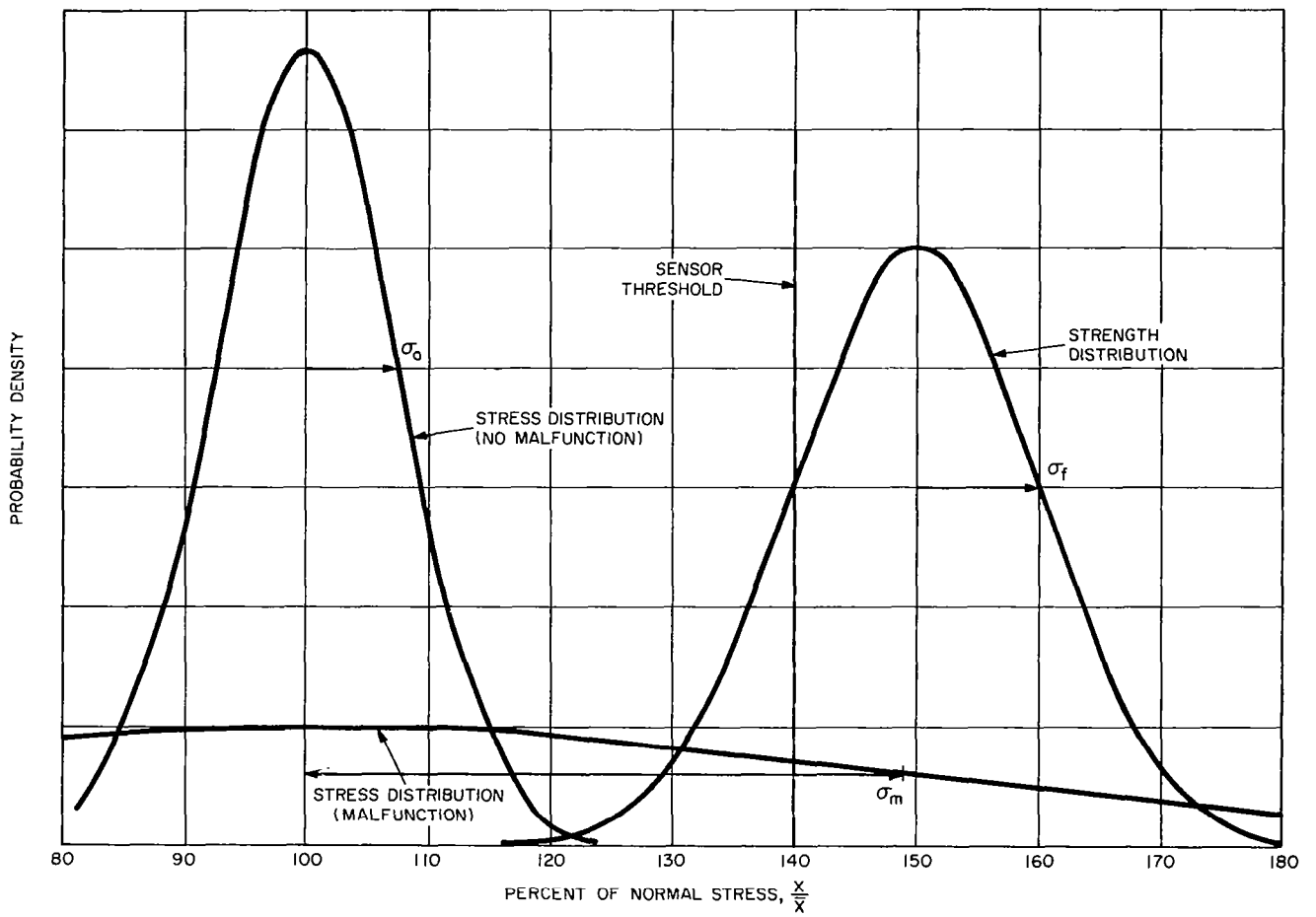

FIGURE 7-4. TYPICAL STRESS AND STRENGTH DISTRIBUTION FOR NORMAL AND MALFUNCTION CONDITIONS

for no READI and an ideal sensor. An ideal sensor is one that will shutdown the engine only when a failure actually occurs. The results for this example show a risk reduction of 75 percent which compares favorably with the 84 percent possibly with a theoretical ideal sensor. The performance of the practical sensor improves with increasing value of the σ_m/σ_f ratio.

7.5 CONCLUSION

A practical READI system will make use of a variety of input measurements ranging from initial to final effects. In general, the measurement of intermediate effects unrelated to stress are preferred. Practical experience in preliminary synthesis of detection equations for the subsystems in Saturn V indicate that, for over 60 percent of the malfunctions, suitable combinations of intermediate measurements may be found to indicate and verify the malfunction. When the measurement of the variable under stress is employed, careful consideration must be given to the selection of the alarm point. For realistic stress and strength distributions a substantial risk reduction can be achieved, even when measuring the stress variable alone.

APPENDIX A

J-2 ENGINE MATHEMATICAL MODEL

The mathematical model that was employed in analog computer simulation of the J-2 engine dynamics consists of a set of equations that define the pressures and flows within the engine as functions of propellant tank pressures and valve positions. Figure A-1 is a simplified engine schematic diagram that shows the locations of the various valves and the discrete points within the engine that are represented in the model equations.

The lox and fuel tank pressures are treated as constants. Figure A-2 shows how the normal engine valve positions were varied for the start and cutoff transients. The lox and fuel bleed valves were normally considered to be closed, except for occasional operation to represent malfunctions or remedial actions. The propellant utilization valve was normally considered in the neutral position, half open. It also was varied occasionally, for remedial action purposes, at a maximum time of 1 second to swing from nominal to full open or full closed.

Table A-1 defines the symbols and units employed in the model equations. The equations themselves are listed in table A-2. In addition, figures A-3 and A-4 give the values of nonlinear functions that are employed in the equations. Figure A-5 shows the value of a nonlinear function that represents the gas generator ignition and combustion limits. The effect of this function is to keep the gas generator chamber pressure at zero until a 1/1 O/F ratio is obtained, and to reduce the pressure to zero if the O/F ratio falls below one half.

Note that in table A-2 there are two equations listed for the hot gas flow to the fuel turbine. Equation (34) is rigorous with respect to maintaining flow continuity, while the alternate, equation (34*), has the effect of introducing an empirical correction for the velocity of the hot gas flow through the turbines. It appeared that equation (34) was preferable for simulation of disturbances from the steady-state operating condition, while equation (34*) was a better representation for large transients such as start of cutoff.

Correlation of the model behavior with actual engine test data was good, but the engine data were limited to normal start transients. Test data that included engine malfunction transients were not available.

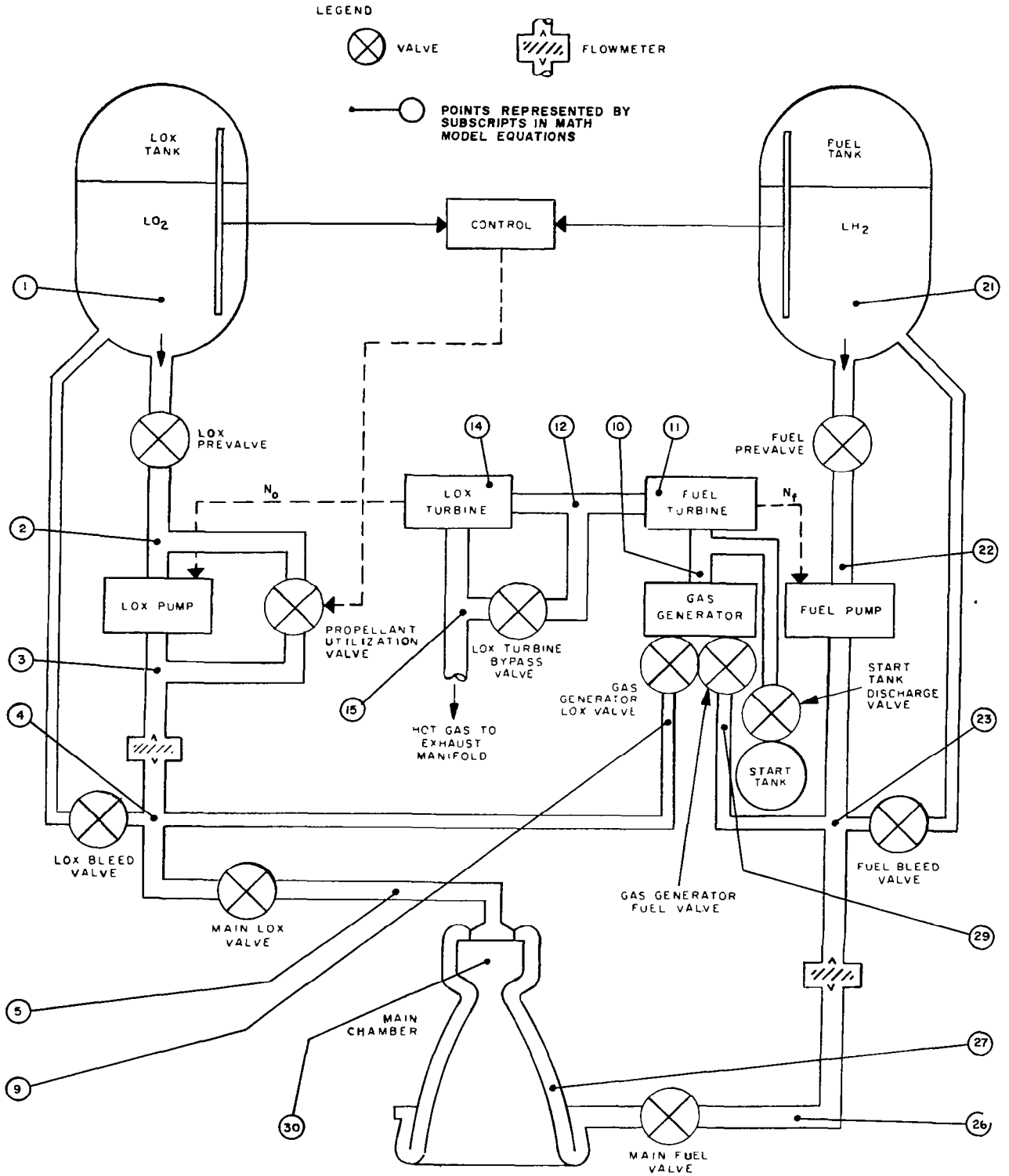

FIGURE A-1. ENGINE SCHEMATIC DIAGRAM SHOWING LOCATION OF MATHEMATICAL MODEL DISCRETE POINTS

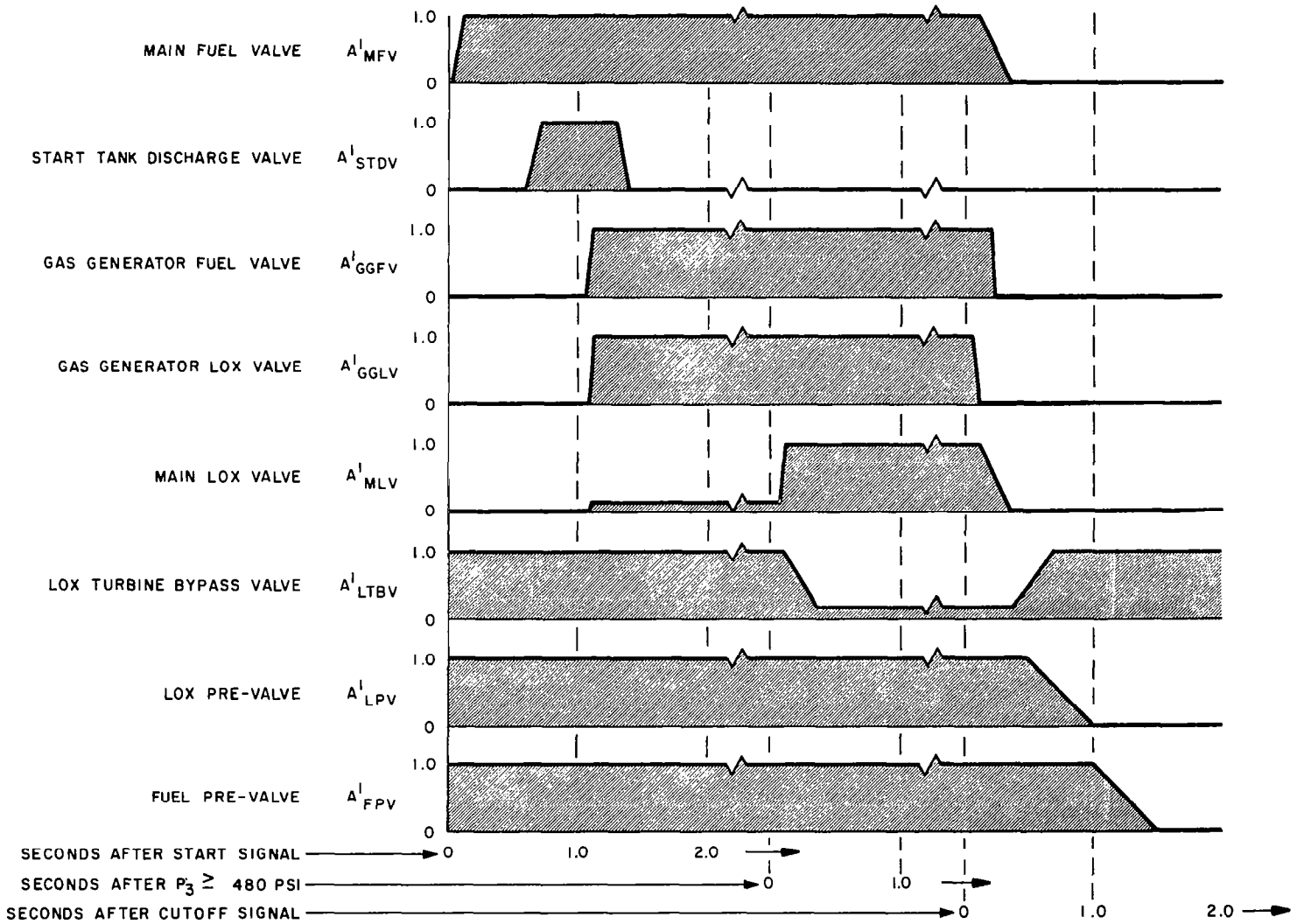

FIGURE A-2. NORMAL ENGINE VALVE POSITIONS DURING START AND CUTOFF

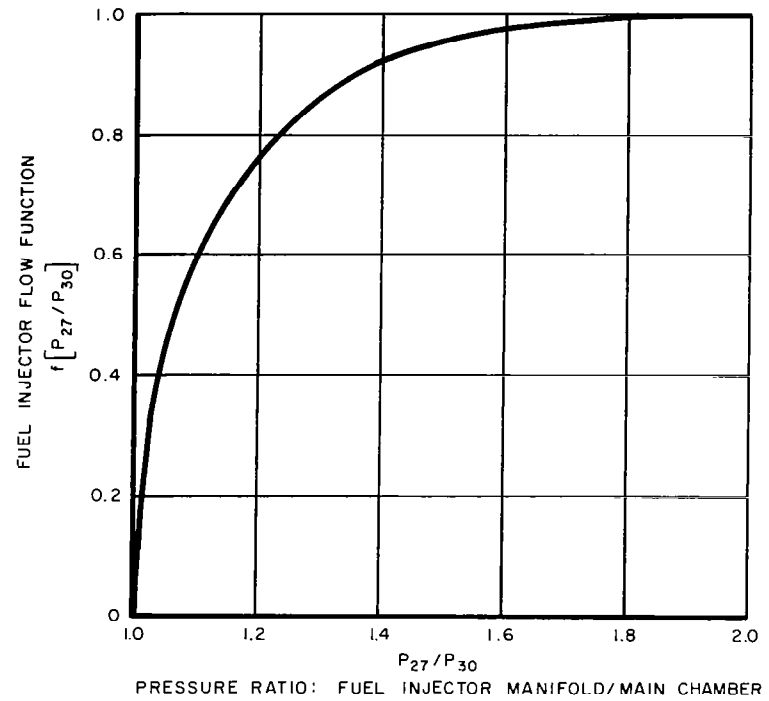

FIGURE A-3. FUEL INJECTOR FLOW FUNCTION VS. PRESSURE RATIO

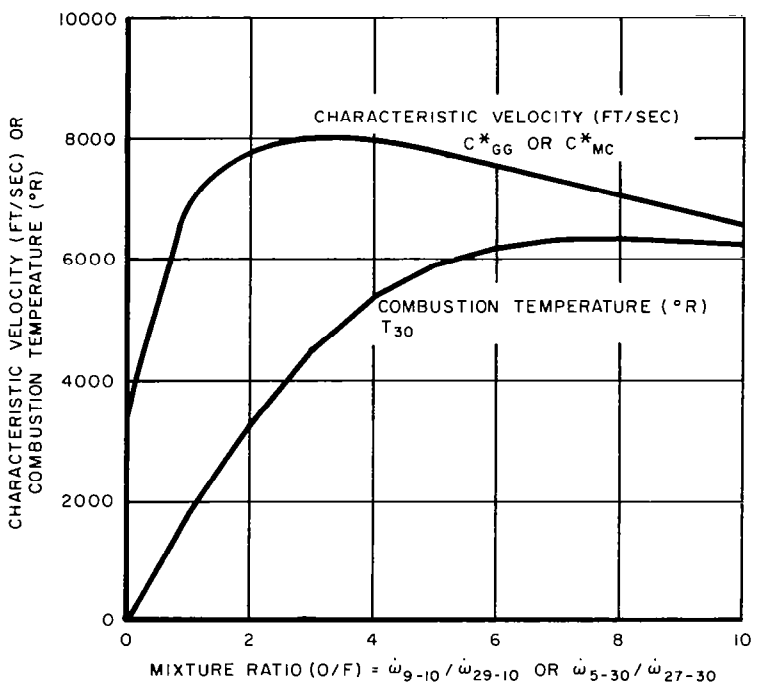

FIGURE A-4. CHARACTERISTIC VELOCITY COMBUSTION TEMPERATURE VS. MIXTURE RATIO

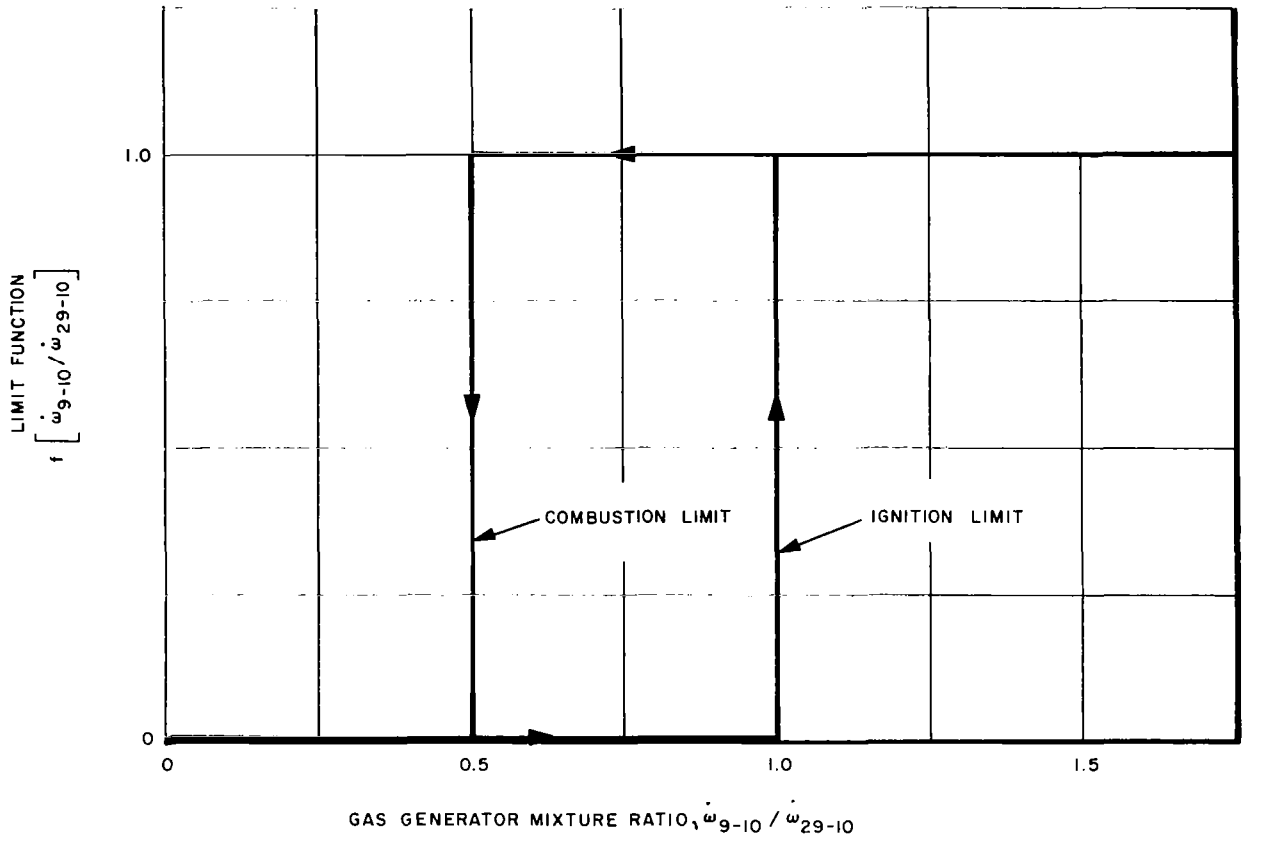

FIGURE A-5. GAS GENERATOR IGNITION AND COMBUSTION LIMIT FUNCTION

Table A-1

SYMBOLS AND UNITS USED IN ENGINE MATHEMATICAL MODEL

Symbol	Definition	Units
A'	Area of valve opening relative to maximum open area	-
C^*	Characteristic velocity	ft/sec
N	Turbopump speed	rpm
$\dot{N}$	Rate of change of turbopump speed	rpm/sec
P	Pressure	lbs/in^2
$\dot{P}$	Rate of change of pressure	$lbs/in^2/sec$
T	Temperature	°R
$\dot{T}$	Rate of change of temperature	°R/sec
$\dot{w}$	Flow rate	lbs/sec
$\ddot{w}$	Rate of change of flow rate	lbs/sec^2

Subscripts:

Numbers in figure A-1 refer to the subscripts after the variables (such as flow and pressure) in table A-2.

o	Lox turbopump
f	Fuel turbopump
FBV	Fuel Bleed Valve
FPV	Fuel Pre Valve
GGFV	Gas Generator Fuel Valve
GGLV	Gas Generator Lox Valve
LBV	Lox Bleed Valve
LPV	Lox Pre Valve
LTBV	Lox Turbine Bypass Valve
MFV	Main Fuel Valve
MLV	Main Lox Valve
PUV	Propellant Utilization Valve
STDV	Start Tank Discharge Valve
GG	Gas Generator
MC	Main Chamber

TABLE A-2. ENGINE MATHEMATICAL MODEL EQUATIONS

Equations		Constants
Oxidizer Flow Equations		
(1) LOX Inlet Duct	$\dot{w}_{1-2} = \frac{1}{K_2}\left[(P_1 - P_2) - \frac{K_1}{A'_{LPV}}(\dot{w}_{1-2})^2\right]$	$K_1 = 0.0000129$ $K_2 = 0.00253$
(2) Pressure Utilization Valve	$\dot{w}_{3-2} = 2K_{14}\, A'_{PUV}\,(P_3 - P_2)^{1/2}$	$K_{14} = 2.3247$
(3) LOX Pump	$\dot{w}_{2-3} = \dot{w}_{1-2} + \dot{w}_{3-2}$	
(4) LOX High Pressure Duct	$\dot{w}_{3-4} = \frac{1}{K_8}\left[(P_3 - P_4) - K_7\,(\dot{w}_{3-4})^2\right]$	$K_7 = 0.00018789$ $K_8 = 0.0072$
(5) LOX Bleed Valve	$\dot{w}_{4-1} = K_{200}A'_{LBV}\,(P_4 - P_1)^{1/2}$	$K_{200} = 5.82$ $P_1 = 39$ psi
(6) LOX Bootstrap Line	$\dot{w}_{4-9} = \frac{1}{K_{12}}\left[(P_4 - P_9) - K_{11}\,(\dot{w}_{4-9})^2\right]$	$K_{11} = 9.99$ $K_{12} = 0.036$
(7) Gas Generator LOX Valve	$\dot{w}_{9-10} = K_{13}A'_{GGLV}\,(P_9 - P_{10})^{1/2}$	$K_{13} = 0.4432$
(8) Main LOX Valve	$\dot{w}_{4-5} = K_9A'_{MLV}\,(P_4 - P_5)^{1/2}$	$K_9 = 73.9$
(9) LOX Injector	$\dot{w}_{5-30} = K_{10}\,(P_5 - P_{30})^{1/2}$	$K_{10} = 36.5$
Oxidizer Pressure Equations		
(10) LOX Pump Head	$P_3 - P_2 = \text{Minimum of}\begin{cases} C_1N_o^2+C_2K_{100}N_o\dot{w}_{2-3}-C_3(K_{100}\dot{w}_{2-3})^2 \\ \text{or} \\ C_6N_o^2+C_5K_{100}N_o\dot{w}_{2-3}-C_4(K_{100}\dot{w}_{2-3})^2 \end{cases}$	$K_{100} = 6.32$ $C_1 = 1.6024 \times 10^{-5}$ $C_2 = 1.009 \times 10^{-5}$ $C_3 = 4.534 \times 10^{-5}$ $C_4 = 1.061 \times 10^{-4}$ $C_5 = 2.795 \times 10^{-5}$ $C_6 = 1.472 \times 10^{-5}$
(11) LOX Pump Discharge	$\dot{P}_3 = K_{15}\,(\dot{w}_{1-2} - \dot{w}_{3-4})$	$K_{15} = 211$
(12) Main LOX Valve Inlet	$\dot{P}_4 = K_{15}\,(\dot{w}_{3-4} - \dot{w}_{4-5} - \dot{w}_{4-1} - \dot{w}_{4-9})$	
(13) LOX Injector Inlet	$\dot{P}_5 = K_{115}\, f[P_5]\,(\dot{w}_{4-5} - \dot{w}_{5-30})$	$K_{115} = 2.0$ $f[P_5] = \begin{cases} 1.0 & 0 < P_5 < 60 \text{ psi} \\ \infty & 60 \text{ psi} < P_5 \end{cases}$
(14) Gas Generator LOX Valve Inlet	$\dot{P}_9 = K_{16}\,(\dot{w}_{4-9} - \dot{w}_{9-10})$	$K_{16} = 1040.0$
LOX Bleed Valve Position		
(15) A'_{LBV} = 1.0 or 0; Nominally 0		

TABLE A-2. ENGINE MATHEMATICAL MODEL EQUATIONS (Continued)

	Equations	Constants
Propellant Utilization Valve Position		
(16)	$0 \leq A'_{PUV} \leq 1.0$; Nominally $A'_{PVV} = 0.5$	
(17)	Maximum $\dot{A}'_{PUV} = \pm 0.5$/sec	
Fuel Flow Equations		
(18)	Fuel Inlet Duct	$\dot{w}_{21-22} = \frac{1}{K_4}\left[(P_{21} - P_{22}) - \frac{K_3}{A'_{FBV}}(\dot{w}_{21-22})^2\right]$	$K_3 = 0.000243$ $K_4 = 0.0112$
(19)	Fuel Pump	$\dot{w}_{22-23} = \dot{w}_{21-22}$	
(20)	Fuel High Pressure Duct	$\dot{w}_{23-26} = \frac{1}{K_{54}}\left[(P_{23} - P_{26}) - K_{53}(\dot{w}_{23-26})^2\right]$	$K_{53} = 0.00388$ $K_{54} = 0.0157$
(21)	Fuel Bleed Valve	$\dot{w}_{23-21} = K_{52} A'_{FBV} (P_{23} - P_{21})^{1/2}$	$K_{52} = 1.45$ $P_{21} = 30$ psi
(22)	Fuel Bootstrap Line	$\dot{w}_{23-29} = \frac{1}{K_{61}}\left[(P_{23} - P_{29}) - K_{60}(\dot{w}_{23-29})\right]$	$K_{60} = 1.2$ $K_{61} = 0.0139$
(23)	Gas Generator Fuel Valve	$\dot{w}_{29-10} = K_{62} A'_{GGFV} (P_{29} - P_{10})^{1/2}$	$K_{62} = 0.193$
(24)	Main Fuel Valve	$\dot{w}_{26-27} = K_{56} A'_{MFV} (P_{26} - P_{27})^{1/2}$	$K_{56} = 6.46$
(25)	Fuel Injector	$\dot{w}_{27-30} = K_{59} P_{27} T_{27-30}^{-1/2} f[P_{27}/P_{30}]$	$K_{59} = 1.508$ See figure A-3 for $f[P_{27}/P_{30}]$
Fuel Pressure Equations		
(26)	Fuel Pump Head	$P_{23}-P_{22}$=Minimum of $\begin{cases} C_5 N_f^2 + C_6 K_{108} N_f \dot{w}_{22-23} - C_7 (K_{108}\dot{w}_{22-23})^2 \\ \text{or} \\ C_8 (K_{108}\dot{w}_{22-23})^2 \end{cases}$	$K_{108} = 102.0$ $C_5 = 9.0 \times 10^{-8}$ $C_6 = 17.04 \times 10^{-6}$ $C_7 = 38.18 \times 10^{-6}$ $C_8 = 28.466 \times 10^{-6}$
(27)	Fuel Pump Discharge	$\dot{P}_{23} = K_{55}(\dot{w}_{22-23} - \dot{w}_{23-26} - \dot{w}_{23-21} - \dot{w}_{23-29})$	$K_{55} = 412.0$
(28)	Main Fuel Valve Inlet	$\dot{P}_{26} = K_{55}(\dot{w}_{23-26} - \dot{w}_{26-27})$	
(29)	Fuel Injector Inlet	$\dot{P}_{27} = K_{58} T_{27}(\dot{w}_{26-27} - \dot{w}_{27-30})$	$K_{58} = 0.64275$
(30)	Gas Generator Fuel Valve Inlet	$\dot{P}_{29} = K_{63}(\dot{w}_{23-29} - \dot{w}_{29-10})$	$K_{63} = 4120.0$

TABLE A-2. ENGINE MATHEMATICAL MODEL EQUATIONS (Continued)

Equations		Constants		
Fuel Temperature Equations				
(31) Thrust Chamber Cooling Jacket	$T_{27} = \frac{1}{2}(T_{27-30} + K_{106})$	$K_{106} = 49.5$		
(32) Fuel Injector Inlet	$\dot{T}_{27-30} = K_{120}\, T_{30} - K_{119}\, T_{27-30}\, \dot{w}_{26-27}$	$K_{119} = 0.065$	$K_{120} = 0.1479$	
Fuel Bleed Valve Position				
(33) A'_{FBV} = 1.0 or 0; Nominally 0				
Hot Gas Flow Equations				
(34) Fuel Turbine	$\dot{w}_{10-11} = w_{9-10} + \dot{w}_{29-10} + K_{21}\, A'_{SDTV}\, e^{-K_{22}t}$	$K_{21} = 15.1768$	$K_{22} = 0.227$	
(34*) Fuel Turbine, Alternate	$\dot{w}_{10-11} = K_{118}\, P_{10} + K_{21}\, A'_{STDV}\, e^{-K_{22}t}$	$K_{118} = 0.00996$	t = time after starting to open the start tank discharge valve, seconds	
(35) LOX Turbine Bypass Valve	$\dot{w}_{12-15} = 12.56\, K_{28}\, A'_{LTBV}\, P_{12}$	$K_{28} = 0.007899$		
(36) LOX Turbine	$\dot{w}_{12-14} = K_{30}\, P_{12}$	$K_{30} = 0.07978$		
Hot Gas Pressure Equations				
(37) Gas Generator Chamber	$\dot{P}_{10} = K_{36}\,[K_{102}\, C^*_{GG}\, (\dot{w}_{9-10}+\dot{w}_{29-10})\, f(\dot{w}_{9-10}/\dot{w}_{29-10}) - P_{10}]$	$K_{36} = 3250.0$	$K_{102} = 0.015$	See figure A-4 for C^*_{GG}
(38) LOX Turbine Inlet	$\dot{P}_{12} = K_{29}\, (\dot{w}_{10-11} - \dot{w}_{12-15} - \dot{w}_{12-14})$	$K_{29} = 3060.0$		See figure A-5 for $f(\dot{w}_{9-10}/\dot{w}_{29-10})$
Turbopump Speed Equations				
(39) Fuel Turbopump	$\dot{N}_f = (K_{25} - K_{26}\, N_f)\, \dot{w}_{10-11} - K_{27}\, (P_{23}-P_{22})\dot{w}_{22-23}/N_f$	$K_{25} = 5879.0$	$K_{26} = 0.06158$	$K_{27} = 9557.225$
(40) LOX Turbopump	$\dot{N}_o = (K_{31} - K_{32}\, N_o)\, \dot{w}_{12-14} - K_{33}\, (P_3-P_2)\dot{w}_{2-3}/N_o$	$K_{31} = 4260.0$	$K_{32} = 0.1003$	$K_{33} = 433.3$
Main Chamber Equations				
(41) Pressure	$\dot{P}_{30} = K_{39}\,[K_{103}\, C^*_{MC}\, (\dot{w}_{5-30} + \dot{w}_{27-30}) - P_{30}]$	$K_{39} = 3250.0$	$K_{103} = 0.000191$	See figure A-4 for C^*_{MC}
(42) Temperature	$T_{30} = f[\dot{w}_{5-30}/\dot{w}_{27-30}]$			See figure A-4 for T_{30}

APPENDIX B

EQUATIONS USED IN THE STAGE PERFORMANCE DEGRADATION MODELS

B.1 SIVB STAGE

Since the SIVB flight is exo-atmospheric and nearly horizontal, the gravity component loss was neglected, and the single ΔV relation was used:

$$\Delta V = Vex \ln\left(\frac{M_o}{M_f}\right)$$

The equation is modified for the three time periods under consideration:

- From launch to start of first burn
- During first burn
- During second burn.

The terms used in the equations are defined below:

$Vexo$ - normal Vexhaust = $I_{spo} \times G_o$

Vex_1 - effective Vex after malfunction

Vex_1' - modified Vex_1 due to PU action

M_{fo} - final mass after second burn

M_{fo}' - final mass with malfunction

$M(t^*)$ - mass of vehicle at time of malfunction

$M(tpu)$ - mass of vehicle when PU unit equalizes mass ratio

M_{01} - mass of vehicle at start of first burn, normal

M_{01}' - mass of vehicle at start of first burn, malfunction

M_{02} - mass of vehicle at start of second burn, normal

M_{02}' - mass of vehicle at start of second burn, malfunction

M_o - mass of vehicle at start of second burn, equivalent

ΔM - orbital boiloff

M_{RP} - normal usable propellant reserve after first burn

M_{RPN} - normalized usable propellant reserve

t^* - time-of-occurrence of malfunction

t_b - burn time

t_{pu} - time of PU correction

$\dot{M}_{PR}$ - normal propellant rate

$\Delta\dot{M}_{PR}$ - change in effective propellant rate

M_{orb} - $M_{02} + \Delta M$

α - $vex_1/vexo$

α' - $vex_1'/vexo$

$\Delta\dot{M}_{PR}$ - $\dot{M}_{PR}$ modified by PU action

- For failure occurring in second burn:

$$Vexo \ln\left[\frac{M_o}{M(t^*)}\right] + Vex_1 \ln\left[\frac{M(t^*)}{M_{fo}'}\right] = Vexo \ln\left[\frac{M_o'}{M_f}\right] \quad (1)$$

$$M_o' = M_{fo}\left[\left[\frac{M_o}{M(t^*)}\right]\left[\frac{M(t^*)}{M_{fo}'}\right]^{\alpha}\right] \quad (2)$$

$$M_{fo}' = \Delta\dot{M}_{PR}(t_b - t^*) + M_{fo} \quad (3)$$

$$t_b = (M_{RP} - t^*\dot{M}_{PR})/(M_{PR} + \Delta M_{PR}) \quad (4)$$

$$M_{prn} = (M_o' + \Delta M - M_{fo})/M_{RP} \quad (5)$$

- For failure occurring in first burn:

$$\text{Vexo} \ln\left[\frac{M_{01}}{M(t^*)}\right] + \text{Vex}_1 \ln\left[\frac{M(t^*)}{M'_{orb}}\right] = \text{Vexo} \ln\left[\frac{M_{01}}{M_{orb}}\right] \quad (6)$$

$$M'_{orb} = M(t^*)\left[M(t^*)/M_{orb}\right]^{1/\alpha} \quad (7)$$

$$M'_{02} = M_{orb} - \Delta M \quad (8)$$

$$M_{fo}' = \Delta\dot{M}_{PR}(t_b) + M_{fo} \quad (9)$$

$$t_b = (M_{02}' - M_{fo}')/(\dot{M}_{PR} + \Delta\dot{M}_{PR}) \quad (10)$$

$$\text{Vex}_1 \ln\left[\frac{M_{02}'}{M_{fo}'}\right] = \text{Vexo} \ln\left[\frac{M_o'}{M_{fo}}\right] \quad (11)$$

$$M_o' = M_{fo}(M_{02}'/M_{fo}) \quad (12)$$

Proceed as in equation (5)

- For failure occurring between launch and first burn (leaks only):
  - PU unit cannot correct mass unbalance

$$\text{Vex}_1 \ln\left[\frac{M_{01}'}{M_{orb}'}\right] = \text{Vexo} \ln\left[M_{01}/M_{orb}\right] \quad (13)$$

$$M_{orb}' = M_{01}'\left[\frac{M_{orb}}{M_{01}}\right]^{1/\alpha'} \quad (14)$$

$$M_{02}' = M_{orb}' - \Delta M \quad (15)$$

$$\text{Vex}_1' \ln(M_{02}'/M_{fo}') = \text{Vexo} \ln\left[\frac{M_o'}{M_f}\right] \quad (16)$$

$$M_o' = M_{fo}(M_{02}'/M_{fo}')^{\alpha'} \quad (17)$$

M_{fo}' as in equation (9) and M_{prn} as in equation (5)

- PU unit corrects mass unbalance in second burn

M_{02}' as in equation (15)

$$\text{Vex}_1 \ln\left[M_{02}'/M_{tpu}\right] + \text{Vex}_1 \ln\left[M(t_{pu})/M_{fo}\right] = \text{Vexo} \ln\left[M_o'/M_{fo}\right] \quad (18)$$

$$t_{pu} = \left[\left[M_{01} - M_{01}'\right]/\Delta\dot{M}_{PR}\right] - \Delta T \text{ (first burn)} \quad (19)$$

$$M_o' = M_{fo}\left[\left[\frac{M_{02}'}{M_{tpu}}\right]^{\alpha'}\left[\frac{M_{tpu}}{M_{fo}'}\right]^{\alpha}\right] \quad (20)$$

- PU unit corrects mass unbalance in first burn

$$\text{Vex}_1' \ln\left[\frac{M_{01}'}{M_{tpu}}\right] + \text{Vex}_1 \ln\left[M(t_{pu})/M_{orb}'\right] = \text{Vexo} \ln\left[M_{01}/M_{orb}\right] \quad (21)$$

$$t_{pu} = \left[M_{01} - M_{01}'\right]/\Delta M_{PR}' \quad (22)$$

$$M_{orb}' = M(t_{pu}) \left[(M(t_{pu})/M_{01}')^{\alpha/\alpha'} \cdot (M_{01}/M_{orb})^{1/\alpha} \right] \quad (23)$$

Follow equations (8) to (12) and (5).

NOTE: $M_{fo}' = M_{fo}$ as the PU has balanced the mass flow.

B.2 SII STAGE

The following list defines the terms used in the SIC, SIVB, and SII performance equations:

- $\dot{M}oxo$ - Initial oxidizer flow rate
- $\dot{M}ox(t)$ - Oxidizer flow rate at time t
- Moxo - Initial weight of oxidizer
- M_{prx} - Residual weight of oxidizer at burnout
- $\dot{M}_{fo}$ - Initial fuel flow rate
- $\dot{M}_f(t)$ - Fuel flow rate at time t
- M_{fo} - Initial weight of fuel
- M_{prf} - Residual weight of fuel at burn out
- M_{so} - Initial weight of structure and payload
- $M_s(t)$ - Weight of structure and payload at time t
- M(t) - Weight of vehicle at time t
- THR_o - Initial thrust of stage
- THR(t) - Thrust of stage at time t
- H_o - Initial altitude of stage
- H(t) - Altitude of stage at time t
- $\dot{H}_o$ - Initial altitude rate of stage
- $\dot{H}(t)$ - Altitude rate of stage at time t
- $V_s(t)$ - Inertial velocity of vehicle at time t
- V_R - Relative velocity of vehicle at time t
- θ_s - Space-fixed flight path angle
- α' - Angle of attack
- R(t) - Range at time t (earth centered coordinates)
- t_{ieco} - Time of in-board engine cutoff
- t* - Time-of-occurrence of malfunction.

The purpose of these equations is to compute M_{PRN} for various values of oxidizer flow (α), fuel flow (β) and thrust (γ). Each set is run for t* = 0, 40, 80,....., 320 (time of occurrence of malfunction).

The equations for SII are used for each iteration of t, until one of the tests fails. The equations for SIV are then used until the SIVB tests fail. M_{PRN} is then computed.

B.2.1 GENERAL CONSTANTS

$G_o = 9.8066$

$M(T_3) = 16,030$

$T_3 = 23.8$

$R_o = 6,378,000$

$V_{circ} = 7800$

$H_{circ} = 185,000$

$V_{\psi_o} = 2550$

$K_1 = 0.151$

$K_2 = 0.05$

$K_3 = 0.133$

$K_4 = 0.05$

$K_o = 0.008096$

$\Delta t = 4.0$

B.2.2 SII PERFORMANCE EQUATIONS

B.2.2.1 Constants

$$\left.\begin{aligned}\dot{M}_{oxo} &= 1800.0\\ \dot{M}_{fo} &= 380.0\end{aligned}\right\}\ \text{Assumed Values}$$

$$H_o = 65{,}300$$

$$\dot{H}_o = 950$$

$$M_{so} = 450{,}000$$

$$M_{oxo} = 780{,}000$$

$$M_{prx} = 6600.0$$

$$M_{fo} = 153{,}000$$

$$M_{prf} = 9900.0$$

$$THR_o = 925{,}000.0$$

$$T_2 = 3.8.$$

B.2.2.2 Initial Conditions

$$t = 4.0 \text{ sec.}$$

$$M_{ox}(t) = M_{oxo}$$

$$M_f(t) = M_{fo}$$

$$H(t) = H_o$$

$$\dot{H}(t) = \dot{H}_o$$

$$V_\psi(t) = V_{\psi_o}$$

B.2.2.3 Propellant Utilization Model

$$DIFF = \begin{cases} K_4 \left(\frac{M_{ox}(t)}{4.7} - M_f(t)\right) & \text{if } t>8 \\ 0.6 & \text{if } t\leq 8 \end{cases} \quad (1)$$

$$PU = \begin{cases} DIFF & \text{if } -0.4 \leq DIFF \leq 1.6 \\ -0.4 & \text{if } DIFF < -0.4 \\ 0.6 & \text{if } DIFF > 1.6 \end{cases} \quad (2)$$

$$\dot{M}_{ox}(t) = \dot{M}_{oxo}\,(1 + K_1(PU)) \quad (3)$$

$$\dot{M}_f(t) = M_{fo}\,(1 + K_2(PU)) \quad (4)$$

$$THR(t) = THR_o\,(1 + K_3(PU)) \quad (5)$$

B.2.2.4 Malfunction Effect Control

if $t \geq t^*$ add $\begin{cases} \dot{M}_{oxo}\ (\alpha) \text{ to } \dot{M}_{ox}(t) \\ \dot{M}_{fo}\ (\beta) \text{ to } \dot{M}_f(t) \\ THR_o\ (\gamma) \text{ to } THR(t) \end{cases}$

B.2.2.5 Mass Equations

$$M_{ox}(t) = M_{ox}(t) - \dot{M}_{ox}(t)\,\Delta t \quad (6)$$

$$M_f(t) = M_f(t) - \dot{M}_f(t)\,\Delta t \quad (7)$$

Test for end of burn. If

$$M_{ox}(t) - M_{prx} \leq 0$$

or

$$M_f(t) - M_{prf} \leq 0$$

proceed to SIVB equations.

$$M_s(t) = \begin{cases} M_{so} & \text{if } t < T_3 \\ M_{so} - M_{t3} & \text{if } t \geq T_3 \end{cases} \quad (8)$$

$$M(t) = M_s(t) + M_{ox}(t) + M_f(t) \quad (9)$$

B.2.2.6 Control and Guidance Equations

$$V_s(t) = \sqrt{V_\psi(t)^2 + \dot{H}(t)^2} \quad (10)$$

$$\theta_s = \sin^{-1}\left(\frac{\dot{H}(t)}{V_s(t)}\right) \quad (11)$$

$$\alpha' = (H_{circ} - H(t))\,K_o - \dot{H}(t) \quad (12)$$

$$X = \begin{cases} \theta_s + \alpha' & \text{if } -90^\circ \leq \theta_s + \alpha' \leq 90^\circ \\ 90^\circ & \text{if } \theta_s + \alpha' > 90^\circ \\ -90 & \text{if } \theta_s + \alpha' < -90^\circ \end{cases} \quad (13)$$

B.2.2.7 Equations of Motion

$$R(t) = H(t) + R_o \qquad (14)$$

$$ACC = \frac{G_o \cdot THR(t)}{M(t)} \qquad (15)$$

$$I_1 = \begin{cases} 0 & \text{if } t < T_2 \\ ACC \cdot \sin X \cdot \Delta t & \text{if } t \geq T_2 \end{cases} \qquad (16)$$

$$I_2 = G_o \left(\frac{R_o}{R(t)}\right)^2 \Delta t \qquad (17)$$

$$I_3 = \frac{V_\psi(t)^2}{R(t)} \Delta t \qquad (18)$$

$$I_4 = \begin{cases} 0 & \text{if } t < T_2 \\ \frac{R(t)}{R_o} ACC \cdot \cos X \cdot \Delta t & \text{if } t \geq T_2 \end{cases} \qquad (19)$$

$$\Delta\dot{H} = I_1 - I_2 + I_3 \qquad (20)$$

$$H(t) = H(t) + (\dot{H}(t) + 1/2\ \Delta\dot{H})\ \Delta t \qquad (21)$$

$$\dot{H}(t) = \dot{H}(t) + \Delta\dot{H} \qquad (22)$$

$$V_\psi(t) = V_\psi(t) + I_4 \qquad (23)$$

Let t = t + 4.0 and repeat from B.2.2.3 equation (1).

B.2.3 SIV PERFORMANCE EQUATIONS

B.2.3.1 Constants

$$M_{ox}(t) = \dot{M}_{oxo} = 390$$
$$\dot{M}_f(t) = \dot{M}_{fo} = 80$$
$$M_s(t) = M_{so} = 130{,}000$$
$$M_{oxo} = 180{,}000$$
$$M_{prx} = 1{,}800$$
$$M_{fo} = 40{,}000$$
$$M_{prf} = 3{,}000$$
$$THR(t) = 196{,}000$$
$$T_2 = 0.0$$

B.2.3.2 Initial Conditions

$$M_{ox}(t) = M_{oxo}$$
$$M_f(t) = M_{fo}$$

B.2.3.3 Mass Equations

$$M_{ox}(t) = M_{ox}(t) - \dot{M}_{ox}(t)\ \Delta t \qquad (1)$$

$$M_f(t) = M_f(t) - \dot{M}_f(t)\ \Delta t \qquad (2)$$

If $V_{circ} - V_\psi(t) \leq 0$ compute M_{PRN} by method 1, B.2.2.5 equations (6) and (7) and end.
If $M_{ox}(t) - M_{prx} \leq 0$ or $M_f(t) - M_{prf} \leq 0$ compute M_{PRN} by method 2, B.2.2.5 equations (8) and (9) and end.
} SIVB first burn termination test

$$M(t) = M_s(t) + M_{ox}(t) + M_f(t) \qquad (3)$$

B.2.3.4 Guidance Equations

$$V_s(t) = \sqrt{V_\psi(t)^2 + \dot{H}(t)^2} \qquad (4)$$

$$\theta_s = \sin^{-1} \frac{\dot{H}(t)}{V_s(t)} \qquad (5)$$

$$\alpha' = (H_{circ} - H(t))\ K_o - \dot{H}(t) \qquad (6)$$

$$X = \begin{cases} \theta_s + \alpha' & \text{if } -90° \leq \theta_s + \alpha' \leq 90° \\ 90° & \text{if } \theta_s + \alpha' > 90° \\ -90° & \text{if } \theta_s + \alpha' < -90° \end{cases} \qquad (7)$$

B.2.3.5 Equations of Motion

$$R(t) = H(t) + R_o \qquad (8)$$

$$ACC = \frac{G_o \cdot THR(t)}{M(t)} \tag{9}$$

$$I_1 = \begin{cases} 0 & \text{if } t < T_2 \\ ACC \cdot \sin X \cdot \Delta t & \text{if } t \geq T_2 \end{cases} \tag{10}$$

$$I_2 = G_o \left(\frac{R_o}{R(t)}\right)^2 \cdot \Delta t \tag{11}$$

$$I_3 = \frac{V_\psi(t)^2}{R(t)} \cdot \Delta t \tag{12}$$

$$I_4 = \begin{cases} 0 & \text{if } t < T_2 \\ \frac{R(t)}{R_o} \cdot ACC \cdot \cos X \cdot \Delta t & \text{if } t \geq T_2 \end{cases} \tag{13}$$

$$\Delta\dot{H} = I_1 - I_2 + I_3 \tag{14}$$

$$H(t) = H(t) + (\dot{H}(t) + 1/2\ \Delta\dot{H})\ \Delta t \tag{15}$$

$$\dot{H}(t) = \dot{H}(t) + \Delta\dot{H} \tag{16}$$

$$V_\psi(t) = V_\psi(t) + I_4 \tag{17}$$

Let $t = t + \Delta t$ and repeat from B.2.3.3 equation (1).

B.2.4 DISCUSSION OF RESULTS

Method 1: $M_{PRN} = M(t) - 129{,}000.0$

Method 2: $V = V_{circ} - V_s(t)$

$$M_{PRN} = M(t)e^{-\Delta V/4300.0} - 129{,}000.0$$

M_{PRN} is then normalized by dividing by 135,219.07 (the unnormalized M_{PRN} from $\alpha = \beta = \gamma = t^* = 0$)

B.3 SIC STAGE

Performance computation (equation set)

(1) Set up at t=o:

$H(t) = o$

$\dot{H}(t) = o$

$\psi(t) = o$

$\dot{\psi}(t) = \Omega$

$M_{ox}(t) = M_{oxo}$

$M_f(t) = M_{fo}$

$T_M = T_o$

$t_{ieco} = 146$ seconds.

(2) Mass flow equations

$$\dot{M}_{ox}(t) = \dot{M}_{oxo} \cdot (1 + \alpha(t \geq t^*) + \dot{M}_{ox}\, t_{ieco}\ (t \geq t_{ieco}) \quad (1)$$

$$\dot{M}_f(t) = \dot{M}_{fo} \cdot (1 + \beta(t \geq t^*) + \dot{M}_f(t_{ieco})\ (t \geq t_{ieco}) \quad (2)$$

$$M_{ox}(t) = M_{ox}(t) - \dot{M}_{ox}(t) \cdot \Delta t \quad (3)$$

$$M_f(t) = M_f(t) - \dot{M}_f(t) \cdot \Delta t \quad (4)$$

$$M(t) = M_s + M_{ox}(t) + M_f(t) \quad (5)$$

(3) Thrust

$$THR(t) = THR(o) \cdot \left(1.15 - 0.15\, e^{-\beta \cdot H(t)}\right) \left(1 + \alpha\left|_{t \geq t^*} + THR(t_{ieco})\right|_{t \geq t_{ieco}}\right)$$

Test:

If $M_{ox}(t) - M_{prx} \leq o$, or if $M_f(t) - M_{prf} \leq o$, exit to SII stage or else continue.

(4) Flight parameters

$$\rho(t) = \rho_o\, e^{-\beta \cdot H(t)}$$

$$R(t) = R(o) + H(t)$$

$$V_R^2(t) = \left[R(t) \cdot \left(\dot{\psi}(t) - \Omega_o\right)\right]^2 + \dot{H}^2(t)$$

$$Q(t) = 1/2\rho(t) \cdot V_R^2(t)$$

t_x = the lesser of $\left(M_{ox}(t) - M_{PRX}\right)/\dot{M}_{ox}(t)$ or $(M_f(t) - M_{PRF})/\dot{M}_f(t)$

$$X(t) = X(t) - \left(\frac{X(t) - X_2}{t_x}\right)\Delta t, \quad t \geq t_2; \quad X(t) = 90°, \quad t < t_2$$

$$t_{ieco} = t + t_x - 4$$

$$C_S = 347\ (T_m/A_o)^{1/2}$$

$$M_A = V_R/C_S$$

$M_A \leq B_1$; $C_{DA}(t) = \left(C_1 + \frac{C_2}{M_A} + \frac{C_3}{M_A^2}\right)\frac{1}{M_A}$

$B_1 < M_A \leq B_2$; $C_{DA}(t) = C_4 + C_5\, M_A$

$B_2 < M_A$; $C_{DA}(t) = C_6 + C_7\, e^{C_8 M_A}$

Test: MA $\leq$ 100. If yes, continue, if no, M_A = 100, continue.

(5) Equations of motion

$$\psi(t) = \psi(t) + \dot{\psi}(t) \cdot \Delta t \quad (1)$$

$$\phi(t) = X(t) + \psi(t) \quad (2)$$

$$ACC = \left[G_o \cdot THR(t) - C_{DA}(t) \cdot Q(t)\right]\frac{1}{M(t)} \quad (3)$$

$$I_1 = ACC \cdot \sin\phi(t) \cdot \Delta t \quad (4)$$

$$I_2 = Go\left(\frac{R(o)}{R(t)}\right)^2 \Delta t \quad (5)$$

$$I_3 = \left[R(t) \cdot \dot{\psi}(t)^2\right] \Delta t \quad (6)$$

$$I_4 = \frac{R(t)}{Ro} \cdot ACC \cdot \cos \phi(t) \cdot \Delta t \qquad (7)$$

$$\Delta \dot{H} = I_1 - I_2 + I_3 \qquad (8)$$

$$H(t) = H(t) + (\dot{H}(t) + 1/2\ \Delta \dot{H}) \cdot \Delta t \qquad (9)$$

$$\dot{H}(t) = H(t) + \Delta \dot{H} \qquad (10)$$

$$\dot{\psi}(t) = \frac{Ro}{R(t)^2} I_4 + \dot{\psi}(t) \qquad (11)$$

$$V_\psi = R(t) \cdot \dot{\psi}(t) \qquad (12)$$

$$V_S = \sqrt{V_{\psi_1}^2 + \dot{H}^2(t)} \qquad (13)$$

$$T_M = A_o + A_1 H + A_2 H^2;\ H \leq 32{,}000 \qquad (14)$$

$$T_M = A_3 + A_4 H + A_5 H^2;\ H > 32{,}000 \qquad (15)$$

Test: $T_M \geq 222$. If yes, continue, if no, $T_M = 222$, continue, proceed to 2.

(6) Constants

R_o - 6,378,260

G_o - 9.8066

ρ_o - 0.1423

β - 1/7170

X_2 - 20.0

t^2 - 8 sec

T_o - 288.8

A_o - 288.8

A_1 - 0.00394

A_2 - 1355 x 10^{-10}

A_3 - 22.0

A_4 - 0.0155

A_5 - 0.315 x 10^{-6}

B_1 - 0.6

B_2 - 1.1

C_1 - 22.0

C_2 -(-) 2.88

C_3 - 0.168

C_4 -(-) 27.2

C_5 - 92.0

C_6 - 87.9

C_7 - 87.9

C_8 -(-) 0.415

$TH_{t_{ieco}}$ -(-) 0.2

$\dot{M}_{ox}\ t_{ieco}$ - (-) 0.2

$\dot{M}_f\ t_{ieco}$ - (-) 0.2

M_S - 1,740,000

M_{oxo} - 3,000,000

M_{prx} - 69,000

$\dot{M}_{oxo}$ - 20,000 (Assumed)

M_{fo} - 1,370,000

M_{prf} - 69,000

$\dot{M}_{fo}$ - 8,700 (Assumed)

Ωo - 0.64068 x 10^{-6}

THR_o - 7,500,000

α - change in oxidizer flow

β - change in fuel flow

γ - change in thrust level.

APPENDIX C
REFERENCES

1. Preliminary Design and Feasibility Investigation of Rocket Engine Analyzer and Decision Instrumentation (READI) for Saturn V, furnished by Sperry Gyroscope Company to Marshall Space Flight Center, under Contract No. NAS 8-11290, March 1965

2. Purser, Faget and Smith, Manned Spacecraft: Engineering Design and Operation, New York, Fairchild Publications, Inc., 1964

3. Minutes of the Eighth Crew Safety Panel Meeting of March 31 - April 1, 1964, Marshall Space Flight Center, Huntsville, Alabama

4. S. Glasstone, "The Effects of Nuclear Weapons", United States Atomic Energy Commission, 1962

5. Marshall Space Flight Center Memorandum, M-AERO-D-1-63, "Saturn V Performance Summary and Trajectory Data Based on Specification Weights", MSFC, Huntsville, Alabama, 29 April 1963, CONFIDENTIAL

6. NASA, TM X-880, Apollo System Descriptions, (Volume 1).

"The aeronautical and space activities of the United States shall be conducted so as to contribute . . . to the expansion of human knowledge of phenomena in the atmosphere and space. The Administration shall provide for the widest practicable and appropriate dissemination of information concerning its activities and the results thereof."

—NATIONAL AERONAUTICS AND SPACE ACT OF 1958

NASA SCIENTIFIC AND TECHNICAL PUBLICATIONS

TECHNICAL REPORTS: Scientific and technical information considered important, complete, and a lasting contribution to existing knowledge.

TECHNICAL NOTES: Information less broad in scope but nevertheless of importance as a contribution to existing knowledge.

TECHNICAL MEMORANDUMS: Information receiving limited distribution because of preliminary data, security classification, or other reasons.

CONTRACTOR REPORTS: Technical information generated in connection with a NASA contract or grant and released under NASA auspices.

TECHNICAL TRANSLATIONS: Information published in a foreign language considered to merit NASA distribution in English.

TECHNICAL REPRINTS: Information derived from NASA activities and initially published in the form of journal articles.

SPECIAL PUBLICATIONS: Information derived from or of value to NASA activities but not necessarily reporting the results of individual NASA-programmed scientific efforts. Publications include conference proceedings, monographs, data compilations, handbooks, sourcebooks, and special bibliographies.

Details on the availability of these publications may be obtained from:

SCIENTIFIC AND TECHNICAL INFORMATION DIVISION

NATIONAL AERONAUTICS AND SPACE ADMINISTRATION

Washington, D.C. 20546